Design, construction and performance testing of a solar powered refrigerator and heat-pump for urban streets vendors

by

GRACIA WA MWAMBA MUSIFU

Thesis submitted in fulfilment of the requirements for the degree

Master of Engineering in Mechanical Engineering

in the

Faculty of Engineering and the Built Environment at Cape Peninsula University of Technology

Supervisor: Dr Tiyamike Ngonda

Co-supervisor: Mr Cletus Magoda

Bellville Campus
January 2023

DECLARATION

I, Gracia Wa Mwamba Musifu, declare that the contents of this thesis represent my own unassisted work, and that the thesis has not previously been submitted for academic examination towards any qualification. Furthermore, it represents my own opinions and not necessarily those of the Cape Peninsula University of Technology.

14 January 2023

Signed **Date**

ABSTRACT

Solar powered refrigeration systems have been a prominent topic in recent years. Designing a system that relies on entirely solar energy will help in achieving some goals of developing countries, to have a clean source of energy and to reduce reliance on fossil fuels and national electricity grids. The main objective of this study is to design and conduct testing analysis of a refrigerator and heating-pump unit driven by solar energy; it is intended to introduce a hybrid system which can satisfy both cooling as well as heat collection.

However, this research aimed at analysing an optimum solar powered cooling (refrigeration) and heating system that work as one unit by creating a solar cooler and solar warmer that is powered by the same compressor. Given that, the warming (heating-pump) system is dependent entirely on the performance of the condenser while the cooling system is made widely from available domestic refrigerator components based on the vapour compression principle, which components are to be matched to each other and to the solar PV system.

The idea of using the heat (rejected to the atmosphere) from the condenser to warm up foods is a unique approach of research. Experimental and analytical methodologies are applied to give technical details on how this hybrid system will fit with the existing facility, to provide reasons why the model will be in small scale for street vendors, and to promote small enterprises in rural communities.

This paper illustrates the design procedures and calculations necessary to properly size main components such as the battery, PV panel, charge controller and compressor as well as determine the heat load of the entire system. The model was designed and built in the mechanical engineering workshop of Cape Peninsula University of Technology, and the prototype was installed and tested under atmospheric conditions for performance evaluation at the Bellville campus. The design methodology applied was supplemented by both MATLAB programming and ANSYS simulation for validation; readings for wind speed, ambient temperature and solar radiation were taken from the Campbell scientific weather station and analysed. The testing was undertaken at no loads and then fully loaded compartments to evaluate the performance of the system. Experimental results showed that both systems work well at peak hours and also when there is more sunray. Irregularities occurred when the doors were left open for an extended period which caused loss of energy. Although the average COP of the entire system was 3.3, the data revealed that there is still room for improvement, especially if the prototype is to be marketed.

Key words: photo-voltaic system; refrigeration cycle; solar heat pumping; solar powered refrigeration; vapour compression refrigeration

ACKNOWLEDGEMENTS

I would like to express my gratitude to the following:

- God for always being present during my studies and making it possible all the way through.
- Prof Kant Kanyarusoke, Dr Tiyamike Ngonda and Mr Cletus Magoda for giving me complete freedom and flexibility to work on this topic.
- The mechanical workshop technicians for their guidance and supervision.
- My family and friends for their constant love and support.

Knowledge is power and unity is strength.

DEDICATION

I honourably dedicate this thesis to my family,
Especially to my dear father, Doctor Emile Mwamba Mayola Wa Nkulula,
For all that he has sacrificed to have me do great.
He has been my strength and joy, the main provider my entire life.
Wherever you are, I LOVE AND ADORE YOU DAD.

TABLE OF CONTENTS

LIST OF FIGURES

LIST OF TABLES

TERMS AND DEFINITIONS

A. Definition of key words

Photo-voltaic system
Power system designed to supply electric energy by directly converting solar energy through the photovoltaic effect; a process in which semiconducting materials generate voltage and current when exposed to light.

Refrigeration cycle
A thermodynamic cycle that generates refrigerating effect with the use of evaporator, compressor, condenser and expansion valve. It is a cycle of mechanical system in which transmission of heat flow from one place at a lower temperature (the source) to another place at a higher temperature by continuously circulating, evaporating, and condensing a fixed supply of refrigerant in a closed system.

Solar heat pumping
Engages the use of solar energy to produce heating effect. Thus, a heat pump is called as a "heater" if the objective is to warm the heat sink; if the home or a given space is used as a sink, thermal energy will be added, heating the space.

Solar powered refrigeration
Refrigeration system where solar energy is used as the primary source of energy to drive the cooling process. It is operated using electricity directly produced from solar radiation using photovoltaic cell.

Vapour compression refrigeration
Refrigeration cycle in which the refrigerant undergoes phase changes, where it is alternately compressed and expanded, changing it from liquid to vapour.

CHAPTER 1:
INTRODUCTION

1.1 General

1.1.1 Outline of the research problem

The use of renewable energy sources is typically a reliable alternative in rural areas and developing countries, where electric grid line does not exist or are at a great distance. Electrical energy is considered the most convenient form of energy source in rural and urban areas (Cho & Thida, 2018); however, energy poverty is one of the major challenges in Africa and many countries rely on traditional biomass such as firewood, dung and crop residues to meet energy demands (Karekezi *et al.,* 2012). Research to resolve problems relating to energy is quite important since life is directly affected by energy and energy consumption.

Clean energy generation becomes more and more crucial day by day due to the growing significance of environmental issues; intensive efforts are being made worldwide to narrow the gap between renewables and conventional energy sources. It is overwhelming to know in 2012 that 1.4 billion people lacked access to electricity, with 85% living in rural areas. As a result of this, rural communities reliance on the traditional use of biomass was projected to rise from 2.7 billion in 2012 to 2.8 billion in 2030, just eight years from now (Kaygusuz, 2012). Among the clean energy technologies, solar energy is recognised as one of the most promising choices since it is free and provides clean and environmentally friendly energy (Cuce & Cuce, 2012).

According to the International Funds for Agricultural Development (2015), approximately 70% of inhabitants of Africa reside in rural areas, areas characterised by poverty and inadequate access to modern fuels. The term ‘modern’ energy is used to differentiate traditional forms of energy like firewood and agricultural residue from commercial (modern) forms of energy like electricity and liquefied petroleum gas (Brew-Hammond, 2010). Due to the lack of access to modern fuels, the majority of the rural population relies heavily on traditional fuels to meet their energy needs; consequently, this situation causes serious ecological problems such as deforestation. Therefore, there is growing awareness and increasing attention concerning the renewable energy options to meet the heating and cooling requirements of all people. It is well known that most of the populated countries from various parts of the world are blessed with abundant solar radiation with mean daily illumination intensity and more than 275 sunny days in a year, according to Muthusivagami *et al.* (2010). These considerations all point towards the solar cooling and heating systems as part of a sustainable way of life since this is clearly a critically important need.

The importance of foods, air and water to human life are widely documented; food provides energy to the bodies and supplies the necessary chemicals for growth and protection against diseases. Thus, fresh foods are continuously grown due to the consistent high demand for a healthy and convenient diet; because most foods (fruits and vegetable products, meat, grains and fish) are perishable by nature and are seasonal, they must be preserved and stored in controlled conditions prior to long-term consumption (Alkilani, 2017). The idea of using solar energy for refrigeration is not a new one; in particular, solar energy has been suggested as a power source because it is available globally and generally in phases with the cooling and heating demand. This research revolves around designing and commercialising a solar power refrigerator and heat-pump and also involves a prototype that will demonstrate some of the technical accomplishments.

1.1.2 Refrigeration

Various economic and ecological reasons make it necessary to look more in detail at the potential performance improvements of refrigeration systems. A refrigeration system is a system which can reduce the temperature or heat of a substance under a controlled condition; the aim being to cool some product or space to the required temperature. It has many applications including household refrigerators, industrial freezers, cryogenics and air conditioning. More energy efficient systems are needed to curb the greenhouse effect which is caused by an increase of carbon dioxide (CO2) and other gases in the atmosphere in addition to refrigerants. The subject of refrigeration and air conditioning has evolved out of our human need for foods and comfort, so its history dates back many centuries. In olden days, refrigeration was achieved by natural means such as the use of ice or evaporative cooling; however, technology has rapidly evolved in the last century and is now one of the inevitable processes in today's life for preserving food materials, medicinal products and other substances, and giving human comfort via air conditioning. In transporting temperature-sensitive foodstuffs and other materials by trucks, trains, airplanes and seagoing vessels, refrigeration is a necessity.

1.1.3 Solar refrigeration

Solar refrigeration engages a system where solar power is used for cooling purposes. Solar energy can provide cheap and clean energy for cooling and refrigeration applications all over the world. Cooling can be achieved through two basic methods: the first is a PV based solar energy system where solar energy is converted into electrical energy and used for refrigeration much like conventional methods; the second utilises a solar thermal cooling system, where a solar collector directly heats the refrigerant through collector tubes and circulates it for cooling instead of using solar electric power. For the purpose of this research, solar photovoltaic technology has been considered.

a. Solar photovoltaic refrigeration system

Solar photovoltaic (PV) refrigeration systems which use batteries have existed for several decades but have only been used in limited applications. Recent technological developments and experimentation in the field are refining 'solar refrigerator'; coupled with the decreasing cost of PV, this is expected to lead to more wide-spread acceptance and use (Michael *et at*., 2001).

b. Commercial refrigeration

The production of cold temperature through a sustainable process has been a subject of study for long now. Cold is essential in several aspects of human life: it is needed in the food processing field, conservation of medical products like vaccines and certain drugs and the air conditioning sector as well. However, refrigeration of foods and drinks is problematic in parts of the world where there is no electricity or where the electricity supply is unreliable.

Due to warm weather, it has become increasingly common to seek a cold drink in hot weather; thus, cold drinks are preferable by people and the demand for them is unceasing since this is a good way to cool the body temperature. As a result, people began to commercialise cool drinks and look for a better method to arrange cold drinks within a certain period. Commercial refrigeration, then, refers to units with larger capacity than domestic units; they are used by retailer outlets for storage and to display frozen and fresh food and beverages. Therefore, the purpose of using solar assisted refrigeration in an open market is to help vendors sell cooled and fresh products and promote small businesses.

1.1.4 Heat-pump

By definition, a heat pump is a device that transfers heat energy from a source of heat to what is called a 'thermal reservoir'. It moves thermal energy in the opposite direction of spontaneous heat transfer by absorbing heat from a cold space and releasing it into a warmer one. The term 'heat-pump' is more general and applies to many heating, ventilation and air conditioning devices for space heating or cooling. When a heat-pump is used for heating, it employs the same basic refrigeration-type cycle used by a refrigerator or cold room, but in the opposite direction, releasing heat into the conditioned space rather than the surrounding environment. As we think of a heat-pump as a heat transporter, the term 'heating' will be used throughout the paper to avoid misperception.

1.2 Statement of the research

In countries with a high intensity of sunshine, there is a considerable demand for both a cold and heating supply. The main problems in these populated areas are often logistics and the lack of infrastructure; against this background there is a major demand for new decentralised and

combined cooling and heating processes. Refrigerated storage, which is believed to be best method for storing foods or drinks in fresh form, is not available in rural or remote locations where grid electricity is rarely or never available. The effort of addressing the importance of small enterprises on one side and the emphases on cleaner and cheaper energy on the other side, has brought attention to the introduction of this work. So, the present study was undertaken to arrange for a small, portable, cost-effective refrigeration and heating system (unit) that street vendors can use to simultaneously keep their liquid merchandise cold and their solid food snacks warm.

1.3 Purpose of the research

The proposed research is part of a master project in solar energy utilisation in refrigeration and heating-pump (warming) systems, aimed at the development of one or more prototype units demonstrating the usefulness and economic viability of solar energy for rural and urban street vendors in various parts of Africa. However, the goal in this research is to have a combined unit that intends to cool drinks, water or other beverages and while also being capable of utilising the heat rejected to the atmosphere by the condenser for warming up foods of any type at a considerable temperature; therefore, the system should be durable, feasible and economically affordable. It also aims at promoting, on much larger scale, renewable energy sources for sustainable local economic development purposes by demonstrating the efficiency of such a system.

1.4 Research objectives

The main objective in this study is to design and build a combined unit (cooling and heating) which uses solar energy as the source power to get cool fresh drinks and warm foods within a short time, using the same heat rejected by the condenser coil.

Here are the specification for this study:

- The design and construction of a solar powered refrigeration and heating system that runs on a vapour compression cycle;
- The simulation of the model; and
- The testing of the actual unit.

1.4.1 Research design and methodology

The main research methodologies, experimental and analytical approaches, will be broken down into four steps:

i. *Literature review:* Theories are vital in research because they allow a clear approach to the study undertaken. The first step was to summarise the rationale of how this project fits into the sustainable energy strategy of the African community. Therefore, a brief

review of the refrigeration and heating system will provide a structured way to develop the unity of the system.

ii. *Design and calculation:* This step focused on the recommended technology, how it would fit into the existing system, and what advantages would be exploited. It will also describe and compare alternative options that could be used instead. It is important to develop the most suitable project that best matches the vision and needs of vendors and current conditions.

iii. *ANSYS simulation:* This step is to compare system performance from different angles. Then the results are applied to an engineering economics model to determine the unit energy costs and ascertain whether the additional costs are justifiable.

iv. *Construction and testing:* In the final step, the system is built by selecting the equipment and materials (dimensions and shapes) according to the design specifications, and then tested, and various data are recorded and analysed to determine the effectiveness of the system according to the research objectives. Conclusions taken in the form of results are drawn and recommendations are offered for future improvement.

1.4.2 Delimitation of the research

In this research:

- The prototype uses solar PV as a power source; the detailed design was limited to 90Wp mono crystalline silicon panel under Cape Town weather conditions (CPUT Bellville campus site).
- The capacity and volume of the combined system are ± 25L and ± 0.03 m^3 respectively.
- The targeted temperatures range between 5°C - 10°C for the cooling room and between 40°C - 50°C in the heating room
- The system was suitable for street vendors in the urban area of Africa.

1.4.3 Research questions

- Is it possible to attain and maintain cooling and heating at the same time?
- What is the ideal tilt angle to get maximum radiance?
- What are the cost implications for the smallest working prototype?

1.5 Study area

This study was conducted at Cape Peninsula University of Technology (CPUT) in Cape Town, Western Cape, South Africa, between 2019 and 2021. CPUT, one of the distinguished

universities in Cape Town, has a reputation for having appropriate technical equipment for practical and experimental engineering. The workshop of Mechanical Engineering was the location chosen to carry out the manufacturing and experiments of the unit since it has a scientific weather station on top of the building for testing and collecting data such as wind speed, solar radiation intensity and ambient temperature.

1.6 Significance of the research

This research engenders a number of implications; for example, the innovation of solar energy will benefit people and the African community at large. The outcomes of this research can be advantageous to street vendors in rural as well as urban areas without access to electricity. Use of the designed system or its larger versions can create small businesses, reduce environmental pollution and degradation, and overall improve socio-economic productivity. In the long run, this fulfils the target of the study: creating opportunities for a better life against poverty within the African community.

1.7 Thesis organisation

Each chapter of the thesis is structed as follows:

Chapter 1 briefly introduces the solar system together with the project background, objectives and aims.

Chapters 2 & 3 give a literature review and a brief review on refrigeration and heat-pump systems.

Chapter 4 details the design analysis focusing on heat load calculation, component selection, concepts and detailed design processes.

Chapter 5 focuses on CFD development with ANSYS modelling given and discussed.

Chapter 6 deals with the system construction, the experimental set-up and the methodologies implemented in the study. This includes data collection techniques, experimental set-up, testing procedures and instrumentation.

Chapter 7 provides performance evaluation of the hybrid system. Discussions on results and key performance indicators are presented in this section.

Chapter 8 offers conclusions and recommendations emanating from the findings of results.

CHAPTER 2:
LITERATURE REVIEW ON SOLAR REFRIGERATION AND HEATING SYSTEMS

2.1 Introduction

The human keeps searching for new sources of energy to meet his growing needs in the developed applications of life in which he lives. Some sources of energy are known of being exhausted, high cost of their utilization and negative impact of their use on the environment.
Returning to renewable energies to help mitigate climate change is an excellent approach which must be sustainable in order to meet the energy demands of future generations (Edenhofer *et al.,* 2011). Qualitative research, employed by reviewing peer-reviewed papers in the area of study, will bring to light the opportunities associated with solar refrigeration and heating-pump systems and the beneficial economic development of these units.
Many advanced countries in the world today take the lead in promoting research and development of renewable energies such as solar energy, wind energy, biomass energy etc. The importance of research and development on green energy has attracted much attention. Although their cost is high, continuous research and development will achieve the stable, easy to use and reasonably priced renewable energy in some day.

Research and development in solar heating and cooling have been aimed almost entirely at applications in the temperate climates of industrialised countries. Technological feasibilities are being assured. The best methods of obtaining cooling with solar energy in developing countries are clearer than ever at this time and the immediacy and extent of needs for heating are known. There are many refrigeration cycles and systems that can be considered and a substantial number of open questions regarding refrigeration, and application has the attractive possibility of better utilisation of available foodstuffs since it is successfully provided. The next step, then, is to conduct a preliminary study aimed at the development of a basic refrigeration and heating systems for food and drink storage.

2.2 Research papers

Most of these papers demonstrates the ability of solar PV to collect heat at the required temperatures necessary for operating compression cooling and heating systems. Several important lessons have been learnt and useful results achieved. Here are some research papers reviewed along the following lines.

Previous solar refrigeration projects have been based primarily on solar thermal energy from concentrating or flat plate solar collectors; the heat would power an adsorption refrigerator, working dependent on the collector outlet temperature, cold store and ambient temperatures.

The main advantage of this design principle is the relatively low cost of the solar collectors as compared with photovoltaics, but it suffers from a poor COP of the cooling circuit and therefore requires a large solar collector surface (Ivan *et al.*, 2010).

Mehmet Azmi Aktacir (2011) worked on a multi-purpose photovoltaic refrigerator system, which objective was to investigate experimentally the daily and seasonal operation performance of the system.
Not only had that, in 2011, Abdulateef *et al.*, published their work on combined solar assisted ejector absorption refrigeration system. In this paper, results related to both conventional and combined systems driven by solar energy using Ammonia-water were presented and the effects of operating temperatures were investigated. The results showed that, the combined cycle provided potentially high COP than that of the conventional absorption machine. The maximum increase in COP was about 50% higher than the basic cycle. It was seen that if higher cooling capacity and also lower evaporator temperature are desired from the system, the generator temperature should be increased considerably.

Electricity is the major source of power for most of the economic activities of a country; but in Palestine, there are still villages and remote areas that are affected by poor and inadequate sources of energy which results in a very low quality of life. To overcome this situation, Saadi and Ameen (2015) worked on developing a solar system that can be used on an AC load which is the refrigerator. In their studies, the main focus was not only the construction of the conventional refrigerator that works on the vapour compression system, but they focused more on designing a specific inverter to invert the DC power into an AC power to produce a pure sine wave which is necessary to avoid noise while operating the refrigerator. This design, which can be used in domestic and commercial appliances, can help launch small businesses within the community and thereby elevate the quality of life.

Norie and Kumar (2016) developed a portable hybrid solar refrigeration system which carried two refrigeration systems of 40 liters capacity. The objective was to design and study three solar refrigeration systems such as solar compression, solar absorption and solar thermoelectric and compare their thermal performancesHowever, the comparative study showed that the thermal performance of solar vapor compression system is much higher than other two solar refrigeration systems. The cooling potential of Solar Absorption system was found to be better than Solar Thermoelectric system in terms of minimum temperature achieved.

Another interesting work was on solar semiconductor refrigerator by Ragil *et al.* (2016). The conventional refrigeration worked on the principle of cooling through evaporation. In this research, the aim was to design and implement a solar powered semiconductor to cool a required volume. While the authors intended to produce cooling by the principle of the Peltier effect, results in this investigation were not spectacular since the cons of this design are that it is typically more expensive and less efficient.
Similarly, Rani *et al.* (2017) worked on the design of a refrigeration system using refrigerant R134a for macro compartment. The main objective of this study was to analyse and design an

optimum cooling system for macro compartment. The current product of the refrigerator was not specified for single function and not compact in size. Hence, a refrigeration system using refrigerant R134a was intended to provide instant cooling in a macro compartment with sizing around 150x150x250 mm. The compartment was purposely designed to fit a bottle or drink can, which was then cooled to a desired drinking temperature of about 8°C within a period of one minute. This study was not only concerned with the analysis of heat load of the macro compartment containing the drink can, but also intended to determine a suitable heat exchanger volume for both evaporator and condenser, calculating compressor displacement value and computing suitable resistance value of the expansion valve. Due to the warm weather in Malaysia, people prefer cold drinks so the demand never ceases since this is a good way to cool the body temperature down. Consequently, people have started to commercialise them, seeking better ways of creating cold in the shortest time. This is by far the closest project to this current investigation study.

Refrigerators used in a daily life are one of the indispensable tools, a reason uninterrupted power should be supplied to them to sustain a cooling service. The Nigerian author Makinde and his two colleges designed and fabricated a micro-controller mobile cold room powered by solar energy; the cold room was built on a tricycle (cart) to facilitate easy displacement (Makinde *et al.*, 2019). For designing and building the system, many guides provide information to correctly select the compressor, battery, solar array, room materials, wiring, evaporator and condenser pipes and charge controller. The cold room was about 500 litres of total volume and the selected compressor was filled with R600a refrigerant. A 12V solar battery and charge controller were used as well as a 600-watt solar panel. The system was able to run for 18 hours at night when the battery was fully charged (Makinde *et al*., 2019). Their research bridged the gaps of non-availability of cold drinks and eradication of perishable food spoilage that was occurring as a result of inconsistent or inadequate power supplies in rural areas of Nigeria.

In addition, billions of people eat food cooked or warmed on wood or biomass fires, a practice with enormous environmental, health, social and economic impact. Meanwhile in many of these areas, sunlight is a plentiful energy resource. Much research has been undertaken to show that people's cooking and warming habits can be changed and new habits sustained.

Horace de Saussure is recognised for the first recorded attempt in solar cooking in 1767. In 1950, Maria Telkes developed the classic solar cooker. It featured a plywood-insulated box, four reflectors and an inclined top made of two layers of glass, which had a tiny airspace in between them. This design is still seen in modern solar cookers in numerous variations. Several research works were conducted in different areas of solar cooking ranging from thermal testing and performance evaluation of various types of solar cooking devices. Such devices include concentrating solar cookers, parabolic solar cookers, panel solar cookers, and hot box solar cookers, square and rectangular box type of solar cookers, double exposure solar cookers, and solar cookers with thermal storage and several others by various authors with the aim of improving the efficiencies of these cookers.

These projects align themselves with this current research study, whereby solar refrigerator and heating pumps are high in demand because they prohibit their use in off-grid applications and maintain a dependence on fossil fuel for power. With reference to the above study, the projected hybrid system will small scale, made from available materials; the vapour compression refrigerator and heating pump will not be coupled or combined with the thermoelectric system (TER). Even though TER could potentially be a better alternative for the conventional refrigeration system due to their distinct advantages, they are still expensive to purchase and less efficient when used alone. The solar warmer, in this case taken as the heating compartment of the unit, will be insulated with appropriate materials instead in order to trap and keep the heat produced by the condenser within the room. Most of the research so far deals with the purpose of increasing energy efficiency of domestic devices; however, as per the objectives listed, the aim of this study is to provide a budgeted system that is efficient and affordable for one rural street vendor.

2.3 Economic impact

Economic performance is a key factor for the application of the solar cooling and heating technologies. Many researchers have studied the economic performance of these systems. In recent years, several studies have shown that the performance of the solar PV cooling system is better than that of solar photo-thermal conversion cooling system in some areas. Mokhtar *et al.* (2010) compared 25 kinds of solar cooling systems which were different in structure in his study based on the conditions of Abu Dhabi. The results indicated that the performance of the solar PV cooling consisting of the vapour compression chiller and polysilicon PV cells was better than that of the solar absorption cooling system consisting of the single effect absorption chiller and flat plate collectors or evacuated tube collectors. However, Otanicar *et al.* (2012) predicted that the equipment cost of the PV cooling system would drop significantly by the year 2030.

Infante and Kim (2014) compared the performance of the solar PV cooling system and solar photo-thermal cooling systems in the conditions of Spain and Dutch. The results indicated that the cooling system consisting of PV cells and vapour compression chiller had the best performance. Other researchers, undertaking similar experiments using a different place condition, have all arrived at the same conclusion as the two first researchers. In the past, the application of a PV cooling system was limited due to its high cost; however, above studies show that the performance of the PV cooling technology has improved significantly in recent decades. The price reduction of PV cells and the most recent PV subsidy policies are also beneficial to the economic performance of PV cooling technology. Even more, the solar PV cooling and heating system is simpler in structure and easier to maintain, compact with a high power-to-weight ratio compared with other solar cooling systems.

The solar photovoltaic system has no moving parts and probably yields the highest overall conversion of the solar energy into electricity. There are several cases where small or medium sized PV powered refrigerators and heating pump are required. Those have to be optimised in size – both the PV generator and its components, as well as the refrigerator volume – to efficiently meet the start-up power and cooling load (Cho & Thida, 2018). The cooling and heating load to be met by the PV generator depends essentially on the ambient temperature and the room temperature of both the refrigerator and heating pump and is determined by the operational conditions of the systems, the size of the cooling (and heating) space and the matching conditions between the PV generator and the power consuming compressor.

So far, most of the work on solar cooling and heating has been concerned with absorption machines, possibly because only large systems have been built and also because of their reduced maintenance compared with mechanical compression systems. Vapour compression refrigeration systems are available to suit almost all applications with the refrigeration capacities ranging from a few watts to few megawatts; and a wide range of refrigerants can be used in these systems to suit different applications and capacities. PV cells open the field for small mechanical systems using a reciprocating type of compressor that are widely developed. This leaves solar refrigeration (cooling) and heating-pump (warming) applications as a possible area of study and answers the research questions on system design and cost implication. It should be noted that solar cooking is the use of the heat from the sun to cook foods, but in this research the temperature is very low (40˚C - 50˚C) and thus the name 'solar warmer' for warming up foods.

2.4 Conclusion

It is interesting to note the possibility of cooling by the evaporator and simultaneous heating by the condenser in continuous closed vapour-compression systems. This brings the theory back to the research considerations where the system required will therefore be both a **solar cooler** for cooling drinks and some other beverages, and **solar warmer** combined in one unit and sharing the same power source. This theory can be realised if it is possible to maintain pressures corresponding to the required temperatures in the evaporator and the condenser. Generally, it might not be economical for a vapour-compression system because of increased compression ratios and therefore increased power consumption; for that reason, experimental verification of this deduction drawn from the theoretical analysis is required to determine the limits of this option.

CHAPTER 3:
BASIC REFRIGERATION AND HEATING SYSTEMS

3.1 Introduction

Theories are very important in research because they provide a way to tackle the study undertaken. Solar energy research appears to have gathered momentum during the last two decades. Therefore, a brief review on refrigeration and heating pump systems will be a way to develop the system unit.

3.2 Refrigeration

As mentioned in the previous chapter, refrigeration is the transfer of heat from one cooled substance to another location. The most common method of refrigeration is one in which the gas used does not come into actual contact with the substance to be cooled and is recompressed and again condensed for reuse. This can be done using one of two systems: the vapour compression system and the absorption system.

3.2.1 Vapour-compression system

Refrigeration systems are commonly used to provide cooling to sub-ambient processes. The most commonly used refrigeration system today is the vapor compression refrigeration cycle (VCR). Heat is extracted from a lower temperature heat source and pumped to a higher temperature by means of the work of the compressor (Asma, 2017). The four main components are the compressor, condenser, evaporator and expansion valve.

3.2.1.1 Analysis of vapour-compression refrigeration cycle

VCR cycles are the most used in domestic and industrial refrigeration and also in air-conditioning (Alkilani, 2017; Dincer & Kanoglu, 2010). The key function is to create a cold region by rejecting heat to the atmosphere, as shown in Figure 3.1 below.

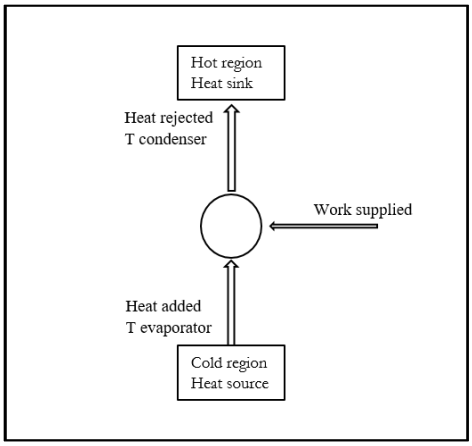

Figure 3.1: Schematic of a VCR

In the VCR cycle, the compressor compresses the refrigerant liquid at high temperature and pressure to state 2; this refrigerant liquid then passes into the condenser to decrease the temperature where it passes at constant pressure to saturated liquid in state 3 and returns to state 4 at the inlet of the evaporator by expanding adiabatically through a pressure reducing valve. Now this low temperature, low pressure liquid goes to the evaporator and becomes vapour. Thus, cooling is obtained in the evaporator. The refrigerant vapour is then moved to the compressor in state 1 with a quality of x = 1 where it is again compressed at high pressure and high temperature, and the cycle continues as shown in Figure 3.2. A temperature-entropy and pressure-enthalpy diagram is shown in Figures 3.3 and 3.4.

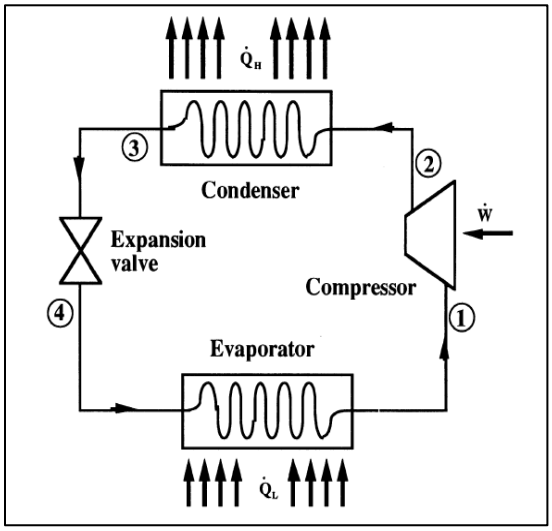

Figure 3.2: VCR cycle (*Edwin, P. & Rex, M., 1986).*

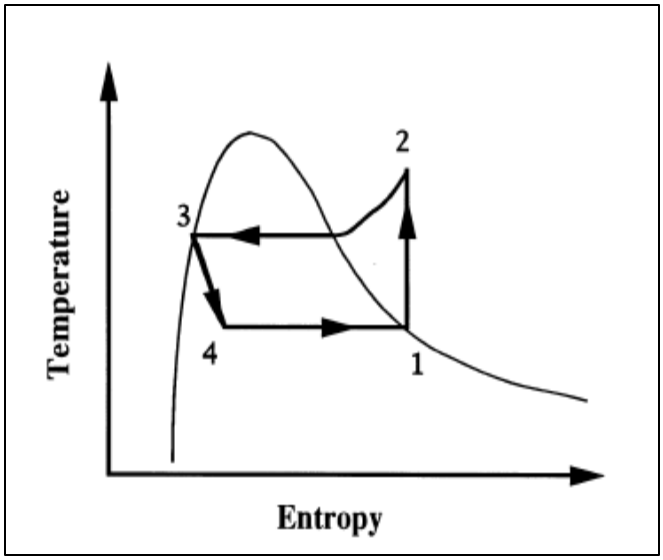

Figure 3.3: Temperature-entropy diagram for a VCR (Edwin, P. & Rex, M., 1986).

The refrigerant is continuously circulating through the cycle and its different states are described beginning at the inlet of the evaporator.

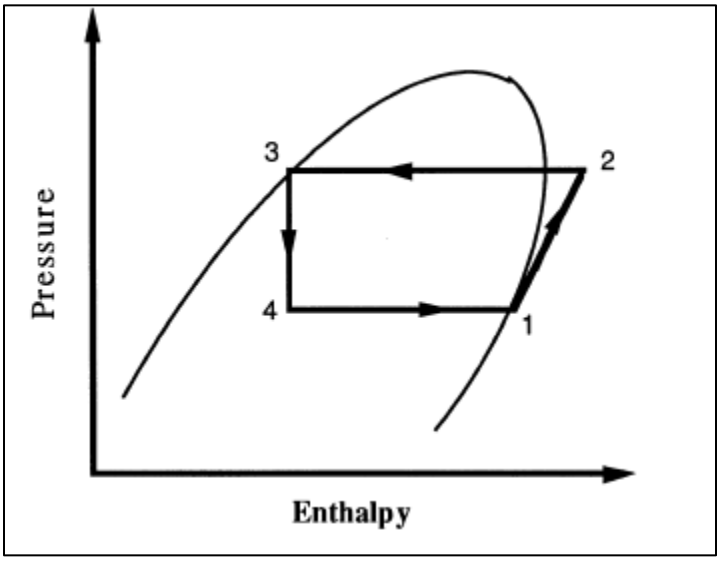

Figure 3.4: Pressure-enthalpy diagram for a VCR (Edwin, P. & Rex, M., 1986).

The refrigeration capacity or the cooling load is determined by the product of enthalpy difference across the evaporator and the mass flow rate of the refrigerant.

$$\dot{Q}_L = \dot{m}_{ref}(h_1 - h_4) \qquad (3.1)$$

- Where, $\dot{Q}_{\mathrm{L}}$ = Heat extracted from cooling space (KW)
  $\dot{\mathrm{m}}_{\mathrm{ref}}$ = mass flow rate of the refrigerant $\left(\frac{\mathrm{Kg}}{\mathrm{s}}\right)$
  h = enthalpy $\left(\frac{\mathrm{KJ}}{\mathrm{Kg}}\right)$

The power required for the entire cycle is found by the product of the mass flow rate of the refrigerant and the enthalpy difference between evaporator outlet and condenser inlet.

$$\dot{W} = \dot{m}_{ref}(h_2 - h_1) \quad (3.2)$$

- Where, $\dot{W}$ = Compressor power input (KW)

The rate of heat rejected to the surroundings from the condenser is given by

$$\dot{Q}_H = \dot{m}_{ref}(h_2 - h_3) \quad (3.3)$$

- Where, $\dot{Q}_{\mathrm{H}}$ = Heat rejected from condenser space (KW)

The throttling device is assumed to be isenthalpic

$$h_3 = h_4 \quad (3.4)$$

The coefficient of performance (COP) is defined as the cooling load or cooling capacity divided by the power supplied to the cycle.

For cooling system, $\mathrm{COP} = \frac{\dot{\mathrm{Q}}_L}{\mathrm{W}} = \frac{\mathrm{h_1 - h_4}}{\mathrm{h_2 - h_1}}$ (3.5)

For heat-pump, $\mathrm{COP} = \frac{\dot{\mathrm{Q}}_H}{\mathrm{W}} = \frac{\mathrm{h_2 - h_3}}{\mathrm{h_2 - h_1}}$ (3.6)

3.2.1.2 Functions of VCR components

a. Compressor

Removing the refrigerant vapour as fast as it is formed maintains the required pressure in the evaporator, and it also raises the pressure of the refrigerant to a level sufficiently high above the equivalent condensing medium temperature to enable the condenser to function.

b. Evaporator

An evaporator is an important part of the refrigerating system, as it is where the cooling effect is produced. The refrigerant absorbs the heat from the substance to be cooled in the evaporator, gets evaporated and is then sucked by the compressor.

c. Condenser

In the condenser, heat is transferred from a hot compressed refrigerant vapour to a cooling medium, usually air or water; this is done so that the same refrigerant may be returned to the evaporator and used again. For condensation to take place, the compressor must be capable of raising the pressure of the refrigerant to such a level that the corresponding saturation temperature is higher than the temperature of the available cooling medium (Michael, 1986).

d. Expansion valve

In this device, the temperature and pressure of the refrigerant are reduced suddenly and drastically.

3.2.2 Absorption system

3.2.2.1 Overview of the system

An absorption refrigeration system uses heat and a refrigerant that may be absorbed into water. Domestic systems use ammonia and industrial systems may use ammonia or lithium bromide. The absorption system of refrigeration differs from that of the vapour-compression system mainly in that it uses heat energy instead of mechanical energy to change the condition required in the refrigeration cycle (Anderson, 1986). The comparison between the functioning of the absorption and compression systems is principally as follows: the absorption system uses heat (usually a gas flame) to circulate the refrigerant, while the compression system employs a compressor to circulate the refrigerant, but some absorption may be operated by gas or electricity (Anderson, 1986).

Anderson (1986) compared three components of the absorption system with the four components of the compression system, as follows:

1. The action of the generator compares with the stroke of the compressor.
2. The condenser and evaporator serve the same purpose in the absorption system as in the compression system.
3. The absorber compares to the law or suction, side of the pump.

3.2.2.2 Principle of an absorption system

The basic principle is the removal of heat from the substance to be cooled by the evaporation of a refrigerant, just as in the compression system; the difference lies in the means adopted for conveying the vapour produced to the condenser. In a simple absorption system, the vapour enters an absorber in which a weak solution dissolves the vapour thereby becoming stronger; heat is produced by this absorption and must be removed by a cooling medium (air or water). The strong solution is then passed to a generator where it is heated, driving off the refrigerant vapour which passes on to the condenser, while the weakened solution returns via a pressure reducing valve to the absorber. From condenser inlet to evaporator outlet, the refrigerant

undergoes changes similar to those which take place in the vapour-compression system adapted from Michael (1986).

3.2.2.3 Disadvantage of the absorption system

As a disadvantage, Michael (1986) noted that the ratio of the refrigeration produced to the heat supplied is quite low (low COP), resulting in a higher running cost in comparison with the compression system unless waste heat is available for large industrial systems.

3.3 Heating system

In this research, the heat used in the system aims to warm up foods that are previously cooked and retain them under a targeted temperature. However, in location with an abundance of sunlight, this practice can use the energy from the sun which is converted into heat energy that is retained for cooking, or as in this case, warming up. This practice can be regarded as another way of introducing and promoting solar cooking, warming and ovens into the traditional community, and creating major opportunities for generating substantial income during the day as a fight against poverty.

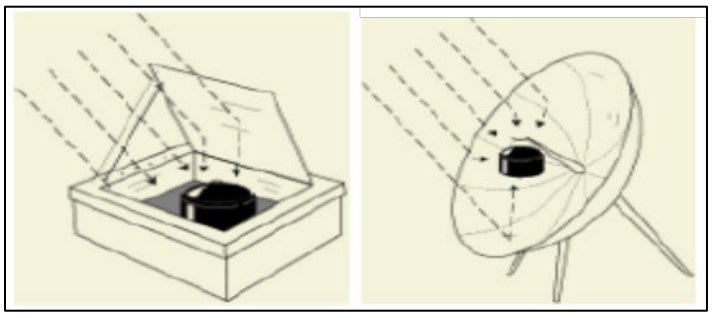

Figure 3.5: Left-solar oven and right-solar cooker

Yet, without undermining the advantages that this technology offers, these solar ovens cannot be used on cloudy days or at night; given that, a system is considered a cooling system when removal of heat Q_L at the evaporator temperature T_{Ev} is the main purpose; and it is considered a heat-pump (heating) if the supply of heat Q_H at the condenser temperature T_{Con} is the main purpose. As a result, the warming (heating) system is dependent entirely on the performance of the condenser since it is a combined unit with refrigeration (using the same compressor power) and letting the energy from the sun serve as additional heat to the system.

CHAPTER 4:
REFRIGERATION AND HEATING:
DESIGN ANALYSIS AND CALCULATION

4.1 Introduction

This analysis deals with detailed design calculations and capacity requirements for the cold room (container or refrigerated space) as well as the heating space. Thus, the heat leakage load through the walls of the structure is first determined, after which the product cooling and air infiltration loads are also calculated. Tabulated data include conductivity factors for various materials, specific heat and condensing capacity when the need for cooling is known. The importance of these calculations is to confirm the total thermal load which will determine the amount of energy required to operate the two systems. This is in parallel with CDF simulation because such data is used to monitor the temperature difference between the two compartments. A schematic explanation is drawn below.

4.2 Preliminary assumptions

One type of refrigeration system that has been proposed for the system is the simple (basic) vapour compression configuration; a schematic of such a device is illustrated in Figure 3.1 above. As shown, a VCR has four major components: evaporator, compressor, condenser and the expansion valve (see Figure 3.2). The system, using R-134a as the refrigerant, is concerned with analysing the heat load in both cooling and heating; therefore, a Mollier diagram is necessary in the process of developing the refrigeration system, and property data of R-134a are taken from the thermodynamic property tables. Below are preliminary assumptions made for the system.

- Evaporator temperature : -2°C
- Cooling product name : 500 ml Coca Cola bottle
- Condenser temperature : 50°C
- Heating product name : Potatoes (French fries) and sausages (meat)
- Refrigerant : R-134a

4.3 Refrigeration design calculation

4.3.1 Cooling cabinet structure

The cooling cabinet is comprised of three main components: the outside cabinet and door, the inner cabinet and the insulation inserted between the two cabinets.

- The outside cabinet

This is made of a particular thermoplastic sheet (high density polyethylene [HDPE]). An HDPE sheet is a tough material with high impact strength and good chemical resistance properties.

- The inner cabinet

The inside room is made of aluminium 'Al' sheets because of their unique properties: lightweight, corrosion resistant and sound and shock absorption.

- The insulation

The insulation that fills the gap between the exterior and inner cabinet is made of expanded polystyrene (EPS) foam because it is an excellent insulator with lightweight, rigid, closed cell insulation properties and is safe and affordable.

Figures 4.1 and 4.2 illustrate the dimensions of a drink bottle: they are considered for determining the space (total area) that the 'bottle' can occupy.

* 77 x 6 columns = 462 mm (L)
* 77 x 4 columns = 308 mm (W)
* 230 x 2 rows = 460 mm (H)

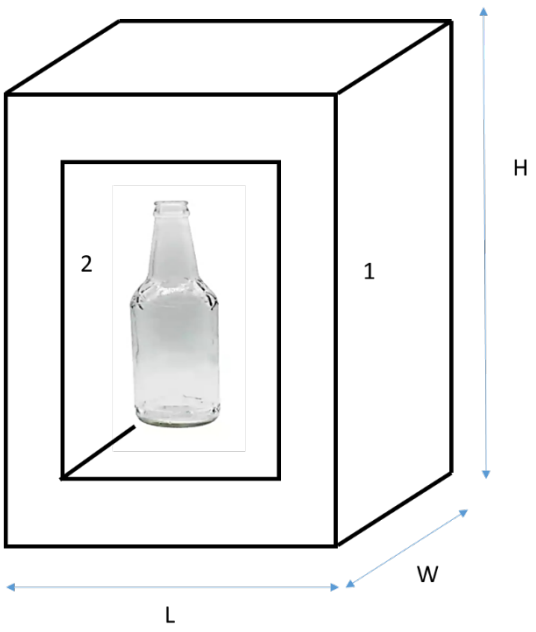

Figure 4.1: Cooling structure unit

Figure 4.2: Illustration of the cooling product's dimensions

- Cabinet size

  Let's take the notation '1' for the outer cabinet and '2' for the inside one (from Figure 4.2 above); therefore, the dimensions of the units are as follows:

  * Outside cabinet
    600 (H_1) x 600 (L_1) x 450 (W_1) mm
    Outside Volume V_o = 0.162 m³
    Total Area A_o = 1.8 m²
    Insulation thickness = 50 mm

  * Inside cabinet
    500 (H_2) x 500 (L_2) x 350 (W_2) mm
    Inside Volume V_i = 0.0875 m³
    Total Area A_i = 1.2 m²
    Capacity = 30 Liters

4.3.2 Heat load in cooling unit

A refrigeration load is measured by the heat units absorbed by the refrigerant while passing through the evaporator. With respect to a cold unit, this load consists of the following items:

i. Heat leakage
ii. Product load
iii. Infiltration load
iv. Miscellaneous loads

4.3.2.1 Heat leakage

Also called 'transmission' load, heat leakage is the heat that leaks through walls, floors, ceilings, glass roofs and other surfaces. Determined by means of a formula, it depends on the type and thickness of the insulation material used. The formula for heat leakage is as follows:

$$Q = U \times A \times \Delta T \quad (4.1)$$

Where, Q = Heat gain (W)
U = Overall Heat Transfer coefficient (W/m² K)
A = Area (m²)
ΔT = Temperature gradient through walls (°C)

The overall heat transfer can be calculated by this equation:

$$U = \frac{1}{\frac{1}{h_0} + \frac{x}{k} + \frac{1}{h_i}} \quad (4.2)$$

With, h = Convection heat transfer coefficient (W/m² K)
k = Conduction heat transfer coefficient (W/m K)
x = Wall thickness (m)

As mentioned above, the unit consists of three different materials. Tabulated data of the conduction heat transfer coefficient 'K' for the specific materials are furnished in Table 4.1.

Table 4.1: Values of K

Material Type	Thickness (m)	k (W/m K)
HDPE Sheet	0.003	0.50
EPS Foam	0.025 0.050 0.075	0.033
Aluminium Sheet	0.002	205

The analysis of the convection boundaries 'h' depends on the temperature distribution and direction of air. It can be calculated using the following formulae:

$$Nu = L \times h / k \quad (4.3)$$

With, Nu = Nusselt Number
L = Length (m)
k = Bulk temperature (°C)

h = Convection coefficient (W/m² K)

4.3.2.2 Product load

Product load, the heat emitted from the product to be cooled, is to be determined in two steps as follows:

∴ Sensible heat load: The amount of heat removed from the product to reach the desired cooling temperature. The formula is as follows:

$$Q = m \times c_p \times \Delta T \quad (4.4)$$

With, Q = Heat removal (kJ)
m = Mass of the product (kg)
c_p = Specific heat capacity of the product (kJ/kg °C)
ΔT = Temperature difference (°C)

∴ Respiration load: The amount of heat generated by living foods. That is why they are being cooled to slow down deterioration and lengthen preservation. This is found by the equation:

$$Q = \frac{10.7f}{3600} \times \left(\frac{9\theta}{5} + 32\right)^g \quad (4.5)$$

With, Q = Heat of respiration (W/kg)
f, g = Respiration coefficients
θ = Average temperature (°C)

The respiration load has been assumed to be zero in the cooling system simply because the products being stored are non-living products. In the heating system, the effect will be minimal on the total heat load since foods (products) will be warmed within a short period.

4.3.2.3 Infiltration load

This is heat caused by the entrance of warm air when the door is open, also termed 'air-change load'. This load is difficult to calculate with accuracy since it is affected by several factors such as the room, the volume and temperature fluctuation. Therefore, an estimated valued will be displayed through calculation, with the equation as follows:

Q = Air changes x Volume x Energy x ΔT (4.6)

With, Air changes = Number of volume changes per day
Volume = Volume of the cold compartment
Energy = Energy per cubic meter per degree Celsius

4.3.2.4 Miscellaneous load

Often referred to as the service loads, these types of loads cannot easily be calculated. They consist of heat from several sources, such as that generated by electrical equipment, motors and lamps in addition to heat from people (the heat load from people will be neglected). A safety factor of 10% is considered in the calculation since they appear more complex, and more importantly, to avoid incompatibility between the design criteria and the actual operation. Since the output voltage of a compressor is always regulated to 12V, a 12V fan must be used for a 12V power supply system. Thus, a DC fan motor with the following specifications is to be used for the system.

- Power: 2W
- Voltage: 12V
- Air flow: 1.46 m^3/min
- Type: Tube axial
- Operating temperature: -10° to 70°C

4.3.2.5 Temperature determination

When designing a refrigeration system and finding the total heat load of a system, the temperatures are often taken as the starting point. In this study, the highest ambient temperature during summer is considered for the heat load calculation because in winter the effect of heat load is negligible. Therefore, the ambient temperature is taken as 32°C, and 7°C is the average temperature of the refrigerated space (inside temperature).

Note: 32°C is the recommended design temperature for Cape Town; occasionally 42°C could be taken from the weather station for some cases on the hottest days (Kanyarusoke et al., 2016).

4.3.3 Heat load calculation

This segment of the chapter deals with refrigeration load calculations for the custom-made cooling unit. In this connection, the scheming is as follows.

4.3.3.1 Heat leakage

As explained in the above subsection, heat leakage through walls can be estimated with fair accuracy. The entire process will be based on the illustration in Figure 4.3 below.

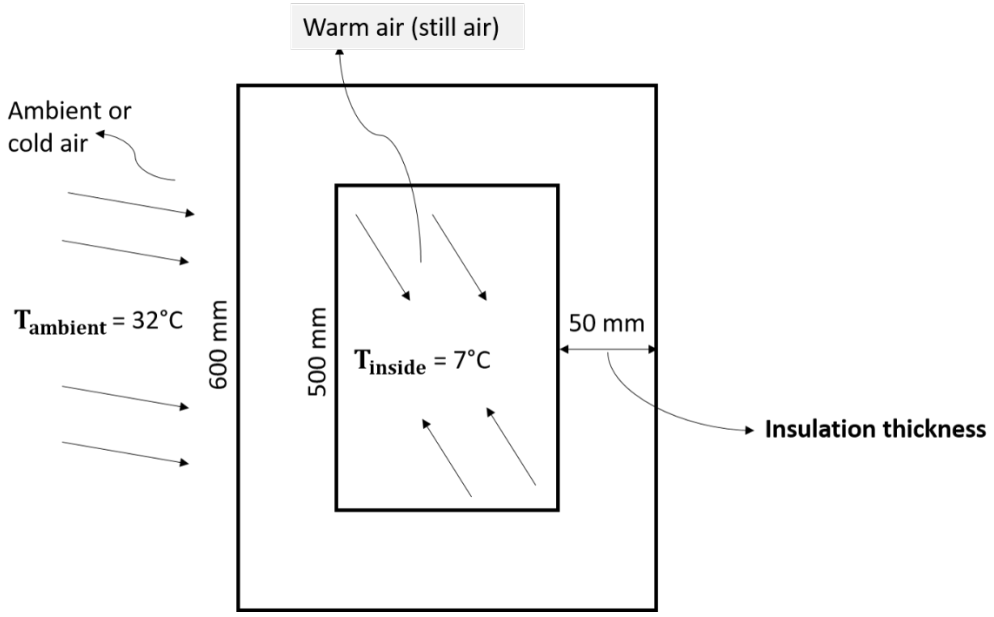

Figure 4.3: Illustration of heal-load parameters

- Convection heat transfer coefficient 'h'

Since the inside convection coefficient is taken based only on the surface type and the outside one is affected by the moving air at a certain velocity, therefore, 'h' is calculated differently.

a. h_{inside} (For height H = 500 mm)

Film temperature T_f = 19.5°C (292.65K)

Temperature difference $\Delta T = 25°C$

Prandtl number Pr = $Pr = \mu \times \frac{C}{k} = 0.706$

Where, $\mu =$ fluid viscocity
C = fluid specific heat
K = fluid thermal conductivity

Grashof number Gr = $L^3 \times \rho^2 \times g \times \Delta T \times \frac{\beta}{\mu^2} = 469585797$

Where, $\rho =$ fluid density
g = gravitational acceleration
$\beta =$ fluid thermal expansion coefficient

Rayleigh number Ra = $Gr \times Pr = 331443316$

Nusselt number Nu = 70.02

From Equation 4.3, the inside convection coefficient $h_{inside} = 3.5\ W/m^2K$

b. Wind convection coefficient $h_{outside}$

When free or natural convection occurs on surfaces or plates exposed to the outside wind (moving air), Equation 4.3 is not applied because the 'free convection' in this case depends on certain factors, among which are flow properties such as wind velocity, viscosity and other flow and temperature-dependent properties. McAdams (1954) provides the equation for finding the convection coefficient which includes the effects of free convection as well as radiation.

$$h = 5.7 + 3.8v \qquad (4.7)$$

Where, v = relative speed between object surface and air (m/s)

However, assuming an average wind speed of 22.2 km/hr or 6.167 m/s at Bellville weather station (Cape Town, SA),

$$h = 5.7 + 3.8 \times 6.167 = 29.1346\ W/m^2K$$

Therefore, the outside convection coefficient $h_{outside} = 29.135\ W/m^2K$

- Overall heat transfer coefficient 'U'

The basic equation for the 'U' is as in as Equation 4.2; but since the cooling unit has three different type of material – high density polyethylene (HDPE), expanded polystyrene (EPS) and aluminium – Equation 4.2 changes into 4.2' as follows:

$$U = \frac{1}{\frac{1}{h_o} + \frac{x_{HDPE}}{k_{HDPE}} + \frac{x_{EPS}}{k_{EPS}} + \frac{x_{Al}}{k_{Al}} + \frac{1}{h_i}} \qquad (4.2')$$

However, in this study, aluminium will not be considered simply because its thermal conductivity (k) is higher than other materials. Therefore, in removing aluminium, Equation 4.2' becomes,

$$U = \frac{1}{\frac{1}{h_o} + \frac{x_{HDPE}}{k_{HDPE}} + \frac{x_{EPS}}{k_{EPS}} + \frac{1}{h_i}} \qquad (4.2'')$$

From Table 4.1 and Equation 4.2'', the value of U is displayed in Table 4.2 with respect to insulation thickness.

Table 4.2: Value of U

Insulation thickness	**$x_{EPS} = 0.025$ m**		**$x_{EPS} = 0.050$ m**		**$x_{EPS} = 0.075$ m**	
Parameters	k_{EPS}	0.033 W/m K	k_{EPS}	0.033 W/m K	k_{EPS}	0.033 W/m K
	x_{HDPE}	0.003 m	x_{HDPE}	0.003 m	x_{HDPE}	0.003 m
	k_{HDPE}	0.50 W/m K	k_{HDPE}	0.50 W/m K	k_{HDPE}	0.50 W/m K
	hi	3.5 W/m² K	hi	3.5 W/m² K	hi	3.5 W/m² K
	ho	29.135 w/m²k	ho	29.135 w/m²k	ho	29.135 w/m²k
U value	**0.923 W/m² K**		**0.543 W/m² K**		**0.385 W/m² K**	

After evaluating the U value for the leakage load, the desired heat transfer coefficient for this process is 0.543 W/m² K taken with an average insulation thickness of 50 mm (parameters highlighted in red) because the more thickness, the more material is needed and therefore the cost escalates as well. Within the cost scope of this project, 50 mm of insulation thickness seems affordable.

- Overall area 'A'

The overall area is presumably the outside area and is determined as follows:

a. Side surfaces: 2 x 0.6 x 0.45 = 0.54 m²
b. Back and front surfaces (including the door): 2 x 0.6 x 0.6 = 0.72 m²
c. Top and bottom surfaces: 2 x 0.45 x 0.6 = 0.54 m²

The total area is assumed to be 0.48 + 0.6 + 0.4 or 1.8 m²

- Heat leakage load 'Q'

Since the cooling compartment is to be kept at 7°C with an ambient temperature of 32°C, the temperature difference is 32°C - 7°C or 25°C, and the thickness of the EPS foam is 50 mm. After the overall heat transfer coefficient is determined, the heat leakage through the surfaces can readily be determined by the application of Equation 4.1.

Q = 0.543 x 1.8 x 25 = 24.435 W

The system is estimated to be working on a 10-hour basis; therefore, the heat leakage in this cooler for 10 hours will be 24.435 x 10 x 3600 = 879.660 kJ.

4.3.3.2 Product load

The product cooling load depends on the temperature of the product to be cooled. The 500 ml Coca-Cola bottle is assumed to be at room temperature initially before being placed into the cooling compartment for the cooling process to occur. Three drinks are carefully chosen to determine the product load and based on *ASHRAE Handbook: Refrigeration.* For this system, only water was selected as reference in the cooling load analysis due to its high specific capacity (see Table 4.3 below). Table 4.4 provides brief information on the cooling product selected.

Table 4.3: Specific heat capacity 'c_p' of selected drinks

Drinks	Specific heat capacity c_p
Orange juice	1.730 kJ/kg K
Water	4.187 kJ/kg K
Cream soda	1.790 kJ/kg K

Table 4.4a: Product specifications (water)

Water specifications	
Product volume	500 ml
Specific heat capacity	4.187 kJ/kg K
Quantity	2 x 24 = 48 bottles
Unit Mass of product	0.56 kg
Room temperature	25°C
Inside temperature	7°C

It is important to consider the mass of the packaging of the water when calculating the product load because not only the liquid but also the packaging (in this case glass bottle) is being cooled to 7°C.

Table 4.4b: Product specifications (packaging)

Packaging specifications	
Product name	Glass
Specific heat capacity	0.8 kJ/kg K
Quantity	2 x 24 = 48 bottles
Unit Mass of product	0.4 kg
Room temperature	25°C
Inside temperature	7°C

As summarised in Table 4.4 (a and b) above, the product load is therefore obtained with the help of Equation 4.4, by adding the product load of both water and glass.

Q_{water} = 2 x 24 x 0.56 x 4.187 x (25-7) = 2025.83808 kJ
Q_{glass} = 2 x 24 x 0.4 x 0.8 x (25-7) = 276.48 kJ
$Q_{product}$ = 2025.83808 + 276.48 = 2302.31808 kJ

4.3.3.3 Infiltration load

This occurs when the door opens so there is a transfer of heat into the space through the air. To determine the air change load for the present study, the following estimations need to be addressed.

a. Volume: The volume of the cooling unit is calculated at 0.5 x 0.5 x 0.35 or 0.0875 m³.
b. Air change: 12 volume air changes per day due to the door being open.
c. Energy: Each cubic meter of new air is assumed to provides 1.2 kJ / °C.
d. Temperature difference: The temperature difference is to be at 25°C.

Applying Equation 4.6, the infiltration load is found to be:

Q = 12 x 0.0875 x 1.2 x 25 = 31.5 kJ

4.3.3.4 Miscellaneous load

The evaporator fan will be used for about two hours to cool down the heat produced by the compressor. Therefore, the power is 2W x (2x3600) or 14.400 kJ.

4.3.3.5 Cooling load

From the foregoing calculations, it follows that the total 10-hour load is obtained by summing up the heat leakage load, product cooling load, infiltration load and miscellaneous load, as shown in Table 4.5.

Table 4.5: Cooling load summary

S. No	Description	Heat load calculation (kJ)
1	Heat leakage load	879.660
2	Product load	2302.31808
3	Infiltration load	31.5
4	Evaporator fan load	14.4
5	**Cooling heat load**	**3227.87808**

4.3.3.6 Safety factor

A safety factor is then applied to the total cooling load to account for errors and variations from the design. It is typical to add 10 to 30% onto the calculation to cover this; the current cooling system assumes 10%.

Total Cooling load = 1.1 x 3213.47808 = 3550.665888 kJ

4.3.3.7 Refrigeration capacity

If a four-hour period is allowed for the cooling process of most domestic refrigerators, in this manner the cooling process will take only two hours per day to cool the temperature of the beverage to the desired temperature of 7°C.

By consequent, Q_{Ref} = 3550.665888 / (2 x 3600) = 493.1 W or 493 W

The refrigeration capacity will decide the value of the compressor displacement volume, design of the heat exchanger volume and the resistance value of the expansion valve.

4.3.3.8 Mass flow rate of the refrigerant

At this point, it is important to determine the operating values of the refrigerated system such as temperature and pressure at the evaporator and condenser as well as the enthalpies at each

respective point of actions (refer to Figure 3.4 in Chapter 3). From the thermodynamics properties chart of refrigerant R-134a, the following values were found.

Table 4.6: Design parameter of R-134a system

State	Parameter	Value
Evaporator, Tev = -2°C	Psat = Pev	272.36 kPa
	s1	0.93253 kJ/kg K
	h1 = hg	249.28 kJ/kg
Compressor	P2	1.3199 MPa
	s1 = s2	0.93253 kJ/kg K
	h2 = hsup	287.29 kJ/kg (by interpolation)
Condenser, Tcond = 50°C	P3 = P2	1319.9 kPa
	h3 = hf	123.49 kJ/kg
Throttling	P4 = Pev	272.36 kPa
	h4 = h3	123.49 kJ/kg

The suggested refrigeration capacity is considered to be the heat extracted from the cooling space, also called '$Q_{Evaporator}$'. With reference to the steady-state equation where kinematic and potential energy are assumed to be negligible,

- Mass flow rate '$\dot{m}$' $= \frac{Q_{Ev}}{h_1 - h_4}$ (Taking $Q_{Ev} = 493$ W)

  $= \frac{493}{(249.28 - 123.49)\text{x } 1000} = 0.0039$ kg/s

- Compressor power 'W_{in}' $= \dot{m}$ x $(h_2 - h_1)$

  $=$ 0.0039 x (287.29 – 249.28) = 148.2 W or 148 W

- Condensing capacity 'Q_{Cond}' = $\dot{m}$ x $(h_2 - h_3)$

  $=$ 0.0039 x (287.29 – 123.49) = 638.8 W or 639 W

4.4 Heating design calculation

4.4.1 Heating cabinet structure

The heating casing consists of some type of heat-trapping enclosure which takes the form of a box made of polycarbonate sheet. The insulating material allows warming temperature to reach similar levels on cold and windy days as on hot days, as well as have the added benefit of blocking any heat leakages that could potentially seep through and lower the heat of the casing.

Polycarbonate is the material of choice for demanding applications, although as transparent as glass and less than half the weight, polycarbonate is virtually unbreakable. It is ideal for glazing as it can be cold bent, easily fabricated and formed. The material also allows for high light transmission and blocks harmful UV radiation.

Plain air is used as an insulator to trap and retain the acquired heat from the sun's rays. Of course, the air itself has to be stabilised by containing or trapping it to form a pocket between the inner and outer surfaces of the casing (moving air will not act as an insulator).

Input data:
The dimensions of the casing are as exact as the cooling cabinet.

* Outside casing
  600 (H_1) x 600 (L_1) x 450 (W_1) mm
  Outside Volume V_o = 0.162 m³
  Total Area A_o = 1.8 m²
  Insulation thickness = 50 mm of air gape

* Inside casing
  500 (H_2) x 500 (L_2) x 350 (W_2) mm
  Inside Volume V_i = 0.0875 m³
  Total Area A_i = 1.2 m²
  ***Featuring food trays to put foods on it

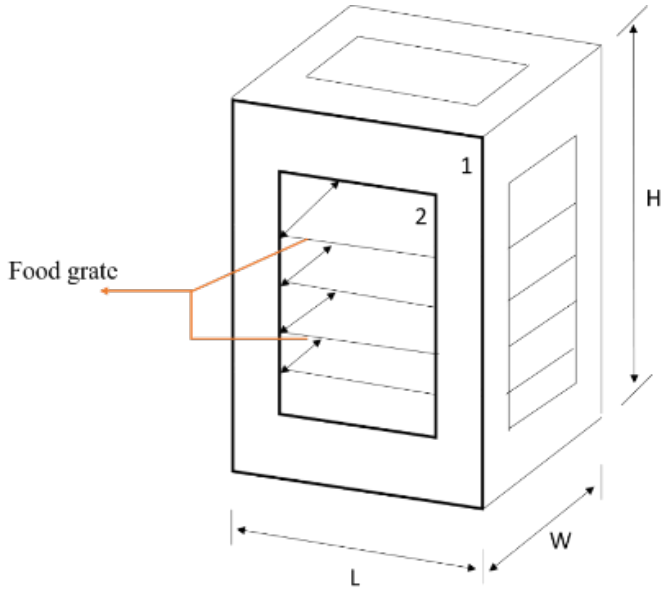

Figure 4.4: Illustration of the heating casing

4.4.2 Heat load in heating unit

The heating load is the amount of heat energy that would need to be added to a space to maintain the temperature at an acceptable range. Indeed, as in the cooling system, the heating load consists of the leakage load, the product load, the air infiltration load and the miscellaneous load.

4.4.3 Heat load calculation

The determination of the heat load occurs by using the same procedure and applying the exact equations as in the cooling load calculation.

4.4.3.1 Leakage load

The basic equation for finding the heat leakage load is '$Q = U \times A \times \Delta T$'. From this point, it is also important to determine the overall heat transfer coefficient 'U', the total area 'A' as well as the temperature difference 'ΔT' to find an accurate leakage load.

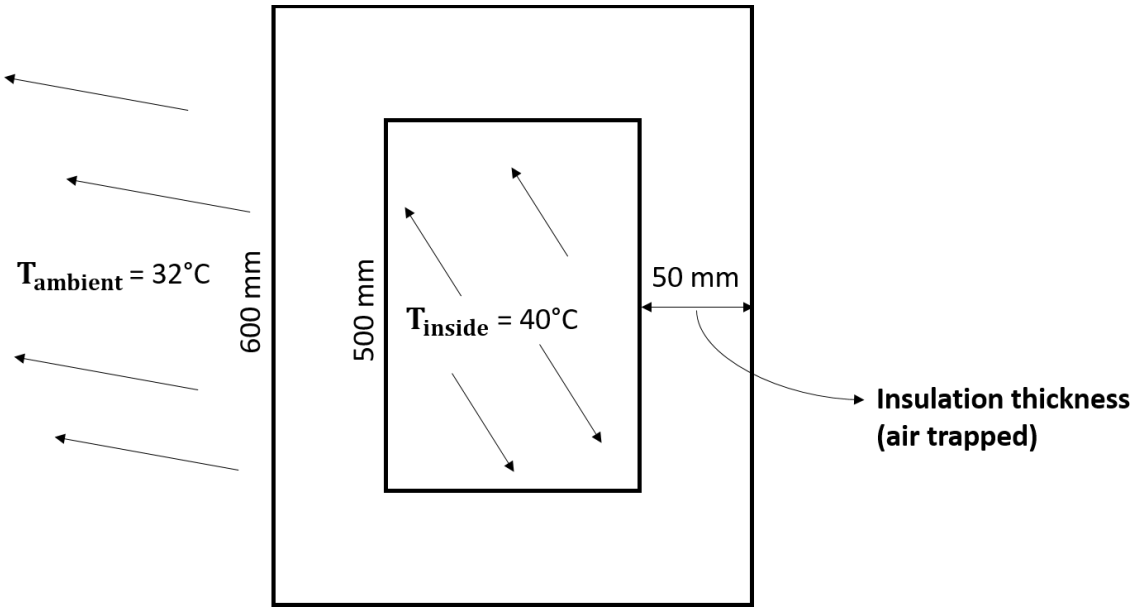

Figure 4.5: Leakage load input data

Table 4.7 below displays technical information on the type of material used for the heating casing, since the leakage load is entirely emitted through the surfaces of the casing.

Table 4.7: Material specifications

Material	Thickness (m)	K value (W/m.K)
Polycarbonate 'PC'	0.003	0.21
Air	0.050	0.026766 (@ 32°C)

Using Figure 4.5 and Table 4.7 above,

- Convection heat transfer coefficient 'h'

  a. h_{inside} (For height H = 500 mm)

Film temperature T_f = 36°C (309.15K)

Temperature difference $\Delta T = 8°C$

Prandtl number Pr = $\Pr = \mu \times \frac{C}{k} = 0.702$

Grashof number Gr = $L^3 \times \rho^2 \times g \times \Delta T \times \frac{\beta}{\mu^2} = 117170340$

Rayleigh number Ra = Gr × Pr = 82257092

Nusselt number Nu = 49.59

From Equation 4.3, the inside convection coefficient $h_{inside} = 2.6\ W/m^2K$

b. Wind convection coefficient $h_{outside}$

Assuming the same conditions as in the cooling system since both units are subjected to the same ambient temperature (32°C) and wind speed (6.167 m/s).

So, from Equation 4.7, the outside convection coefficient $h_{outside} = 29.135\ W/m^2K$

- Overall heat transfer coefficient 'U'

  Using Equation 4.2' as such, $$U = \frac{1}{\frac{1}{h_o} + \frac{x_{PC}}{k_{PC}} + \frac{x_{Air}}{k_{Air}} + \frac{x_{PC}}{k_{PC}} + \frac{1}{h_i}}$$

  The overall U in this case is equalled to

  $$U = \frac{1}{\frac{1}{29.135} + \frac{0.003}{0.21} + \frac{0.050}{0.026766} + \frac{0.003}{0.21} + \frac{1}{2.6}} = 0.431.86\ w/m^2k$$

- Total area 'A'

  The total area is taken as the total outside area of the casing and equalled to 1.08 m². The intermediate calculations are shown below:

  a. Side surfaces: 2 x 0.6 x 0.45 = 0.54 m²
  b. Back and front surfaces (including the door): 2 x 0.6 x 0.6 = 0.72 m²
  c. Top and bottom surfaces: 2 x 0.6 x 0.45 = 0.54 m²

  The total area is assumed to be 0.54 + 0.72 + 0.54 or 1.8 m²

- Heat leakage load 'Q'

  Since the heating space is to be maintained at 40°C with an ambient temperature of 32°C, the temperature difference is 40°C - 32°C or 8°C; and a 50 mm air gape used as an insulator. After the preliminary calculations, the heat leakage through the surfaces can readily be determined by the application of Equation 4.1.

  Q = 0.432 x 1.8 x 8 = 6.2208 W

  By working on a 10-hour basis, the leakage load will then be 6.2208 x 10 x 3600 = 223.9488 kJ or 224 kJ.

4.4.3.2 Product heating load

The product selected in the case of heating are potatoes in the form of French fries and meat sausages in the form of chilli bites. Specifications are provided in Table 4.8.

Table 4.8: Product specifications

Parameters	Potatoes	Meat sausages
Quantity	1	1
Unit Mass	5 Kg	5 Kg
Specific capacity 'c_p'	3.43 kJ/Kg °C	0.56 kJ/Kg °C
Room temperature	40°C	40°C
Ambient temperature	32°C	32°C

- Sensible heat load
  From Equation 4.4, $Q_{Potatoes} = 5 \times 3.43 \times 8 = 137.2$ kJ

$$Q_{Sausages} = 5 \times 0.56 \times 8 = 22.4 \text{ kJ}$$

- Respiration load
  The respiration load should be considered in the calculation because the products chosen (potatoes and meat) are living organisms and therefore should be stored carefully to prevent not only loss of weight but also loss of quality. In general, weight loss and shrink occur only for long term storage (about one to two weeks) if it is not cooked; but in the case of hot (cooked) foods, it takes hours or days (depending on the type of food) to see moisture loss.

  With that said, since in this case the storage time is limited to only 10 working hours per day, the respiration load is considered negligible and the effect on the total heating load insignificant.

  However, the total product load is 137.2 + 22.4 or 159.6 kJ.

4.4.3.3 Infiltration load

To determine the air change load, the following assumptions are made.

a. Volume: The volume of the heating unit is calculated at 0.5 x 0.5 x 0.35 or 0.0875 m^3.
b. Air change: 12 volume air changes per day due to the door being open.

c. Energy: Each cubic meter of new air is assumed to provide 1.25 kJ / °C.
d. Temperature difference: The temperature difference is at 8°C.

Applying Equation 4.6, the infiltration load is found to be,

Q = 12 x 0.0875 x 1.25 x 8 = 10.5 kJ

4.4.3.4 Heating load capacity

The total 10-hour load is obtained by summing up the heat leakage load, product load and infiltration load as follows:
224 + 159.6 + 10.5 = 394.1 kJ

Adding 10% safety factor to compensate some errors

Total heating load = 1.1 x 394.1 = 433.51 kJ

If a time period of 10 to 15 minutes is allowed to raise and retain the heat within a considerable temperature of 40°C, the amount of heat to be added is:

433.51 / (15 x 60) = 481.68 W

Plus, 2W of the energy produced by the evaporator fan, 481.68 W + 2W = 483.68 W.

The total heating load is considered as the condensing load capacity of the heating system
Q_{Cond} = 484 W

4.4.3.5 Mass flow rate

Using the same approach and input as in the cooling load calculation,

- Mass flow rate 'ṁ' $= \frac{Q_{Cond}}{h_2 - h_3}$ (Taking $Q_{Cond} = 484$ W)
  $= \frac{484}{(287.29 - 123.49) \text{ x } 1000} = 0.003$ kg/s

- Compressor power 'W_{in}' $= \dot{m} \text{ x } (h_2 - h_1)$
  $= 0.003 \text{ x } (287.29 - 249.28) = 114$ W

- Evaporating capacity 'Q_{Ev}' $= \dot{m} \text{ x } (h_1 - h_4)$
  $= 0.003 \text{ x } (249.28 - 123.49) = 377.4$ W

4.5 Discussion of results

All design parameters of both cooling and heating systems by using refrigerant R-134a are summarised in Table 4.9.

Table 4.9: Cooling system vs heating system

PARAMETERS	HEATING		COOLING	
Leakage load	224	kJ	879.7	kJ
Product load	159.6	kJ	2302.3	kJ
Infiltration load	10.5	kJ	31.5	kJ
Miscellaneous load	14.4	kJ	14.4	kJ
Total heat load	433.5	kJ	3550.7	kJ
Refrigeration capacity	377.4	W	493	W
Condensing capacity	484	W	639	W
Compressor	114	W	148	W
Mass flow rate	0.003	Kg/s	0.0039	Kg/s

Based on the data gathered from Table 4.9, here are some allocations:

- The compressor is the most important component of this design since the two systems share the same power. Indeed, based on the above information, 148 W and 114 W (cooling and heating respectively) are close enough and therefore 148 W will be used throughout the component design calculation. Then a reasonable motor power (more precise) will be selected in the catalogues of compressors conforming to the two systems and while having a mass flow of approximately 0.0039 kg/s (since the difference between the two systems is quite small).

- The difference in the capacity of the heat exchangers for the two systems ($Q_{Condenser}$ and $Q_{Evaporator}$) is not that big, but also provides a not quite similar "Win" variant. For these reasons, considering a compressor power which has a higher capacity than what was found in the calculations, the unit will operate and achieve the desired performance.

- The overall heat transfer coefficient “U” is affected by the type of materials, available space, temperature conditions and direction of flow (wind speed); therefore, it should be different since the two systems are not similar.

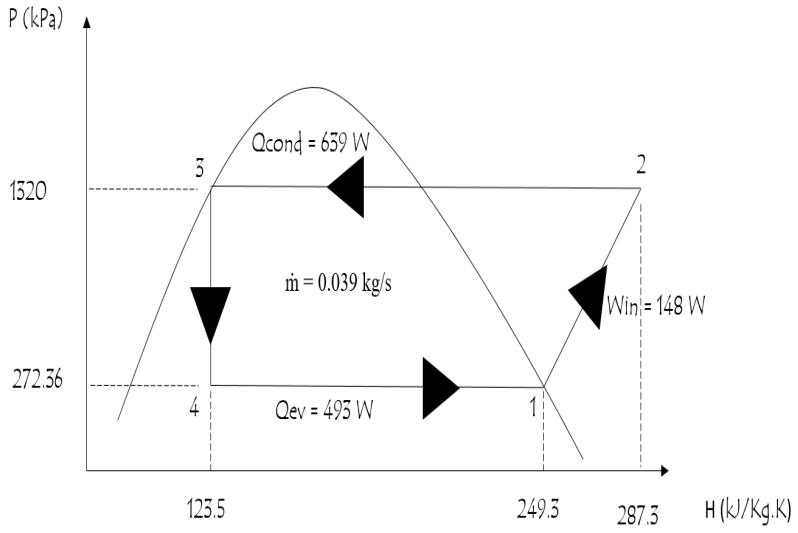

Figure 4.6: p-h diagram of the selected system

Therefore, the coefficient of performance (COP) of the system is found as follows:

a. COP of refrigeration
   From Equation 3.5, COP = $\frac{493}{148}$ = 3.32

b. COP of heat-pump
   From Equation 3.6, COP = $\frac{639}{148}$ = 4.32

The system demonstrates good overall efficiency; under normal conditions, the COP is about 3.32 and 4.32 for the cooling and heating systems, respectively.

4.6 Design of components

This section presents a systematic design analysis of the main components – including the compressor, the evaporator, the condenser and the expansion valve – along with other several components that must be matched to each other to complete the system.

The following factors (see Figure 4.7) should be considered when designing the system components.

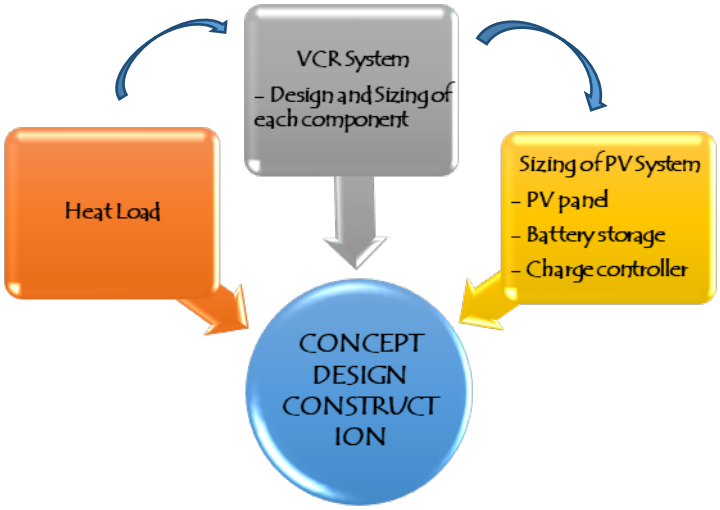

Figure 4.7: Concept study

4.6.1 Compressor

The power demand of the cycle depends strongly on the temperature at which cooling is required, the temperature at which the refrigerant is condensed and the type of refrigerant used (Asma, 2017). The function of the compressor in the vapour compression refrigeration cycle is to compress the low-pressure superheated vapour leaving the evaporator to the high-pressure condenser inlet state. In this study, a reciprocating type of isentropic compressor is considered.

Figure 4.8: 12V DC compressor

The compressor is regarded as the heart of the VCR cycle, designed to handle peak load despite variations of load (from summer to winter, in accordance with the number of warm products or chilled or opening of the doors). Its design is critical in obtaining the necessary level of

refrigeration performance. It is important to select a compressor capacity with a somewhat greater capacity than the total heat load to avoid overloading the compressor motor.

By considering calculated refrigeration capacity of the cooling system 'Q̇ref/ev = 493 W', enthalpy value at the inlet and outlet of the evaporator (h_1 and h_4) as well as an amount of 0.004 kg/s of mass flow rate of refrigerant R-134a allowed in the system, a DC compressor is selected to encounter more than the cooling capacity calculated in the previous section. The more suitable one has the following specifications (Table 4.10) and see appendix A-1.

Table 4.10: Technical specification of the compressor unit

Specifications	Description
Compressor rotation	2000 – 3500 rpm
Cooling capacity	149 – 186 W
Power supply	12V DC
Refrigerant	R-134a
Displacement	2.5 cm³
Working current	2.2 – 9A
Net weight	4.6 Kg

4.6.2 Heat exchangers evaporator

Heat exchangers are devices that facilitate the exchange of heat between two fluids that are at different temperatures while keeping them from mixing with each other. Therefore, in this research, the evaporator and condenser are taken as heat exchangers and are designed as air coolers and heaters based on the convection heat exchange. The data used in the design calculation of heat exchangers are taken from the cooling system since they are recorded to perform well for both cooling and heating systems.

- Evaporator

The design procedure of an evaporator coil is as follows:

Given: $\mathbf{Q_{Evaporator} = 493\ W}$

T_{Ev} = -2°C

Assume: $T_{Air\ in}$ = 32°C and $T_{Air\ out}$ = 5°C

θ_1= 32 - (-2) = 34°C and θ_2= 5 - (-2) = 7°C

LMTD = (34-7) / ln($\frac{34}{7}$) = 17.084°C

∴ Applying Equations 4.2 and 4.3 on pipes in series,

@ Pipe dimeter Φ: 6 mm

Film temperature T_f = 1.5°C (274.65K)
Temperature difference $\Delta T = 7°C$

Prandtl number Pr = $\Pr = \mu \times \frac{C}{k} = 0.711$

Where, μ = fluid viscocity
C = fluid specific heat
K = fluid thermal conductivity

Grashof number Gr = $L^3 \times \rho^2 \times g \times \Delta T \times \frac{\beta}{\mu^2} = 303$

Where, ρ = fluid density
g = gravitational acceleration
β = fluid thermal expansion coefficient

Rayleigh number Ra = Gr × Pr = 215

Nusselt number Nu = 1.92

From Equation 4.3, the outside convection coefficient $h_{outside} = 7.7\ w/m^2k$

From Equation 4.2, the overall heat transfer coefficient U = 7.7 w / m² k

$A_s = \frac{Q_{Ev}}{U \times \Delta T_{LMTD}} = \frac{493}{7.7 \times 17.084}$ = 3.75 m²

A similar calculation is carried out for the pipe diameter Φ of 8 mm and the remaining design calculation of the condenser coil.

@ Pipe diameter Φ: 8 mm, U = 6.8 w / m² k

$A_s = \frac{Q_{Ev}}{U \times \Delta T_{LMTD}} = \frac{493}{6.8 \times 17.084}$ = 4.24 m²

- Condenser

The condenser is a tube coil connected to the outlet of the compressor; its function is to reject heat from the compressed fluid. Its design procedures are as follows:

Given: $Q_{Condenser}$ = 639 W

T_{Cond} = 50°C

Assume: $T_{Air\ in}$ = 20°C and $T_{Air\ out}$ = 45°C

θ_1= 50 - (20) = 30°C and θ_2= 50 - (45) = 5°C

LMTD = (30-5) / ln($\frac{30}{5}$) = 14°C

∴ Applying Equations 4.2 and 4.3 on pipes in series,

@ Pipe diameter Φ: 6 mm, U = 8.3 w/m²k

$$A_s = \frac{Q_{Cond}}{U \times \Delta T_{LMTD}} = \frac{639}{8.3 \times 14} = 5.5\ m^2$$

@ Pipe diameter Φ: 8 mm, U = 7.3 w/m²k

$$A_s = \frac{Q_{Cond}}{U \times \Delta T_{LMTD}} = \frac{639}{7.3 \times 14} = 6.3\ m^2$$

Note: Dimensions of the length for the evaporator and condenser coil are taken for η-tubes; to get the length of a single tube, take the actual dimension and divide it by the number of tube (e.g., for 12 tubes, L = 16 m; therefore, for a single tube, L = 16/12 or 1.33 m).

As demonstrated in the design calculation above, it is important to only consider the higher value for condenser and evaporator capacity to select the most suitable heat exchangers. It is concluded that with 493 W and 639 W of capacity (evaporator and condenser respectively), the system provided areas at pipe diameters of 6 and 8 mm, so the optimum sizes of the condenser and evaporator coils will be selected within those limits.

4.6.3 Capillary tube

The capillary tube is a device in the form of a small orifice fitted between the condenser and evaporator, and which reduces suddenly the pressure and temperature of the refrigerant due to

friction. It is one of the commonly used throttling devices serving almost all small refrigeration systems.

The capillary tube is selected by its length and diameter; so, the specifications are as follows:

- ✓ Capillary tube ID (in): 0.91 mm (0.036”)
- ✓ Capillary tube Length (in): 2.30 m (90.6”)
- ✓ Material: Copper

4.6.4 System piping

Piping is an important part of refrigeration systems. The incorrect design and sizing of the refrigerant pipe could result in faulty operations or even damage to the refrigeration system. The properties of the different piping types have a direct effect on the constructive design. In long pipelines, a low-pressure loss must be ensured in particular; in piping with vaporous refrigerant, the safe transport of oil must be guaranteed. Cold or hot refrigerant must be equipped with insulation to prevent heat loss or condensation on the surface.

- *The suction line:* Of the major sections of line, the suction line is the most critical to size properly. Generally, the suction line is sized for a minimum velocity to ensure good oil return to the compressor. Incorrectly sizing the suction line can lead to oil return problems or a reduction in the system’s capacity. If the pipe chosen is too large, for example, the velocity of the refrigerant flow will be reduced since it helps to push the oil along the suction line. Alternatively, if it is too small, oil return will not be a problem; however, there may be an excessive pressure drop through the suction line which will reduce the system’s capacity.

- *The discharge and liquid lines:* These lines are also important to size correctly size. However, in the discharge line, the refrigerant is traveling at a higher velocity, the oil is pushed along, and the pipe size is not as critical. In the liquid line, since the refrigerant is in its liquid form, it tends to mix well with the refrigerant and is carried along easily.

Pressure differences in the refrigerant pipes have an undesired effect on the boiling temperature of the refrigerant and thus on the operation of the system. Pressure differences can be caused by height, differences in liquid pipes, or also by pressure losses in the piping; it is therefore important to dimension the piping correctly.

Here are the specifications for the piping design as tabulated below.

Table 4.11: Refrigerant line sizing specifications

	Tube OD (In)	Tube ID (In)	Velocity (m/s)	ΔP (KPa)	ΔT (°C)
Liquid line (35°C)	4.7625 mm (3/16")	3.2385 mm (0.1275")	0.3	2	0.1
Suction line (10°C)	6.35 mm (1/4")	4.826 mm (0.1900")	11.6	3	0.3
Discharge line (60°C)	4.7625 mm (3/16")	3.2385 mm (0.1275")	6.9	5	0.2

In refrigeration systems, the refrigerant lines are usually made of copper tubing. Copper is an extremely low-temperature material and therefore is particularly suitable for components in a refrigerating system. Copper tubes meet special purity and strength requirements in refrigeration technology.

4.6.5 Refrigerant

The refrigerant flows through all the internal parts of the system, carrying out the cooling effect in the evaporator, absorbing the heat from the substance to be cooled and throwing it to the atmosphere via the condenser.

In this research, another focus point is the refrigerant R-134a, also known as Tetra Fluoro Ethane (CF3CH2F) of a family of H.F.C refrigerant. With the discovery of the damaging effect of C.F.CS and H.C.F.CS refrigerants to the ozone layer, the H.F.C family of refrigerant has been widely used as their replacement. It is now used as a replacement for R-12 C.F.C refrigerant in the area of centrifugal, rotary screw, scroll and reciprocating compressors. It is safe for traditional handling because it is non-toxic, non-flammable and non-corrosive.

4.6.6 Temperature control and energy storage

With a discontinuous energy supply from the sun, it is necessary for a stable temperature that some kind of energy storage is implied, either thermal or battery.

a. Thermal storage system
   - Ice-slurry or cold liquid in separate tank(s)
   - Integrated ice storage
   - Solid matter storage like rock, concrete or pebble bed

b. Battery storage system
   - DC battery bank
   - AC battery bank (with a converter)

The system will use a battery because it is the simplest way for storing the energy and quite commonly used, especially in solar energy.

4.6.7 Solar PV system

A solar PV system includes different components selected according to certain considerations; the main ones – PV panels, charge controllers and batteries banks – are electrically connected to each other.

- A PV module consists of specific number of PV cells connected in parallel to increase current and in series to produce high voltage.
- A charge controller is basically a voltage and current regulator in the PV system to protect batteries from overcharging and completely draining.
- Solar batteries store excess energy for use during cloudy days or at night.

4.6.7.1 PV module

A PV module is an assembly of photo-voltaic cells mounted in a framework for installation and to convert solar radiation directly to direct current (DC) electricity, with sizes ranging from a few watts to hundreds of kilowatts. A collection of PV modules is called a PV panel, and a system of PV panels is an array. There are several types of PV panels sold on the market; the most available are polycrystalline, monocrystalline and black frames panels (Direct, 1986). Monocrystalline PV modules are found to be most suitable in this research study as they have the highest efficiency rate, are space-efficient and last longer (Maehlnm, 2015).

The performance of the PV module is taken at standard test conditions (STC) which means irradiance of 1000 W/m² and module cell temperature of 25°C. The table below displays the electrical characteristics of the monocrystalline PV panel used in this study.

Table 4.12: PV module specifications

PV module	Specifications
Nominal power 'Pmax'	90 W
Maximum power voltage 'Vmp'	18.40 V
Maximum power current 'Imp'	4.90 A
Open circuit voltage 'Voc'	22.40 V
Short circuit current 'ISC'	5.50 A
Maximum System Voltage	715 V
Maximum Series Fuse	10 A

4.6.7.2 Charge controller

A charge controller regulates the direct current (DC) from the solar panels to make sure that the battery doesn't overcharge. It can measure whether the batteries are fully charged and can stop the current from flowing to prevent the battery from permanent damage. Despite the diversity in charge controllers, the ones commonly used in solar energy are the pulse width modulation (PWM) and the maximum power point tracking (MPPT). Both of these adjust charging rates and monitor the battery's temperature to prevent overheating; also, each one has its own advantages. Thus, selection depends on system components, site condition, size of array and load, and cost. The following table compares the two.

Table 4.13: Comparative facts between PWM and MPPT (FDI Creative, 2014).

	Pulse Width Modulation 'PWM'	**Maximum Power Point Tracking 'MPPT'**
Array voltage	PV voltage and battery voltage have to be matched	PV array voltage can be higher than battery voltage
Battery voltage	Good performance in warm temperature and when battery is almost fully charged	It can be operated above battery voltage so that it enhances the performance in cold temperature and when the charge in battery is lower
System size	More suitable in small system	It has capacity to handle more than what the PWM regulator does
PV array sizing method	PV array is sized in Amps based on current produced when the PV array is operating at battery voltage	The temperature compensated Voc of the array should be less than the maximum input voltage of the regulator
Grid connection	Off-grid	Off-grid and on-grid
Cost	Low	High

Since this research is subjected to areas where there is no electricity, and considering the size of the system, PWM have been selected in this experiment.

4.6.7.3 Solar batteries

Solar batteries are essential components of the solar PV system: they store surplus solar power, extend the use of a PV system's generated energy and provide free, sustainable power on a cloudy day or during the night. To build the battery bank, deep cycle batteries are selected over lead-acid batteries because they meet the requirements of this research study.

4.6.8 Methodology of sizing a PV system

In the introduction of solar photovoltaic (PV) clusters for private or commercial operations, a crucial idea is to determine the merits of the site (Franklin, 2017). Identifying the place and position of the panels is a vital step in designing a PV system as the later components will be streamlined to this step. There are a few concepts and tips to keep in mind while performing the site assessment:

a. *Shade analysis:* Shading can be a problem for the solar panels as they decrease the maximum power that can be generated. Several factors contribute to this issue; the most common causes of shade on a solar panel are shade from neighbouring trees and buildings in the area and typical cloudy weather and shade from adjacent solar panels (Solar Choice, 2016).

   While designing a solar PV system, one must investigate these factors thoroughly so that maximum output can be obtained. One of the tools most commonly used is a solar pathfinder which gives the direction of the sun throughout the year and notes how much sunlight any specific area will receive throughout the year (Solar Pathfinder, n.d.). However, for this research, the Bellville campus of CPUT, SA, is the area chosen to build and perform the experiment analysis as it is properly allocated to provide better testing results.

b. *Sun hours:* Sun hours are important to know how much radiance will be required to generate the needed output wattage. This parameter gives the number of hours an area will receive maximum sunlight (Franklin, 2017). With advances in technology, this data is available online for anyone's use, but for this project the data are provided by the weather station on the rooftop of the Mechanical Engineering building (Bellville campus, CPUT) as it gives direct information of the selected area.

c. *Tilt angle*: Tilt angle is the setting of the panels needed to get maximum radiance. Ideally the tilt angle is the latitude of the geographic location. An adjustable panel frame is suggested as the sun hours change with respect to the tilt in winters and summers. Hence for any area, a specific tilt angle is calculated to get the maximum radiance throughout the year for a fixed panel. Also, it is advised to have the panels facing south to get the maximum afternoon sun. A couple of devices are used in the process of finding the tilt angle and radiance that will fall upon panel at that tilt angle, an inclinometer and pyranometer, respectively.

An inclinometer is kept on the panel and the degrees are read to find the latitude of the area as it is perpendicular to the sun's radiations when at the highest point in the sky. A pyranometer measures the solar irradiance that will fall at a given tilt angle, measuring solar irradiance in watts per meter squared (W/m^2) (Franklin, 2017).

The following steps are important for properly sizing the main components for the PV system and thereby getting intended results (Leonics, 2013, adapted from Ayaz, 2020).

4.6.8.1 Power demand

Every device has a fixed power consumption. The total power consumption needed to run this system matches the input power of the compressor and evaporator fan. The sum of these loads is multiplied by 1.3 (energy losses in the system) to find the total watt-hour per day needed from the PV modules. It is an inherent property of any panel to have internal losses; this factor should be kept in mind (Leonics, 2013).

From the technical specifications of the 12V DC compressor and the one for the evaporator fan, the maximum power consumption at evaporator temperature of 0°C and the motor speed of 2500 rpm is 84.8 W plus the 2 W for the evaporator fan equals a total power of 86.8 W.

Therefore,

86.8 x 8 = 694.4 Wh/day, with running time estimated at about 8 hours a day

694.4 x 1.3 = 902.72 Wh/day

4.6.8.2 Solar radiation

South Africa experiences some of the highest levels of solar radiation in the world with the average daily solar radiation between 4.5 and 6.5 kWh/day (www.energy.gov.za). This compares to about 3.6 kWh/day for parts of the United States and about 2.5 kWh/day for Europe and the United Kingdom.

However, the following table gives the annual solar radiation of the Cape Peninsula University of Technology site based on National Renewable Energy Laboratory data collection and a PV watt calculator (NREL, 2016).

Table 4.14: Annual solar radiation at CPUT Bellville campus

Month	Solar radiation (Kwh/m²/day)	Energy (kWh)
January	4.63	442
February	5.19	451
March	6.00	550
April	6.48	584
May	6.67	600
June	5.85	507
July	5.75	514
August	5.66	507
September	5.46	474
October	5.49	497
November	4.99	449
December	4.48	423
Annual average per day	**5.55**	**5.998**

4.6.8.3 PV module sizing

To determine the size of the PV array, the total peak watt produced by the PV module as well as the average solar radiation are important for this segment of design. Data from Tables 4.12 and 4.14 show the total peak watt is 90 W and the average radiation at CPUT Bellville Campus is 5.55 kWh/day.

As in the energy calculation, the total watt-hours have already been determined. To find the wattage of panels as required, it is necessary to divide the total watt hours by the peak watt and average radiation (Leonics, 2013; Makinde *et al.,* 2019; Ayaz, 2020).

By consequent, the number of PV panels required = 902.72 / (90 x 5.55)

= 1.807

The system should be powered by 2 PV panels of 90 watts each.

4.6.8.4 Battery sizing

The battery type recommended for use in a solar PV system is a deep cycle battery; it is specifically designed to be discharged to a low energy level and rapidly recharged or cycle charged, and discharged day after day. Deep cycle battery bank sizing can be one of the more complex and important calculations in a solar system design. The main objective when sizing a battery is to get one that can handle the load coming from the PV panel array. If the battery bank is oversized, the risk is that it will not stay fully charged; if the battery bank is undersized, it may not last through the intended loads as planned.

Here are a few important pieces of information.

a. *Total load appliance:* This is the amount of energy that is to be consumed per day. It is imperative to do a careful evaluation of exactly what loads it needs and for what lengths of time.
b. *Days of autonomy:* This is the number of days of battery back-up, or in other words, it represents the number of cloudy days in a row that might occur and for which the system may need to operate when there is no power produced by PV panels to get the required ampere-hour capacity of deep-cycle battery.
a. *Depth of discharge:* The depth of discharge (DOD) is the limit of energy withdrawal to which the deep cycle battery will be subjected; it is expressed as a percent of total capacity.
b. *System voltage:* The system voltage is typically 12V, 24V or 48V.
c. *Temperature:* Deep cycle battery life and capacity are affected by temperature; unlike PV modules, batteries perform best in moderate temperatures. In fact, the temperature standard for most battery ratings is 77°F; cold temperatures tend to reduce battery capacity while high temperatures tend to shorten battery life. Consequently, it is important to identify the lowest temperatures that the battery will be exposed to and factor this into the calculation using the temperature-factor table below.

Table 4.15: Temperature (°F) factor

°F	Temp-Factor
80+	1.00
70	1.04
60	1.11

50	1.19
40	1.30
30	1.40
20	1.59

Following is a formula that will calculate what size of battery the system should have and the total load that should be converted to amp-hours (Leonics, 2013).

$$\text{Battery Capacity (Ah)} = \frac{\text{Total Watt-hours per day used by appliances x Days of autonomy}}{\text{(Losses x depth of discharge x nominal battery voltage)}}$$

With,

- 0.85 for battery losses
- 1 for depth of discharge

Applying the above formula to size the ideal battery for this system:

- Total appliance = 86.8 x 8 = 694.4 Wh/day
- Nominal batter voltage = 12V
- Battery efficiency = 85%
- Days of autonomy = 2 days
- Depth of discharge DOD = 100%

So,

Battery capacity (Ah) = (694.4 x 2) / (0.85 x 12)
= 136 Ah

The nearest available battery in the market is 105 Ah; therefore, the battery used for the system is rated 12V, 105 Ah for two days of autonomy (Appendix A-2).

4.6.8.5 Charge controller sizing

The solar charge controller is typically rated against amperage and voltage capacities. Select the solar charge controller that matches the voltage of PV array and battery and then identify which type of solar charge controller has enough capacity to handle the current from PV array. According to standard practice, the sizing of a solar charge controller is to take the short circuit current (Isc) of the PV array and multiply it by 1.3.

For this project, a PWM charge controller is used with the following specifications:

- Voltage level of the system: 12V
- Maximum amperage: 10 A

4.7 Conclusion

The purpose of the design analysis was to determine the amount of energy required to operate the entire system. As the calculations (section 4.6.9.3) show, two identical 90 Wp monocrystalline photovoltaic panels (used in previous research by Kanyarusoke, 2017) were sufficient to power the entire system, which led to the selection of the battery as well as the charge controller. At this stage, the design of each component of the vapour compression system to the solar PV system is completed, so construction and experimental testing can take place with the aim of analysing the performance of the hybrid prototype.

CHAPTER 5:
CFD MODELLING OF THE SYSTEM

5.1 Introduction

Chapter 4 has provided a detailed explanation of the design analysis and underlying assumptions of using the system. Subsequently, the indicators used for calculation have also been noted. This chapter now focuses on the CDF development of the hot and cold chamber, detailing the steps taken before construction occurs.

5.2 ANSYS CFD

Ansys computational fluid dynamics (CFD) reproduction software is a complete set of products that permits a prediction of the influence of fluid flows on product during design and manufacturing as well as through end use. The software's unmatched fluid flow analysis skills are used to design and optimise new equipment capable of troubleshooting already existing connections. Any fluid flow phenomenon can be analysed, whether monophasic or multiphase, isothermal or reactive, compressible or non-compressible. Ansys (CFD) can provide valuable insight into product performance. Ansys' well-known fluid analysis tools include the extensively used and well-authorised Ansys Fluent and Ansys CFX; a reliable result can be obtained thanks to the advanced modelling capabilities, robustness and speed of its solvers. Ansys advanced technology is highly scalable, providing efficient parallel computation of a few to thousands of processing cores; combining Fluent or CFX with the comprehensive Ansys CFD-Post fluid flow post-processing tool enables users to perform cutting-edge measurable analysis or to create high-quality imaginations and animations (Ansys Fluids Software, n.d.).

Based on finite volume method, Ansys CFD solvers are built wherein the domain is divided into a set of a finite control volumes. General conservation (transport) equations for mass, momentum, energy and species are solved with this set of control volumes (Figure 5.1). Then the partial differential equations are divided into systematic algebraic equations, which are solved numerically to make the solution field.

$$\underbrace{\frac{\partial}{\partial t}\int_V \rho\phi\, dV}_{\text{Unsteady}} + \underbrace{\oint_A \rho\phi\mathbf{V}\cdot d\mathbf{A}}_{\text{Convection}} = \underbrace{\oint_A \Gamma_\phi \nabla\phi\cdot d\mathbf{A}}_{\text{Diffusion}} + \underbrace{\int_V S_\phi\, dV}_{\text{Generation}}$$

Figure 5.1: Finite control volumes equation (Ansys Fluids Software, n.d.)

5.2.1 Problem description

Ansys analysis is applied to confirm the use of rejected heat from the condenser while the refrigeration runs on a vapour compression cycle. The heat collection in the isolated space will

have the maximum temperature in the system, while the cooled side will have the minimum system temperature. So, with the computer simulation, the temperature variance will confirm whether it is effective for both heating and cooling with time variations. So far, the analytical solution for the design has given the green light to build the prototype, but it would be prudent for the project to be tested by computer simulation first before construction. Input is measured from a basic normal household refrigerator, mostly with the same specifications as the prototype.

5.2.2 Procedure

5.2.2.1 Geometry

The geometry can be performed by any CAD system, but in this case Ansys Space clime is used to draw the prototype with its specification in administration of the prototype (see Figure 5.2 below). The condenser is lying in the bottom of the heating compartment, where the evaporator is located in the selling of the cooling space. This is based on the physics phenomenon that hot air goes up and cooled air goes down.

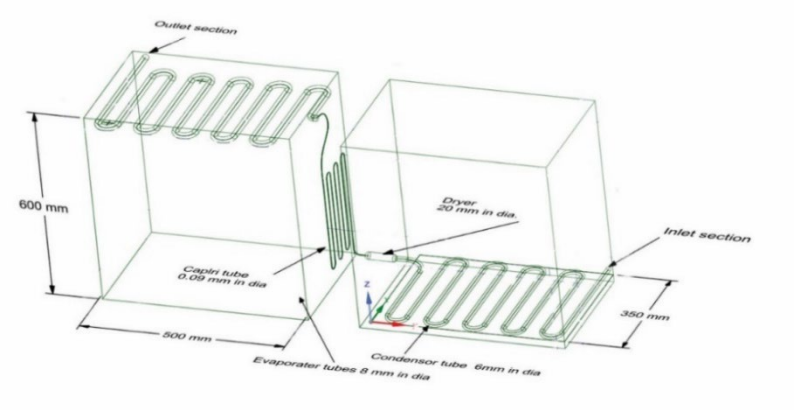

Figure 5.2: Design properties

5.2.2.2 Fluid domains

Fluid domain is where the flow of fluid exists. Thus, there are two fluid domains in this case the piping system where the refrigerant 134a flow, and the second one is the air surrounding the condenser and the evaporator (the flow takes the shape of the pipes and chambers). Figure 5.3 is a demonstration of both fluid domains: the air domain on the right and the refrigerant domain on the left. This condition is called multistage analysis for heat transfer.

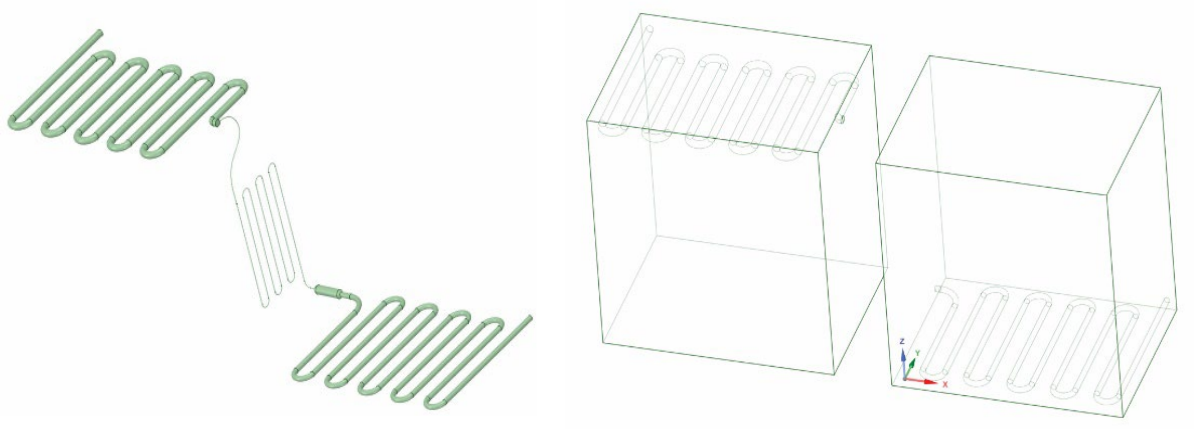

Figure 5.3: Fluid domains: refrigerant (left) and air (right)

5.2.2.3 Meshing

The mesh expression splits the large volume of the domain into small volume and throughout the volume of the flue. These small volumes are grouped into sets, where each set can be solved together, as mentioned earlier. Thus, divided elements are formed in certain shapes, as shown in Figure 5.4, and grouped as follows:

- Hexahedron (hexas, bricks)
- Pentahedron (wedges, prisms)
- Pyramids

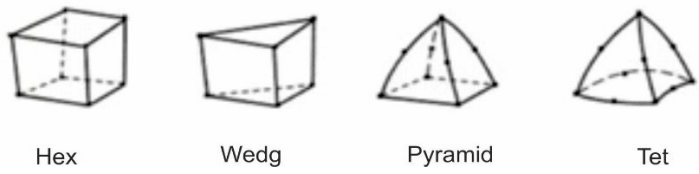

Figure 5.4: Shapes of disintegrated elements

The shape of the mesh parts of the hexahedron can fill the volume more efficiently than other types of mesh shapes. So, six or five tetrahedra can fill one hexahedron, but the solution time consumes more elements. On the other hand, the meshes of the hexahedron are more uniform, which makes it easier to control the distribution of the elements in the volume and more precise when is aligned with the direction of the flow. Mesh and the mesh technique are at the heart of computer simulations. Therefore, the design and management of the mesh requires processing time. The hexahedron mesh can be created by one of two approaches by cutting the geometry into a volume of six faces where each volume has three or four boundary volumes. The other approach is to create a 2D mesh of quadrilaterals and extrude or sweep the 2D mesh to obtain 3-D hexas. Hexahedron meshes can also be created by the advanced mesh tools provided in the software.

5.2.2.4 Preparing

The primary default mesh type for the Ansys workbench is the sweep mesh method, but it requires topologically consistent source and target faces; if these sources topologically are not available, the body cannot sweep and the default mesh technique switches to tetrahedron. Basically, in modular mesh for Ansys, the first thing after loading the geometry is to test whether the geometric mesh is capable or not by selecting 'generate mesh'. As mentioned, the default mesh is the sweep method: if it is not provided with its requirement, a tetrahedron will take place, and if there is an error with the geometry, the mesh processes will stop. After the loaded geometry, the tetrahedron has meshed the prototype geometry (Figure 5.5a). The size and precision of the mesh are very low, while the size of the elements is considered quite high compared to the level of precision (Figure 5.5b). The mesh is adjusted by decreasing the overall size of the elements for more precision, as shown in Figure 5.5c; but the number of size rock elements is more than five million cells, so it will demolish the hardware resources if they were in a limited range (CPU memory and processor). The resolution time will also be longer.

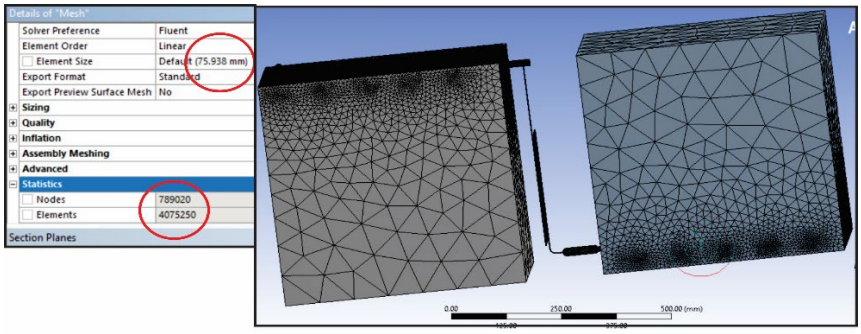

Figure 5.5a: Meshed geometry

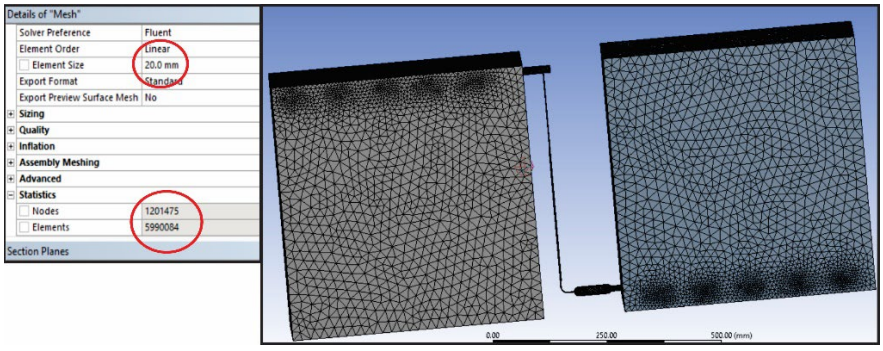

Figure 5.5b: Comparison in meshing size

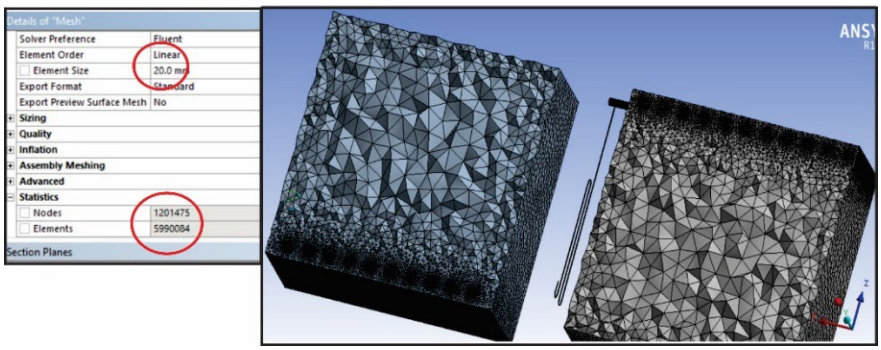

Figure 5.5c: Overall size of the elements

Some work is needed: one for the geometry, one to maintain accuracy then to reduce the number of elements to expedite the calculations. The advance meshing tools such as sweep or multi-zone are the appropriate tools and the geometry is not so complicated if not at the curves of the tubes (condenser and evaporator). Back to the CAD editor (space clam) to surge the geometry mainly slicing.

Figure 5.6a demonstrates the slicing of the compartments to reduce the top and bottom to where the tubs are located (at the red line). The second slice is shown in Figure 5.6b where the slice takes its location at the red line too, to slice the tube curves and the compartments together.

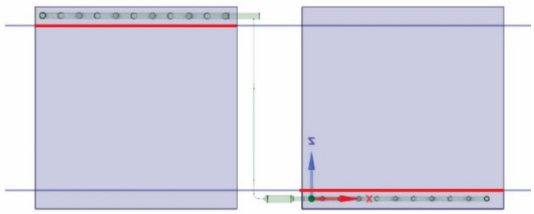

Figure 5.6a: Slicing of both compartments using CAD software

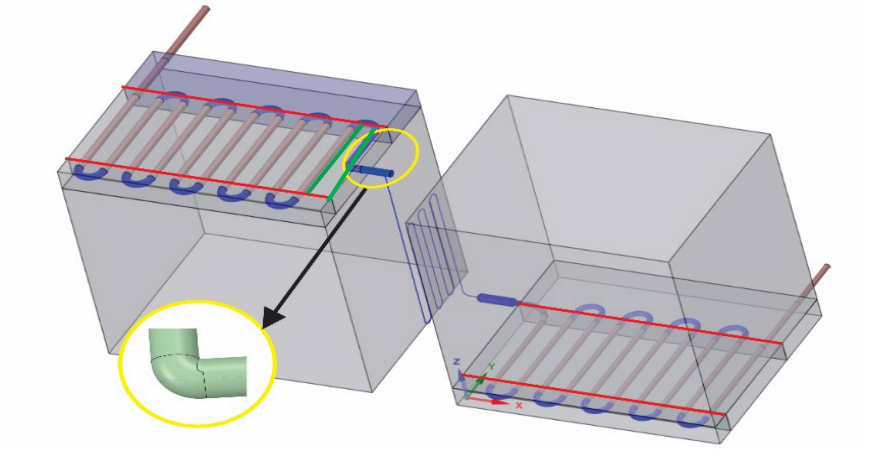

Figure 5.6b: Slicing of the tubes using CAD software

The part with the yellow circle has the wrong geometric shape for the hexagonal mesh at the 90° bend. This would force the tetrahedral mesh to take over and distribute over all the space

between the red lines; so, another cut is made at the green line to limit its border with the rest of the plate in the Y direction between the red lines. By updating the geometry in the Ansys mesh modeler and generating the mesh, the result will be as shown in Figure 5.7a for the default overall size.

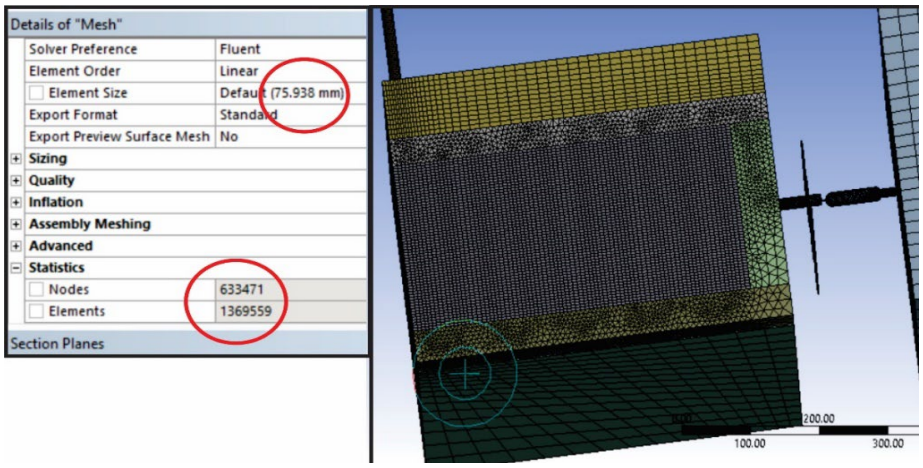

Figure 5.7a: Meshed geometry for the default overall size

Different meshes are mixed between tetrahedral and hexahedral and the number of elements is much lower than before due to the limitation of the tetrahedral mesh which can only be distributed over complex shapes where the hexagonal mesh cannot be achieved. The smooth transition between the two meshes is shown in Figures 5.7b, 5.7c, 5.7d and 5.7e below.

Note: faces and sides in some views are purposely hidden for demonstration.

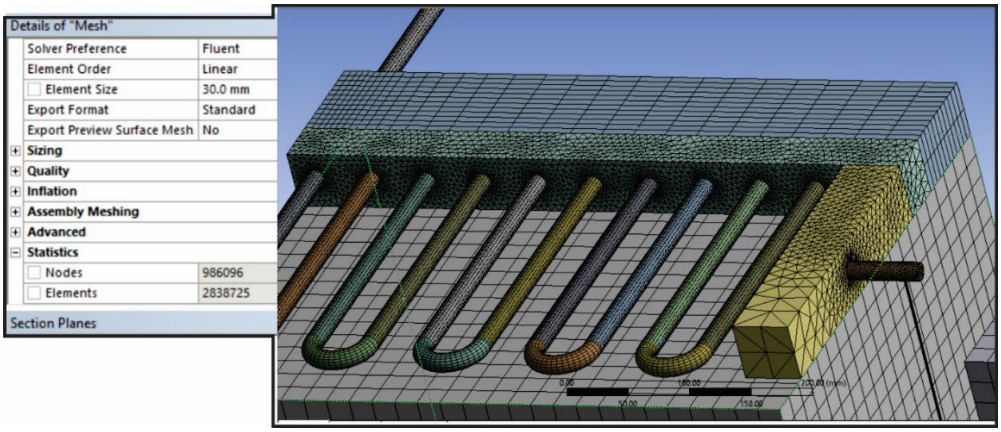

Figure 5.7b: First mesh transition

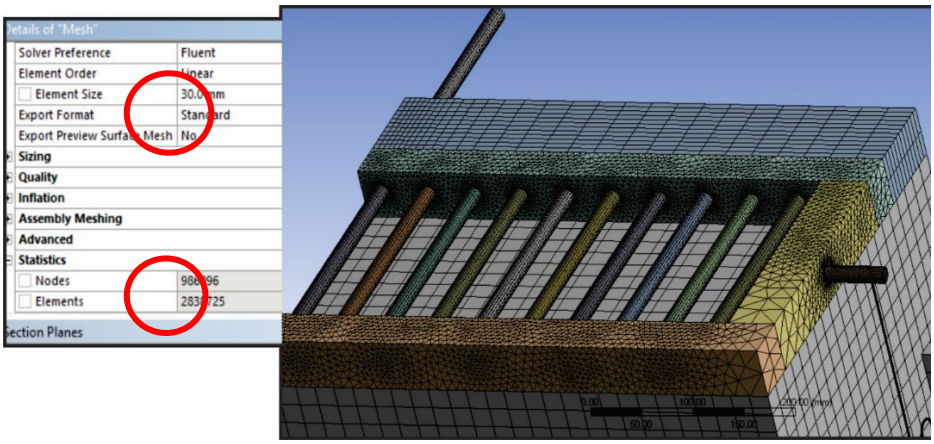

Figure 5.7c: Second mesh transition

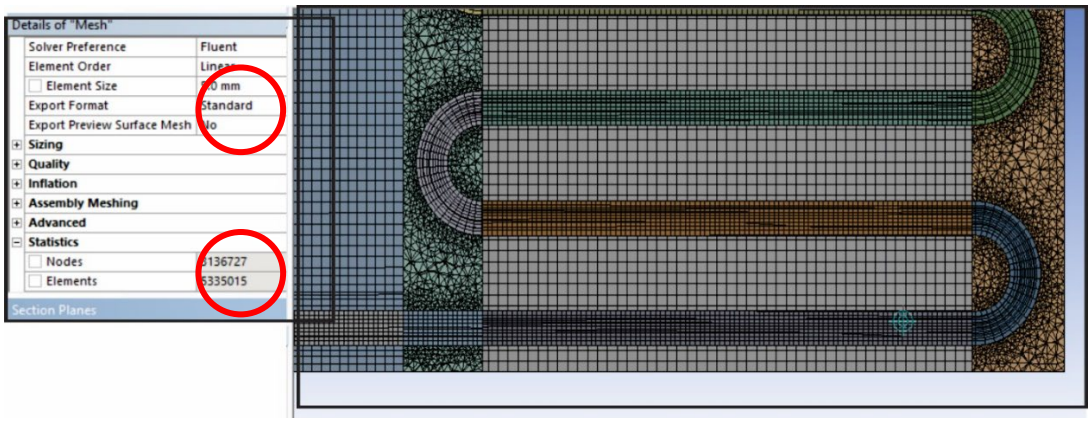

Figure 5.7d: Top view mesh element size 5mm

With an overall element size of 5 mm, the number of elements is always less than that of an overall element size of 30 mm using only a tetrahedral mesh. But due to the limited resources of the CP, an overall size mesh of 30 mm for such a prototype would be sufficient, and the different elements of the components will vary below this size if necessary.

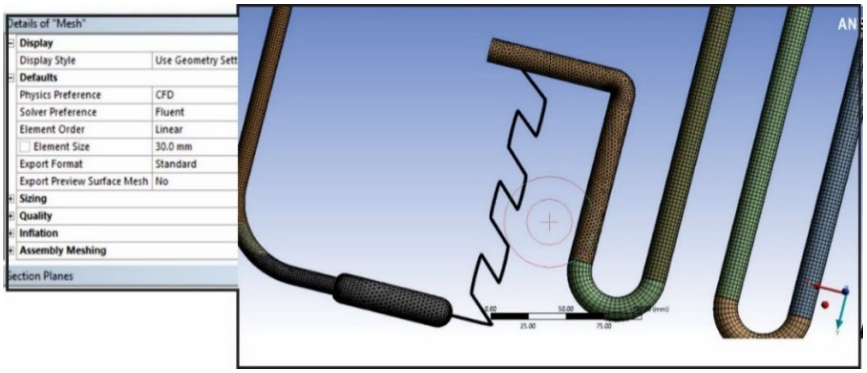

Figure 5.7e: Mesh element size 30mm

It can be seen in Figure 5.8a that the heat generated by the system creates an offset effect in both the cooling and heating compartments, where the pressure in the heating compartment is higher due to the higher temperature of the condenser.

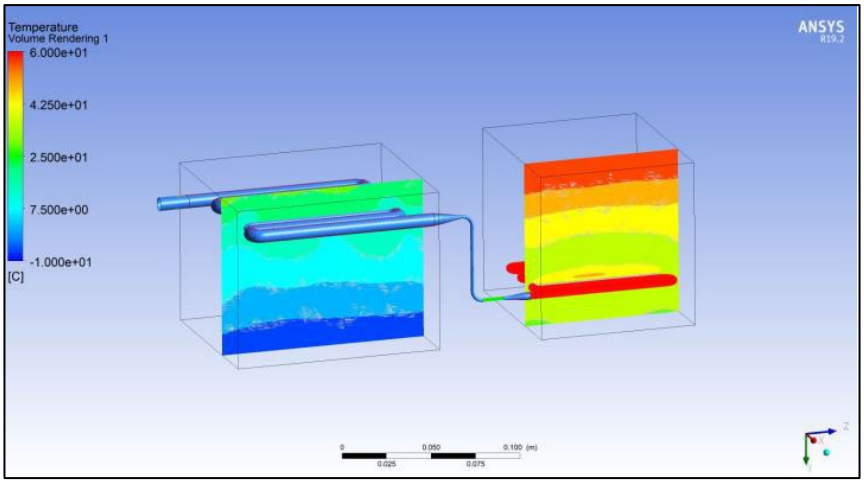

Figure 5.8a: Effect of the heat

Due to the effect of the pressure in both systems, according to Figure 5.8b below, the hot air goes up in the heating compartment which results to the temperature being higher at the top of the room. Simultaneously, it gets colder on the cooling side, and the speed of the air motion behaves respectively.

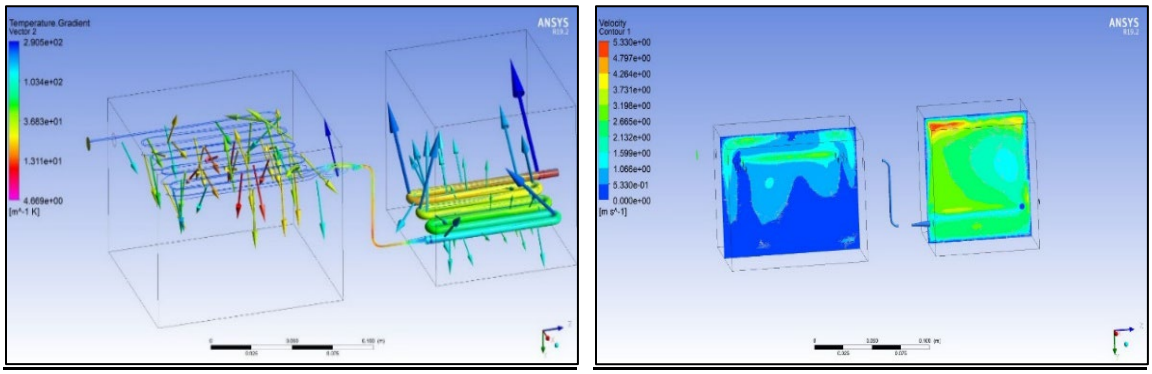

Figure 5.8b: Temperature and air distribution in both compartments

5.3 Conclusion

This chapter covered the simulation development of the prototype. Now that the model has been discussed in detail, the next chapter presents the construction steps and experimental methodologies implemented in the project.

CHAPTER 6:
CONSTRUCTION AND EXPERIMENTAL SET-UP

6.1 Introduction

This chapter introduces the construction of the hybrid solar refrigerator and heat-pump system, as well as the experiment undertaken. It details the steps taken to conduct the experiment and methodology, including data collection techniques, testing procedures and instrumentation.

6.2 System construction

The topology and size of each component have already been discussed in Chapter 4, and the performance of the system is investigated by computer simulation. This section gives a more detailed and comprehensive approach to the method used to construct the combined solar prototype. Components were selected (designed) based on various factors such as strength, cost, manufacturability, weather and weight. Table 6.1 below presents the specifications of the main components used.

Table 6.1: System components

Components	Specifications / Dimensions	Quantity
90 Wp Photovoltaic panel	Mono-crystalline silicon panel 1200*544*25 mm	2
DC battery	12V	1
Charge controller	10A	1
DC compressor	12V	1

The solar mobile prototype comprises a 12V DC compressor, a solar charge controller, solar battery, solar panel and two compartments for cooling and heating purposes. The method adopted in this study is purely experimental; the device, designed using mathematical analysis, was converted into the experiment by following the design results obtained in procuring the needed materials and components for the hybrid.

To make the system simpler and cost effective, a prototype of a modified hybrid system for heating and refrigerating food was developed, with two small household refrigerators used as cooling and heating containers, respectively. The 90 Wp solar panel was used because a pair of identical panels was already available on site. All other aspects of the design were based on the size and specifications of the aforementioned photovoltaic panel. Since the heating unit is dependent on the performance of the condenser, a practical design of the condenser has been rendered and the heating container has been adapted to meet design criteria (see Figure 6.1).

Figure 6.1: Condenser coil placed inside the heating space

The condenser coil was mounted inside the refrigerator to produce heating (hot gas) in the compartment and was welded to the compressor discharge pipe. The other end of the condenser coil was also welded to the dryer (filter). The capillary tube was in turn welded to the dryer and the inlet of the evaporator pipe while the outlet of the evaporator was welded to the suction pipe of the compressor. Finally, the selected 12V DC compressor was mounted with a 2W fan (to dissipate heat) and properly tightened using nuts and bolts, and then filled with R134a refrigerant through the charging pipe and sealed after removing contaminants and moisture by the vacuum pump. Following this, the cooling and heating compartments were tested to ascertain if all parts were assembled correctly.

Figure 6.2: Cooling and heating systems assembled

The combined refrigerator and heat pump systems were assembled and then connected to the solar system in the workshop of the Mechanical Department. The 12V solar battery powered the entire system. The charge controller was connected to the battery and the solar panel to regulate the voltage of the latter. Battery power was needed to run the DC compressor in the absence of sunlight or in instances of low sun intensity. All of the individual parts were assembled correctly to form a single unit.

Figure 6.3: Hybrid prototype assembled

6.3 Experimental set-up and methodology

6.3.1 Zone conditions

The experimental testing of this research was conducted at the Bellville campus (Cape Town) for a period of seven days during summer, between December 2020 and January 2021. The table below overviews the weather in Bellville during the testing period.

Cape Town coordinates: latitude and longitude: 33.9249° S, 18.4241° E.

Table 6.2: Weather overview (extracted from the Campbell data logger)

Months	**Avg. temp.**	**Avg. humidity**	**Avg. daily sunshine**	**Max. wind speed**	**Avg. pressure**
December	21°C	72%	10h	6.25 m/s	1013.7 mbar
January	23°C	73%	11h	7.08 m/s	1012.5 mbar
Avg. wind speed during experimental days				2.55 m/s	
Avg. ambient temperature during experimental days				26.7°C	

6.3.2 Instrumentation and equipment

The following instruments were used during the experimental testing.

- Scientific weather station

The Campbell Scientific weather station situated on the rooftop of the building of the Mechanical Department consists of two pyranometers and an anemometer (see Figure 6.4). The first pyranometer with a shading ring measured diffuse radiation while the other measured the total solar radiation (diffuse and beam); the anemometer measured the air velocity. All of these were connected to the data logger which recorded daily solar beam and diffuse radiation.

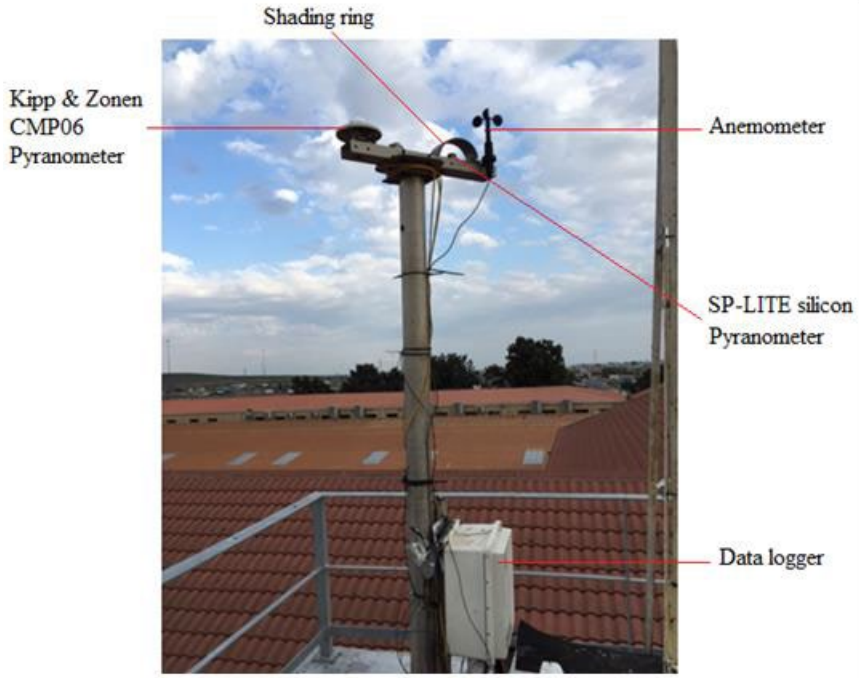

Figure 6.4: Bellville campus scientific weather station

- Solar radiation

The solar radiation was measured by using two different types of pyranometers, the Kipp & Zonen CMP6 and the Kipp & Zonen SP-LITE Silicon pyranometers.

The Kipp & Zonen CMP6 pyranometer, for measuring the total solar radiation intensity, consists of a high-quality blackened thermopile sensor, two glass domes, housing and cable. Its flat spectral sensitivity ranged from 285 to 2800 nm (see Appendix B-1). The Kipp & Zonen SP-LITE Silicon pyranometer, for measuring the diffuse solar radiation, consists of a photodiode complete with frame and cable. To produce a voltage output, the electrical circuit of the photodiode includes a shunt resistor, the photodiode electrical sensitivity changes with the temperature; a nominal value of this change is about 0.2 % per °C (see Appendix B-2).

- Wind speed

A 03101 Young three cup anemometer (Figure 6.5) was used to measure the wind speed. It consists of three cups connected to the shaft. The rotation of the shaft generates a sine wave voltage with a frequency proportional to wind speed. The data logger, directly connected to the anemometer measures the pulse signals and gives the reading of m/s.

Note: More technical specifications of the 03101 anemometer are found in the Appendices.

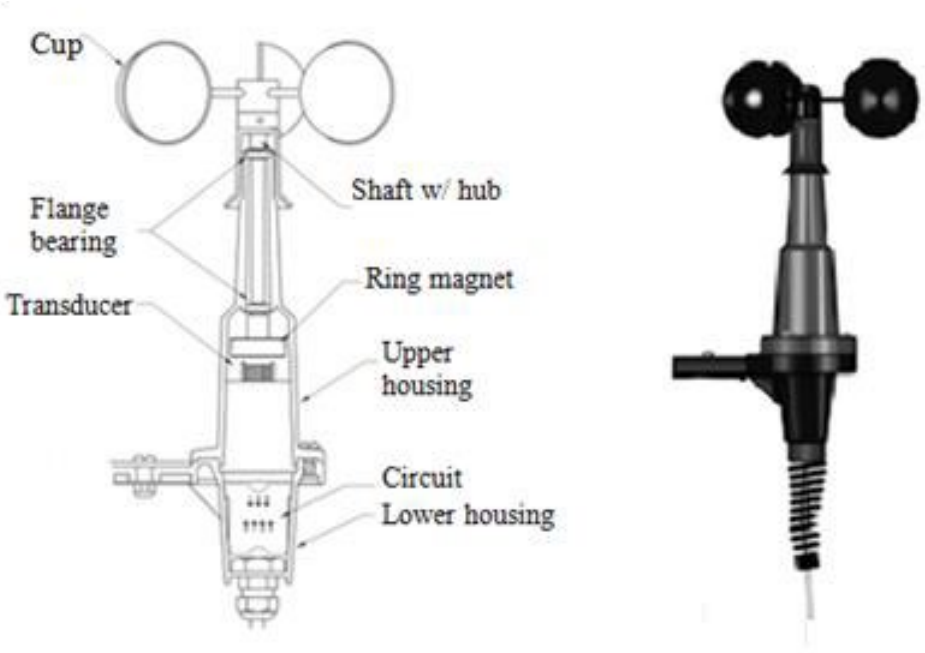

Figure 6.5: 03101 R.M Young anemometer (Campbell, 2015)

- Electrical current

Etekcity MSR-C600 Digital Clamp Meter & Multimeter with AC/DC Voltage Test (Figure 6.6) was used to measure the current consumption of the system. The meter has two jaws that close around the conductor measuring the current; the jaw diameter ranged up to 28 mm.

Figure 6.6: Etekcity MSR-C600 digital clamp meter

6.3.3 Experimental testing

6.3.3.1 Tilt angle

An important factor to consider when trying to increase the energy yield from solar panels is the tilt angle. The angle at which the panel is inclined towards the sun is dependent on the geographical location of the installation. Kamanga *et al.* proposed that the optimum tilt angle for a fixed panel in Zomba, Malawi, for example, should be 25° facing direct north (Kamanga *et al.*, 2014). While Handoyo and Ichsani (2013) suggested an angle between 0 – 40° with seasonal change for Surabaya, Indonesia. Kanyarusoke *et al.* (2016) suggest that the best inclination angle for a PV panel installed in Cape Town would be 30°.

6.3.3.2 Testing procedure

The solar PV system consists of two PV panels of 90 W, a MPPT solar charge controller of 12V and 10A, a 12V deep cycle battery and a 12V DC compressor connected to two small fridges, one for refrigeration and the other for the heating-pump. The panels were both oriented to true north and placed at a slope of 30 °C from the horizontal, on a four-wheel iron frame to facilitate movement of the hybrid prototype; the two containers were bolted to the iron frame to form a combined unit. The charge controller has been screwed to the rear (upper left corner) of the heating compartment to facilitate the connection between the photovoltaic panels, the compressor and the battery. The DC compressor had eight terminal outputs; two terminals were connected to the charge controller, and the others were connected to the evaporator fan, compressor speed controller and thermostat. Two thermocouples were placed inside the cabinets to study the variation of charging temperatures, as well as two temperature controllers which have a digital display indicating the temperature of the different compartments, using temperature sensors (thermocouples). The systems were connected as shown in Figure 6.7 below.

The experiment was performed on top of the Mechanical Engineering building; solar radiation arriving at the site was measured by the existing scientific weather station. Electrical energy recovery was monitored by recording voltages and currents generated by the PV for 15 minutes in the weather station's data logger. Thermal energy in both compartments was monitored every half hour by direct readings from thermometers inserted inside the compartment. Initially, the experiment took place at two levels: on empty and fully loaded compartments, and on a horizontal plane and a plane inclined at 30 degrees. This data was recorded and calculated to study the temperature distribution as well as the performance of the system to achieve heating and cooling in a short time. A comparison was made with the results of the empty and loaded cooling and heating compartments, then at the different tilt angles.

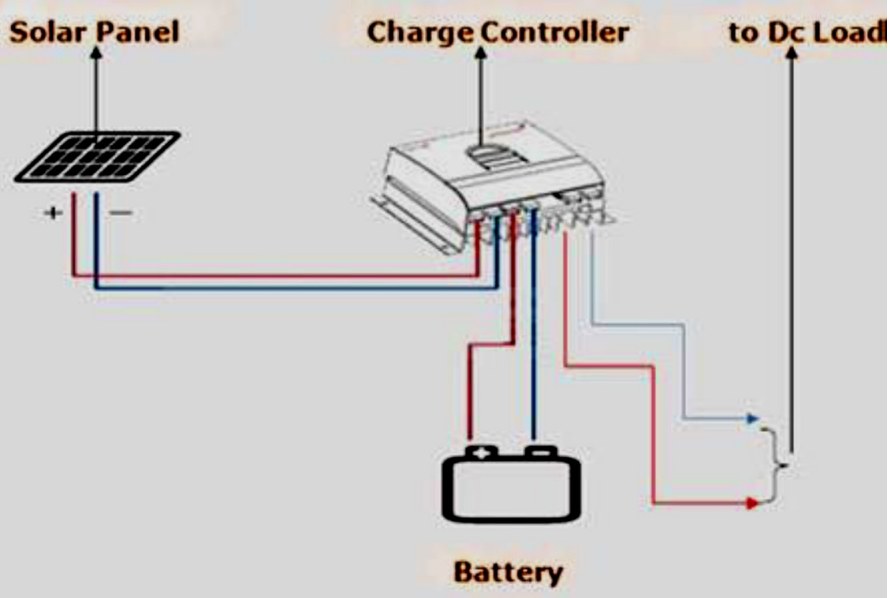

Figure 6.7: Charge controller in a circuit

6.3.3.3 Measured data

The following data were measured and recorded half hourly:

- ✓ Wind speed
- ✓ Total and diffuse radiation
- ✓ Ambient temperature
- ✓ Inside temperature
- ✓ Voltage
- ✓ Current

6.4 Conclusion

This section discussed the methodology applied to construct and assemble the model prototype, and equipment and steps taken to analyse the performance of the solar refrigeration and heat-pump. Results obtained from the experiments and analysis of the same are presented and discussed in the next chapter.

CHAPTER 7:
EXPERIMENTAL ANALYSIS AND RESULTS

7.1 Introduction

Chapter 7 reports the experimental results of the solar hybrid, with a comparison of their performance analysed in detail. Graphical results are displayed, some graphs drawn using Excel and others using MATLAB. The experimental testing was done under the atmospheric conditions of the rooftop of the Mechanical Department building (Bellville, Cape Town), and performed for a period of seven sunny days from 8h30 to 16h30 (8 hours of running time).

7.2 Experimental results

The prototype was tested under the influence of the atmospheric condition at the Bellville campus (Cape Town) of CPUT. Results obtained from the experiments and analysis of the same are presented and discussed in this sub-section. A comparative analysis is made in two ways: firstly, to compare results obtained from empty and fully loaded containers to see the variation of temperature and how much time it takes to reach cooling and heating. The system run for three days on empty cabinets and four days on fully loaded cabinets. Then secondly, to compare the solar radiation results recorded from a horizontal and tilted PV panel with the intention of analysing which provides better solar efficiency.

7.2.1 Variation of weather conditions

The experimental testing took place during summer when there was an abundance of solar rays for a period of seven days, starting with empty spaces and then tested with cabinets loaded with bottles of water in the refrigeration system, and potatoes fries with sausages in the heating system. The meteorological conditions during the testing period included the following: ambient temperature, wind speed, solar radiation and relative humidity. The maximum ambient temperature is seen on the third day of the experiment (or 04/01/2021) and the average wind speed ranged from 1.7 m/s to 3.4 m/s. However, 06/01/2021 was the windiest day during the period of testing with the lowest ambient temperature; then the maximum average solar radiation logged was 655.1 W/m² (on the 22/12/2020). The relative humidity varied depending on the changes in temperatures recorded on the respective testing days. The weather was good for the operation of the PV panel and the results obtained were satisfactory (see appendix D).

7.2.2 Temperatures in empty cooling and heating compartments

As mentioned above, the experiment was conducted in two ways: firstly, in empty compartments and then in fully loaded cooling and heating compartments. The reason was to study the temperature variation as well as the time it takes to bring the products to the designed temperatures: 5°C for refrigeration and 50°C for heat-pump. Figure 6.5 displays the temperature variation on 21 December 2020 when the system run on empty cooling and heating

compartments. It can be seen that the highest temperature reached was 55°C for the heat-pump system, while the refrigerator went as low as 2°C which was quite good for keeping drinks as cold as possible throughout the day; this was due to good radiation occurring around 11:00 AM. However, it was observed that once the door was left opened for more than 15 minutes, a drop in temperature was evident at 15:00 on the graph while running the heat-pump system.

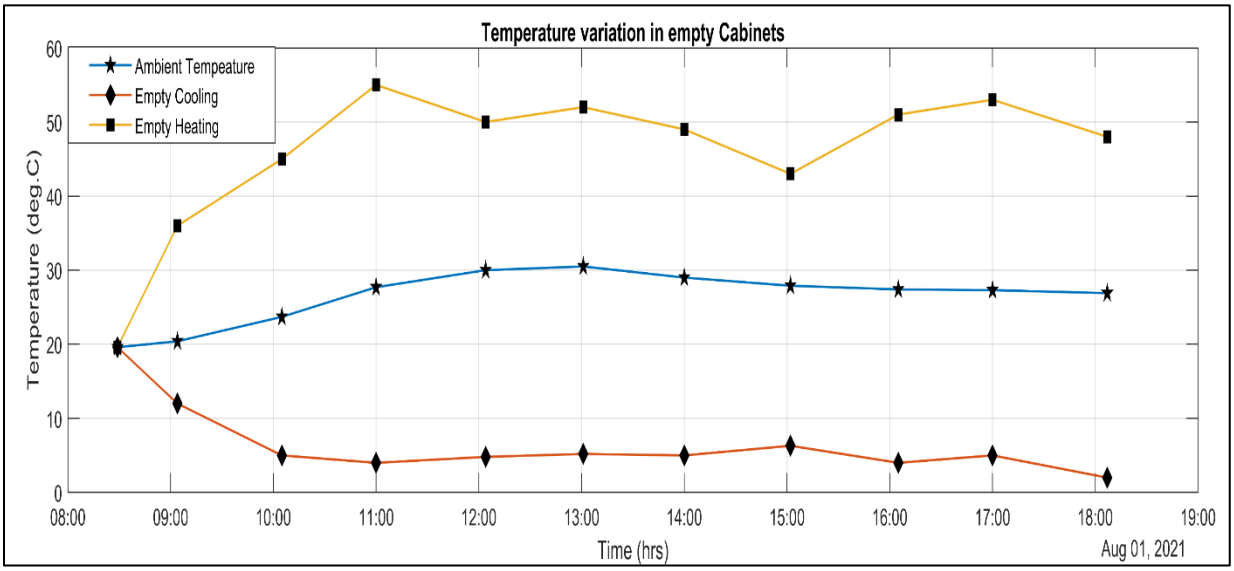

Figure 7.1: Temperature variation in empty cabinets

7.2.3 Temperature in fully loaded cooling and heating compartments

The cooling system was packed with bottles of water while the heating system was fully loaded with potatoes fries and sausages. Data recorded on 04 January 2021 from the weather station are graphically displayed in Figure 7.2 below.

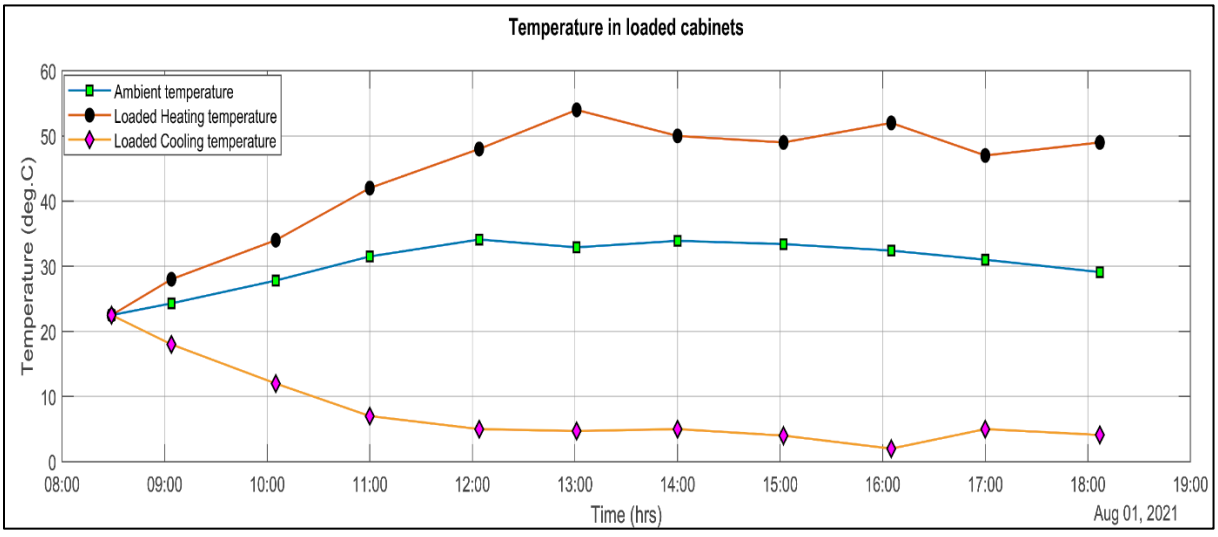

Figure 7.2: Variation of temperature on loaded cabinets

7.2.4 Solar radiation on horizontal surface

The solar radiation on the horizontal plane (0° tilt angle) is graphically presented in Figure 7.3 below. The trend shows that the highest value recorded is approximately 850W/m² and then slightly decreasing as the day continues.

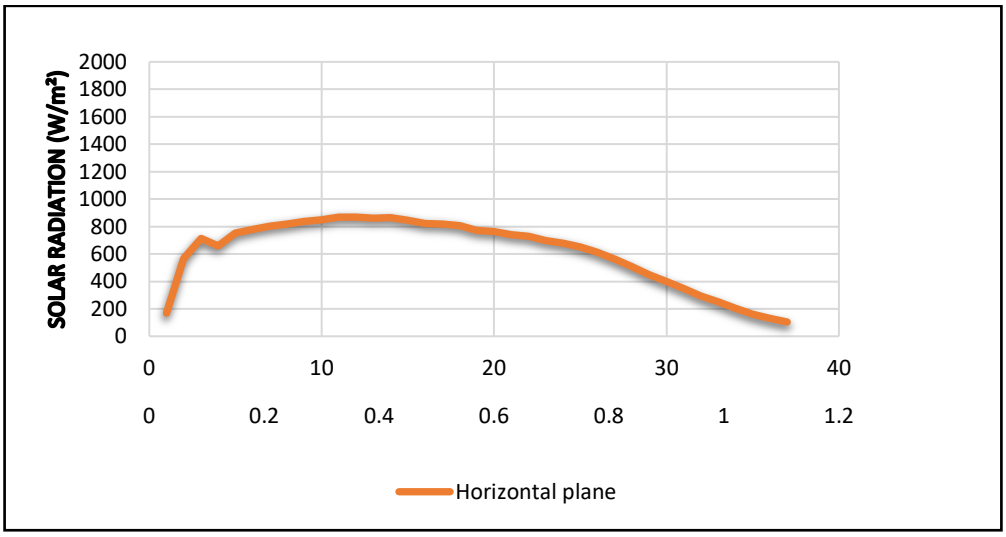

Figure 7.3: Solar radiation onto the horizontal plane

7.2.5 Solar radiation on the inclined surface

The total solar radiation on a 30° inclined PV panel was computed using the Perez model. It was observed from the graph of Figure 7.4 that the variation of the solar radiation on the inclined PV panel was more than that on a horizontal surface (see Figure 7.3 above); this agrees with the findings of Kanyarusoke *et al.* (2012).

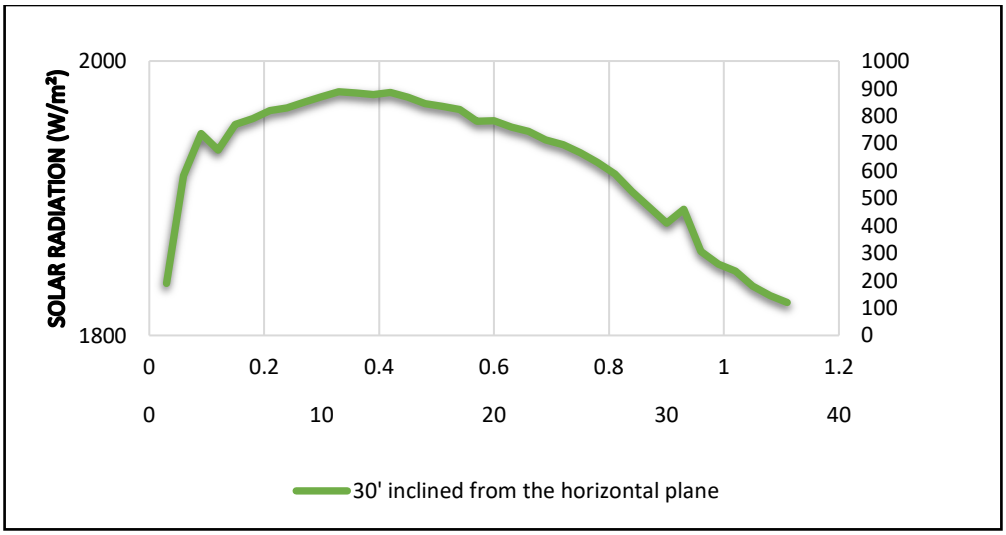

Figure 7.4: Solar radiation onto the 30-degree tilt PV panels

7.2.6 0° vs 30° tilt angle

It was indicated that the experiments were undertaken in two levels to get better solar radiation: initially at 0° slope and then at 30° PV panel. Therefore, it is important to note that the 30° tilt angle was recommended by Kanyarusoke *et al.* (2016) as suitable for Cape Town. Figure 7.5 represents the solar energy reaching the PV module at 0° and 30° tilt angle. However, while running the PV panels at different angles, it was observed that the results in solar radiation onto the 0° PV panel were low compared to the ones from the 30° tilt angle. The 30° PV panels produced the highest results.

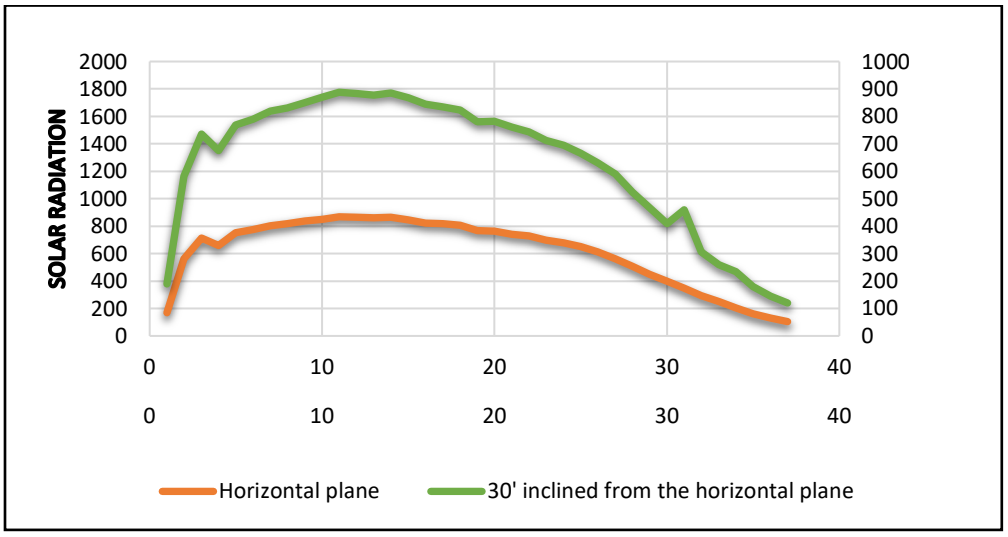

Figure 6.5: Horizontal PV panels vs 30° tilted PV panels

Figure 7.6 displays the solar radiation components (beam and diffuse), the total solar radiation and the solar radiation onto the 30° tilted PV panels. It is evident that while running the system throughout the day, beam radiation was always higher than the diffuse radiation.

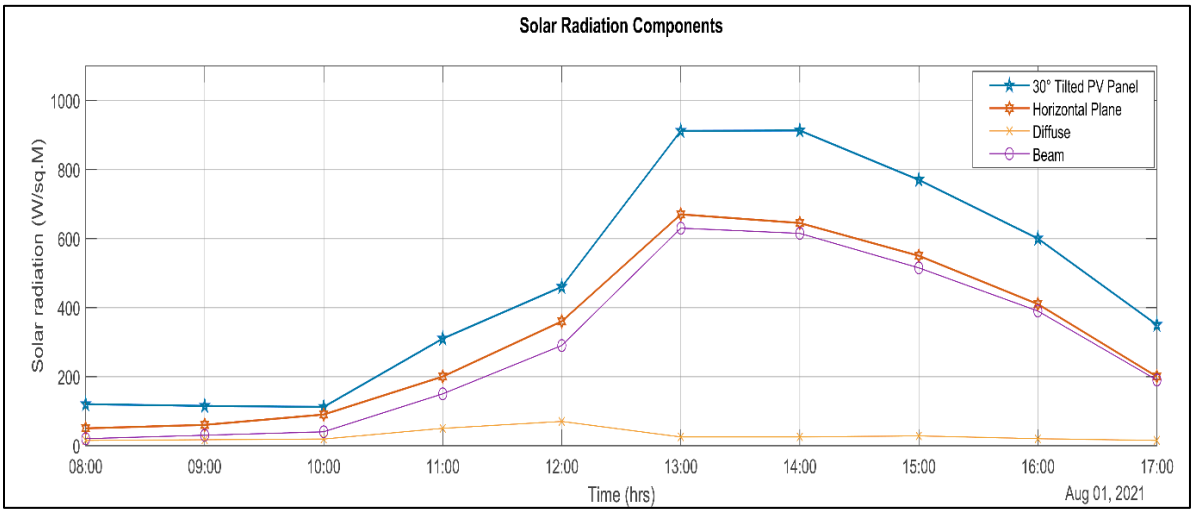

Figure 7.6: Example of the variation of solar radiations on 05 January 2021

The intensity of solar radiation falling on the panels depends on many factors such as time, season and location. Consequently, solar radiation will have an effect on the output of the panel. The amount of energy generated from the PV panels often increases with the level of solar radiation it receives; as radiation increases, so does the power.

The variation of the temperature and solar radiation is displayed in Figure 7.7 below. The experiment reported that the highest sunshine hour, clear and sunny day, allowed the PV surface to receive the maximum solar radiation during the testing period. A sudden increase in solar irradiance was observed which caused both systems to reach their design temperatures shortly before noon.

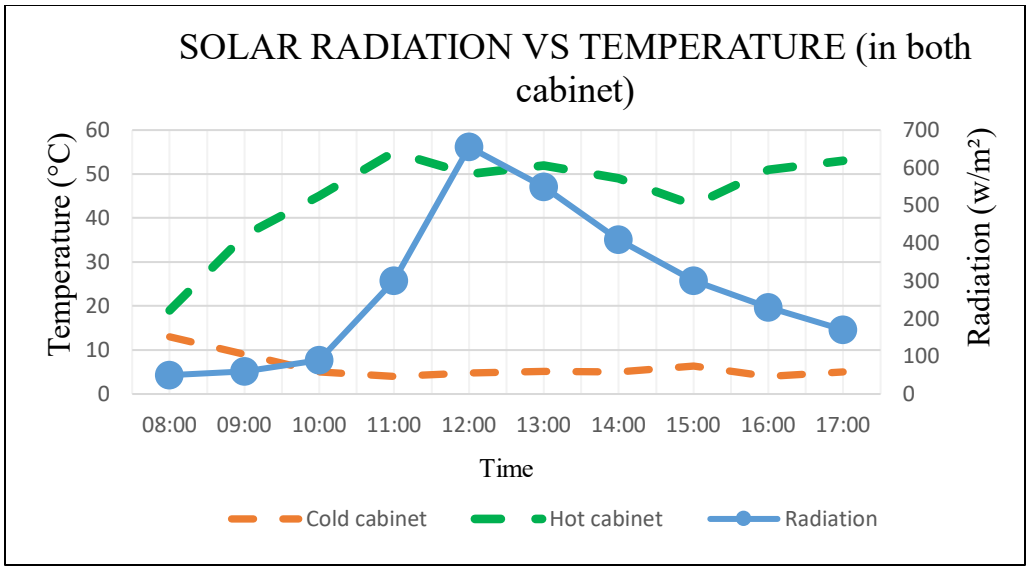

Figure 7.7: Radiation vs temperature

7.2.7 Effect of tilt angle

Different tilt angles were simulated using MATLAB to evaluate the amount of solar radiation available on the panel in winter and spring. Consequently, solar radiation on panels inclined at 25°, 30° and 34° proves best since it gives the highest radiation on the panel. However, these values were validated for Cape Town only and should not be used to estimate the best slope for different location. Figure 7.8 illustrates how the tilt angle affects the amount of solar radiation onto the panel.

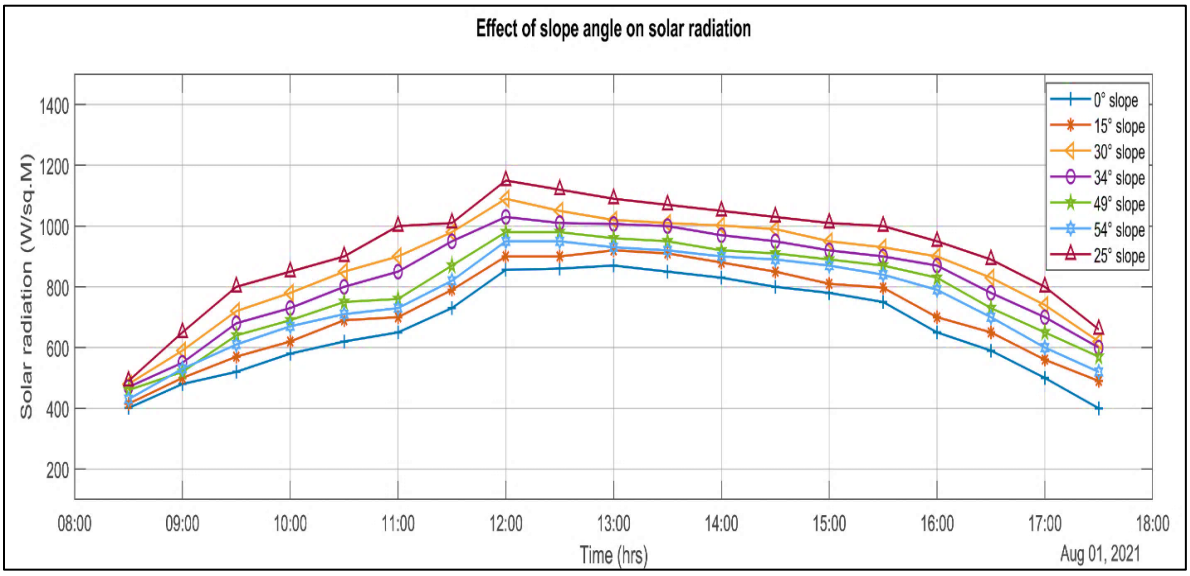

Figure 7.8: Effect of slope angle on solar radiation

7.2.8 Effect of weather and temperature

Meteorological parameters had an impact on the overall performance of the PV panels; the weather and temperature do not stay constant throughout, nor does the performance of the panels. The PV panels performed better on sunny days as clouds and rain made the system ineffective.

7.3 Hybrid prototype performance

The solar radiation for the day was sufficient to run both systems. There were days where it took longer to reach the cooling temperature (5°C) than it did to rise the temperature to 50°C (required heating temperature), but other days provided better timing with better results, as occasionally it only took 30-45 minutes from the ambient temperature to reach cooling and heating temperatures. The thermostat was set to operate between -30°C and +30°C and once the designed temperatures were reached, the 2W fan was switched on to cool down the heat by the compressor below the pre-set temperature. Due to good solar radiation, the battery stayed charged for the entire day.

However, there was an exchange of energy – a rise of temperature in the refrigerator cabinet as well as a drop of temperature in the heating – every time that the door opened. So, the number of opening doors was crucial in the process of improving both systems.

7.3.1 Temperatures

The variation of temperatures on 21 December 2020 and 04 January 2021 in the refrigerator and the heat-pump is shown in Figures 7.9 and 7.10 below. The starting time is 8h30 AM at ambient temperature. The graph shows that both cabinets reach their designed temperature between 10:00-11:00 AM which is a long time if the vendor needs to make a substantial profit by end of day. This is a disadvantage for someone who urgently needs a cold drink on a hot day; however, for the heating system, the foods will be warm and ready to be sold. A temperature comparison between the empty and loaded cabinets showed a difference in temperature distribution that is almost regularised for about two hours from 12:00 AM in both the refrigerator and heat-pump cabinets. Ideal temperatures were reached when the system was experiencing the highest ambient temperatures.

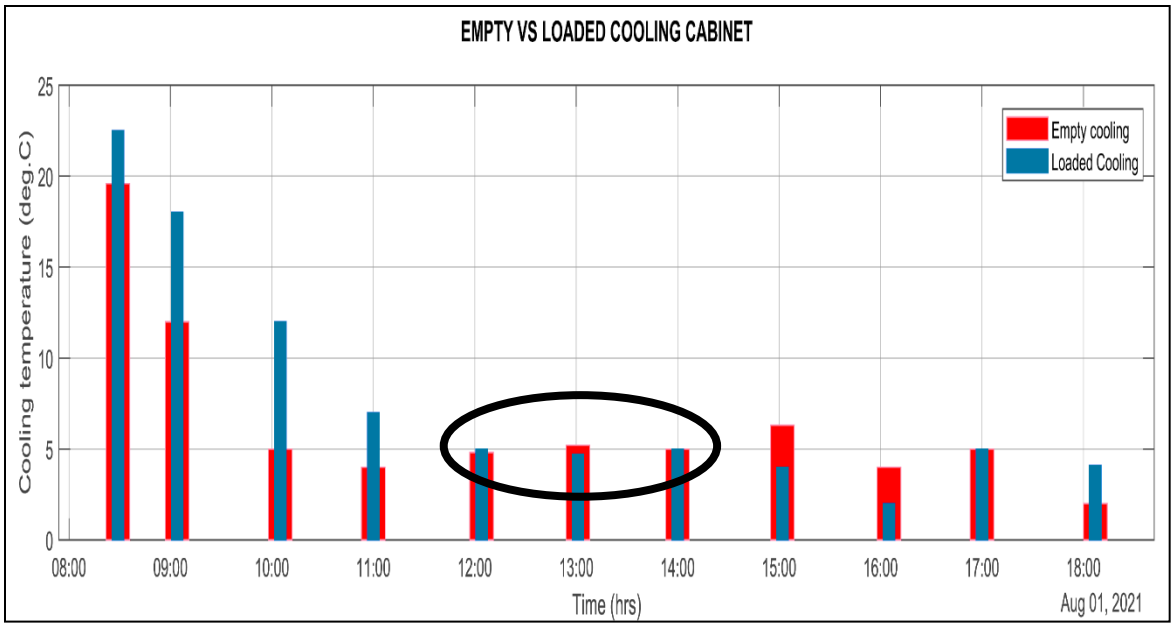

Figure 7.9: Temperature comparison on empty and loaded cooling system

Figure 7.10: Temperature comparison on empty and loaded heating system

7.3.2 Heat load and power consumption

The experiment also revealed that the total loads of the model with empty spaces were nearly stable because it only included heat from the walls (heat leakage) but fluctuated during the first four hours of the loaded spaces before becoming stable, a variation caused by the difference in food temperature. It was then observed that heat loads increased with the increase in ambient temperature but the variation of wind speed had no significant impact on the total heat load. The power consumption, on the other hand, was affected by the quantity of products and how

long the door was left open. At some point, the power consumption drew to zero when the compressor was at rest.

7.3.3 Coefficient of performance (COP)

The variation of performance COP of the system on 04 January 2021 (first day of loaded cabinets) was calculated using the temperature of the refrigerant R134a at the entrance and the exit of the evaporator and the condenser. The R134a charts were used to get the corresponding enthalpy; subsequently, the average COP for the hot and cold cabinet was 2.91 and 3.8 respectively.

The system demonstrates good overall efficiency under normal conditions; higher COP means higher efficiency and less power consumption. However, the efficiency of a heat pump, COP_h, depends on several factors, especially the temperature difference between waste heat source and potential user as an important factor. Major reasons for lower efficiency of the heating system are mechanical and fluid friction, and heat loss to the surroundings; other factors that may affect the efficiency are system controls and efficiency of peripheral equipment like fans.

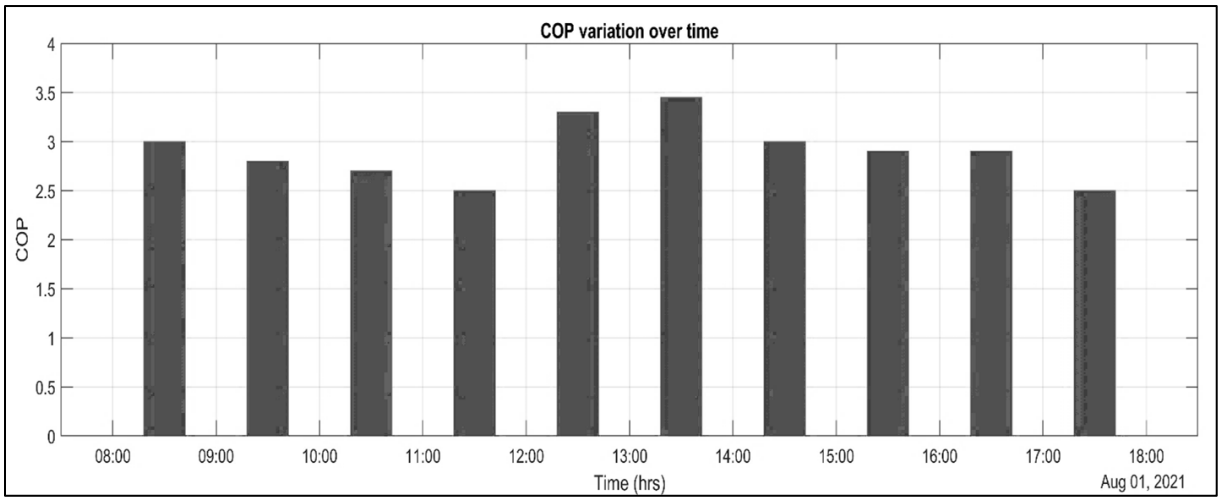

Figure 7.11: Variation of the COP on 04 January 2021

On a clear and sunny day, the variation of solar radiation presented a maximum value at noon, decreased with the decrease of solar altitude and became least (zero) in the evening and morning. However, due to the presence of a cloud in the path of the sunlight, some irregularities were found in the trend (the red dot on the graph). The maximum value of solar radiation recorded on that day was 655.1 W/m² exactly at 12:00 AM. Again, the increasing or decreasing trend of solar radiation is almost symmetrical on a sunny day and the reason the system performance was at its best and the COP remained constant during those periods (see Figure 7.12).

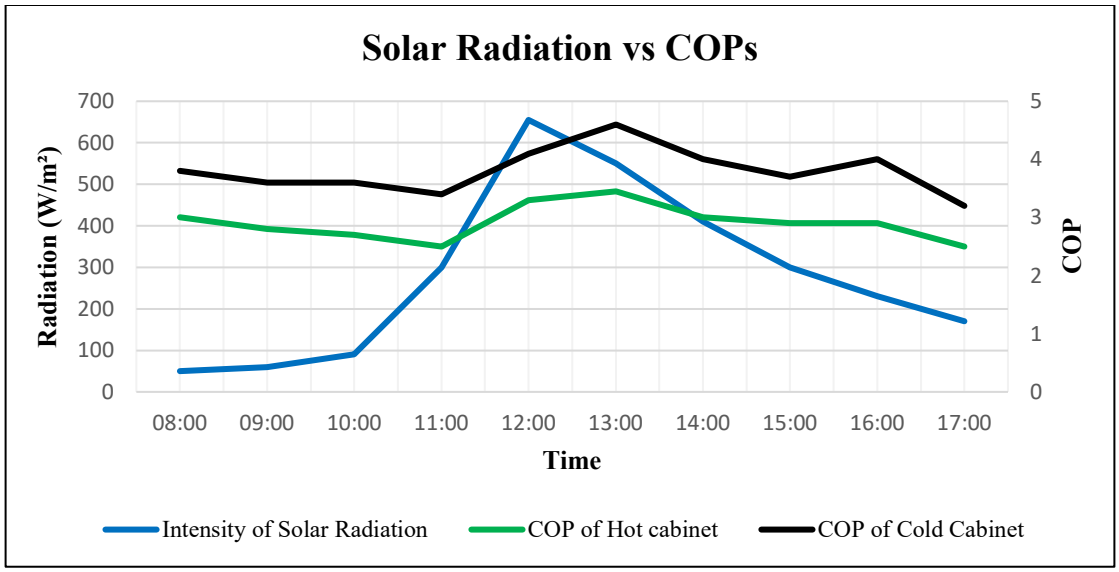

Figure 7.12: Effect of solar radiation on the COP of both system

7.4 Conclusion

Experimental results from analysis of the refrigeration and heat-pump systems have been presented in this chapter. An evaluation of the performance of the PV system as well as the cooling and heating systems have been scrutinised. Results showed that the tilted PV panels harbour great potential in terms of increasing solar radiation and thereby system performance. The following chapter concludes this study by highlighting its most important aspects.

CHAPTER 8:
CONCLUSIONS AND RECOMMENDATIONS

8.1 Summary

The cooling effect is found only in a refrigerator whereas the heating effect can only be found in a heat-pump. Consequently, the main objective of this present research study is to provide cooling and heating simultaneously using one system, the conventional vapour-compression system, while being powered by solar energy. Such a type of technology can be advantageous in places where grid electricity is not available or in term of investments costs.

The design involved sizing all individual components correctly, by finding the total heat load and then matching the components of the household refrigerator to the PV system. Construction and testing took place at Cape Peninsula University of Technology under the atmospheric conditions; data were recorded from the Campbell scientific weather station and analysed to monitor the performance of the prototype.

The model discussed above will bolster a sustainable future more than any separate cooling and heating system. Since the system was designed to take energy from a low temperature source and raise it to a higher grade (temperature), this prototype is useful for any application where that is required within practical operating ranges. This, in the long run, fulfils the target of African countries in increasing rural energy access, helping to alleviate poverty in rural African community by creating small businesses.

8.2 Conclusion

After carrying out this research, it is evident that cooling and heating can be achieved through the use of solar energy. Results have led to the following conclusions:

- The suggested idea of having a PV system with a 12V DC compressor has been proven: the capacity of the refrigeration system can be increased in accordance with an appropriate PV system size.
- The variation of incident solar radiation and ambient temperature has significant effects on the performance of the solar PV refrigerator and heat-pump systems. The wind speed has only minor impact on the total heat load of the system.
- The systems (cooling and heating) were able to reach ideal temperatures and maintain these temperatures for longer.
- Several degrees, 25°, 30° and 34°, prove to be the ideal tilt angle since they give maximum solar radiance on the panel in Capet Town.
- For performance of the solar mobile refrigerator and heat-pump, two conditions were considered – at no load and full load – and tested during summer for seven days. When fully loaded, the refrigerator took time to bring the drinks to cold, due to the size of the evaporator. But on hot days, the performance of both systems was quite efficient.

- Considering the economics, the author attempted to adapt two small, low cost, equally well functioning fridges to meet the requirements of the project.

The prototype is suitable for small-scale businesses to use as pre-cooling and pre-heating units. The importance of this work is that in remote areas, a solar PV refrigerator and heat-pump systems have the potential to create business opportunity and enhance development in the rural community.

8.3 Recommendations

Although the solar hybrid prototype was capable of doing both works, there are still improvements that could be implemented. Here are several recommendations to improve system performance based on results:

- An investigation of the size of the evaporator could influence the refrigerator system performance.
- A proper sizing of heat exchangers (evaporator and condenser) could bring the system to an even better performance.
- The system must be properly designed to remedy the loss of energy caused by opening the doors.
- The effect of the intensity of direct sunlight could increase the heat leakage and improve overall system performance.

If the above-mentioned improvements were possible, this would serve the ideal system in remote areas because it will curtail barriers and put simultaneous heating and refrigerating within the reach of the general population to run small businesses.

REFERENCES

Abulateef, J.M., Murad, N.M., Alghoul, M.A., Zaharim, A. & Sopian, K. 2011. *Experimental Study on combined solar assisted ejector absorption refrigeration system*. University Kebangsaan Malaysia, Malaysia.

Aktacir, M.A. 2011, February. *Experimental Study of a multi-purpose PV-refrigerator system*, International Journal of Physical Sciences Vol. 6(4), pp. 746- 757.

Alkilani, F.M. 2017, February. *A Solar assisted high temperature refrigeration system for postharvest pre-storage fruit cooling.* CPUT.

American Society of Heating. 2006. *ASHRAE Handbook: Refrigeration.*

Ansys Fluids Software. https://www.ozeninc.com/products/fluid-dynamics/ansys-cfd/ . Accessed April 4, 2021.

Asma, E. 2017, August. *A simple approach to calculate / minimize the refrigeration power requirements*. DOI: 10.5772/intechopen.69130.

Ayaz, A.K. 2020. *Design Methodology of Off-Grid PV Solar Powered System (A Case Study of Solar Powered Bus Shelter).*

Brew-Hammond, A. 2010. Energy access in Africa: Challenges ahead. *Energy Policy*. 38: 2291-2301.

Campbell, 2015. *SP Lite2.* https://www.campbellsci.ca/products. Accessed February 11, 2021.

Cho, L.N. & Thida, O. 2018. *Design and Analysis of Solar Powered Vapour Compression Refrigeration System.* Available online at www.ijrp.org

Cuce, P.M. & Cuce, E. 2012. A novel model of photovoltaic modules for parameter estimation and thermodynamic assessment. *International journal of low-carbon technologies* 7: 159-165.

Dincer, I. & Kanoglu, M. 2010. *Refrigeration system and applications.* 2nd ed. Channai: John Wiley & Sons.

Direct, S. 1986. *SOLAR Direct.* http://www.solardirect.com/pv/pvlist/pvlist.htm Accessed October 2, 2020.

Edenhofer, O., Pichs-Madruga, R., Sokona, Y., Seyboth, K., Matschoss, P., Kadner, S., & von Stechow, C. 2011. *Renewable Energy Sources and Climate Change Mitigation*. Cambridge: Cambridge University Press. 10.1017/CB09781139151153.

Edwin, P.A. & Rex, M. 1986. *Refrigeration: Home and Commercial*. Macmillan Publishing Company: New York.

FDI Creative, 2014. *PMW vs MPPT Solar Charge Controllers.* http://www.solarcraft.net/resources/articles/pmw-vs-mppt-solar-charge-controllers Accessed February 2, 2021.

Franklin, E. 2017. *Solar Photovoltaic (PV).* Cooperative extensions: https://extension.arizona.edu/sites/extension.arizona.edu/files/pubs/az1697-2017.pdf Accessed January 9, 2021.

Handoyo, E.A. & Ichsani, D. 2013. International Conference on Sustainable Energy Engineering and Application. *The optimal tilt angle of a solar collector*. Physics Procedia, 32: 166–175. https://www.researchgate.net/publication/256981847-The-Optimal-Tilt-Angle-o_f-a-Solar-Collector Accessed January 21, 2021.

Infante F.C. & Kim, D. 2014. Techno-Economic review of solar cooling technologies based on location specific data. *International Journal of Refrigeration*, 39: 23-7.

Ivan, k., Per, H.P. & Emil, J. 2010, December. *Standalone cool/freeze cluster driven by solar photovoltaic energy.* DTI.

Kanyarusoke, K., Gryzagoridis, J., & Oliver, G. 2012. *Issues in solar tracking for sub-Sahara Africa*. Stellenbosch, South Africa: Proceeding of Southern African Solar Energy Conference.

Karekezi, S., McDade, S., Boardman, B. & Kimani, J. 2012. *Chapter 2-Energy, Poverty and Development. In Global Energy Assessment-Toward a Sustainable Future.* Cambridge University Press, Cambridge, UK and New York, USA, and the International Institute for Applied Systems Analysis, Luxenberg, Austria, pp. 151-190.

Kaygusuz, K. 2012. Energy for sustainable development: a case of developing countries: *Renewable and sustainable energy reviews*. 16, 1116-1126.10.1016/j.rser.2011.11.013.

Leonics. 2013. *How to design solar PV system*. http://www.leonics.com/support/article2_12j/articles2_12j_en.php Accessed January 3, 2021.

Maehlnm, M.A. 2015. *Energy Informative.* http://energyinformative.org/best-solar-panel-monocrystalline-71polycrystalline-thin-film Accessed December 15, 2020.

Makinde, K., Man, A.S., & Amao, E. 2019. *Design and Fabrication of Solar Powered Mobile Cold Room.* International Journal of Trend in Scientific Research and Development, 3(6): 342-350. ISSN: 2456-6470, https://www.ijtsrd.com/papers/ijtsrd28099.pdf

McAdams, W.H., 1954. *Heat Transmission*. 3rd ed. Publisher: McGraw-Hill, New York, 1954.

Michael, F.G.B. 1986. *Refrigeration and air conditioning*. William Heinemann, 1986.

Michael, K., Jim, F., David, J.B., & David, B. 2001. *Experimental Evaluation of a Solar PV Refrigerator with Thermoelectric, Stirling and Vapor Compression Heat Pumps.* Houston, 2001.

Mokhtar, M., Ali, M.T., Brauniger, S. *et al.* 2010. Systematic comprehensive techno-economic assessment of solar cooling technologies using location-specific climate data. *Applied Energy,* 87: 3766-78.

Muthusivagami, R.M., Velraj, R., & Sethumadhavan, R. 2010. Solar cookers with and without thermal storage: A review. *Renewable and Sustainable Energy Review* 14: 691-701.

Norie, A.A. & Kumar. V. December, 2016. *Development of a portable hybrid refrigeration system*. International Journal of Engineering Research & Technology. ISSN: 2278-0181 Vol. 5 Issue 12, December-2016. Available online at www.ijrp.org

NREL. 2016. National Renewable Energy Laboratory 's PV Watt calculator. https://pvwatts.nrel.gov/ Accessed January 5, 2021.

Omni. 2009. *CMP6 Pyranometer*. http://www.omniinstruments.co.uk/cmp6-pyranometer.html Accessed February 13, 2021.

Otanicar, T., Taylor R.A. & Phelan, P.E. 2012. Prospects for solar cooling: *An economic and environmental assessment*. Solar Energy 86: 1287-99.

Perez, Richard, Ineichen, Pierre, Seals, Robert, Michalsky, Stewart & Ronald. 1990. *Modeling daylight availability and irradiance components from direct and global irradiance*. Solar Energy, 44(5): 271-289.

Rani, M.F.H., Razlan, Z. M., Shahriman, A.B., Yong, C.K., Harun, Desa, H. 2017. *Design of refrigeration system using refrigerant R134a for macro compartment.* IOP Publishing DOI :10.1088/1742-6596/908/1/012054

Ragil, K., Sebin, K.B., Vijil, K.V., & Vinod, P.B. 2016. *Solar Semiconductor Refrigerator.*

Renewable Energy| Department: Energy| REPUBLIC OF SOUTH AFRICA. http://www.energy.gov.za/files/esources/renewables/r_solar.html Accessed February 9, 2021.

Saadi, J., & Ameen, A. 2015. *Solar Powered Refrigerator.* https://hdl.handle.net/20.500.11888/11695 Accessed June15, 2019.

Solar Choice. 2016. *Why even partial shading is bad for solar power systems.* https://www.solarchoice.net.au/blog/partialshading-is-bad-for-solar-panels-powersystems Accessed January 5, 2021.

Solar Pathfinder. (n.d.). https://www.solarpathfinder.com/PF Accessed January 7, 2021.

APPENDICES

Appendix A: Technical specification of components

Appendix A-1: 12V DC Compressor specifications

Code numbers

BD50F without electronic unit	101Z1220
Electronic unit 12-24V DC - standard	single: 101N0210, 30 pcs: 101N0211
Electronic unit 12-24V DC - w. metal shielding	single: 101N0220, 30 pcs: 101N0221
Electronic unit 12-24V DC - with AEO	single: 101N0300, 30 pcs: 101N0301

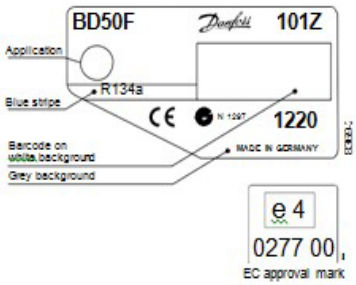

Application

Application		LBP/MBP/(HBP)
Evaporating temperature range	°C	-30 to 0 (10)
Voltage range / max. voltage		12 - 24V DC / 31.5V DC
Max. machine compartment temperature	°C	55
Comp. cooling at ambient temp. 43°C		S or F_1*

S = Static cooling normally sufficient
O = Oil cooling
F_1 = Fan cooling 1.5 m/s (compressor compartment temperature equal to ambient temperature)
F_2 = Fan cooling 3.0 m/s necessary

Design * depending on application

Displacement	cm³	2.50
Oil quantity	cm³	150
Maximum refrigerant charge	g	300
Free gas vol. in compressor	cm³	870
Weight: Compressor/Electronic unit	kg	4.3/0.25

Motor

Motor type		Variable speed
Resistance, all 3 windings (25°C)	Ω	2.0
Approvals (electronic unit)		E4 72/245 95/54 0277 00

Dimensions

Height	mm	A	137
		B	135
		B1	128
		B2	73
Suction connector	location/I.D. mm	C	6.2 ±0.09
Process connector	location/I.D. mm	D	6.2 ±0.09
Discharge connector	location/I.D. mm	E	5.0 +0.12/+0.20
Compressors on a pallet	pcs.		150

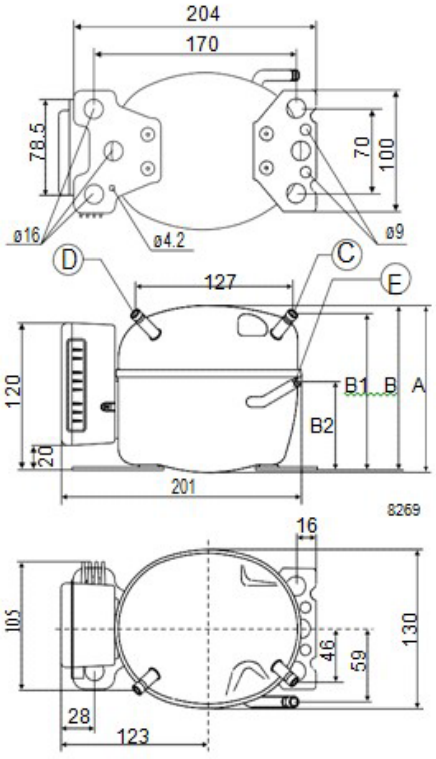

Standard battery protection settings (no connection C - P)

12V cut-out [V]	12V cut-in [V]	24V cut-out [V]	24V cut - in [V]
10.4	11.7	22.8	24.2

Optional battery protection settings

Resistor (R2) [kΩ]	12V cut-out [V]	12V cut-in [V]	12V max. Voltage	24V cut-out [V]	24V cut-in [V]	24V max. Voltage
0	9.6	10.9	17.0	21.3	22.7	31.5
1.6	9.7	11.0	17.0	21.5	22.9	31.5
2.4	9.9	11.1	17.0	21.8	23.2	31.5
3.6	10.0	11.3	17.0	22.0	23.4	31.5
4.7	10.1	11.4	17.0	22.3	23.7	31.5
6.2	10.2	11.5	17.0	22.5	23.9	31.5
8.2	10.4	11.7	17.0	22.8	24.2	31.5
11	10.5	11.8	17.0	23.0	24.5	31.5
14	10.6	11.9	17.0	23.3	24.7	31.5
18	10.8	12.0	17.0	23.6	25.0	31.5
24	10.9	12.2	17.0	23.8	25.2	31.5
33	11.0	12.3	17.0	24.1	25.5	31.5
47	11.1	12.4	17.0	24.3	25.7	31.5
82	11.3	12.5	17.0	24.6	26.0	31.5
220	9.6	10.9				31.5

Capacity (EN 12900/CECOMAF) watt

rpm \ °C	-30	-25	-23.3	-20	-15	-10	-5	0	5	10
2,000	20.1	31.0	34.9	42.8	56.3	72.2	91.6	115	144*	178*
2,500	27.0	39.0	43.4	52.7	68.9	88.9	113	144*	181*	
3,000	31.0	45.4	50.6	61.5	80.7	104	134*	171*		
3,500	38.1	53.2	59.1	71.9	95.0	124*	159*			

Capacity (ASHRAE) watt

rpm \ °C	-30	-25	-23.3	-20	-15	-10	-5	0	5	10
2,000	24.7	38.3	43.1	52.9	69.5	89.3	113	143	178*	221*
2,500	33.3	48.1	53.6	65.0	85.1	110	140	178*	224*	
3,000	38.2	56.0	62.5	75.9	100	129	166*	212*		
3,500	47.0	65.7	72.9	88.7	117	153*	196*			

Power consumption watt

rpm \ °C	-30	-25	-23.3	-20	-15	-10	-5	0	5	10
2,000	25.1	31.8	34.0	38.2	44.7	51.3	58.3	65.8	74.2*	83.5*
2,500	34.1	40.5	42.9	47.8	55.8	64.7	74.3	84.8*	96.1*	
3,000	39.9	49.2	52.2	57.8	66.5	76.4	88.4*	104*		
3,500	50.2	59.3	62.5	69.0	80.2	93.4*	109*			

Current consumption (for 24V applications the following must be halved) A

rpm \ °C	-30	-25	-23.3	-20	-15	-10	-5	0	5	10
2,000	2.2	2.6	2.8	3.1	3.8	4.4	5.1	5.8	6.4*	6.9*
2,500	2.9	3.4	3.6	4.0	4.7	5.4	6.2	7.0*	7.8*	
3,000	3.5	4.2	4.4	4.9	5.6	6.5	7.4*	8.5*		
3,500	4.2	4.9	5.2	5.8	6.7	7.8*	9.0*			

COP (EN 12900/CECOMAF) W/W

rpm \ °C	-30	-25	-23.3	-20	-15	-10	-5	0	5	10
2,000	0.80	0.98	1.03	1.12	1.26	1.41	1.57	1.75	1.94*	2.13*
2,500	0.79	0.96	1.01	1.10	1.24	1.37	1.53	1.70*	1.88*	
3,000	0.78	0.92	0.97	1.06	1.21	1.37	1.51*	1.65*		
3,500	0.76	0.90	0.95	1.04	1.19	1.32*	1.45*			

COP (ASHRAE) W/W

rpm \ °C	-30	-25	-23.3	-20	-15	-10	-5	0	5	10
2,000	0.99	1.21	1.27	1.38	1.56	1.74	1.94	2.16	2.40*	2.65*
2,500	0.98	1.19	1.25	1.36	1.53	1.70	1.89	2.10*	2.33*	
3,000	0.96	1.14	1.20	1.31	1.50	1.69	1.87*	2.04*		
3,500	0.94	1.11	1.17	1.28	1.46	1.64*	1.80*			

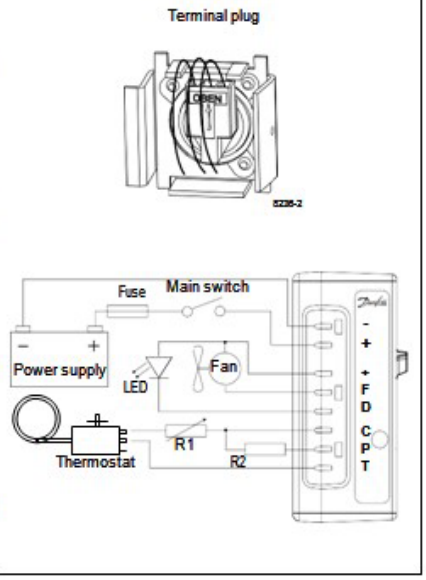

Test conditions EN 12900/CECOMAF
ASHRAE Condensing temperature 55°C 55°C
Ambient and suction gas temp. 32°C 32°C
Liquid temperature 55°C 32°C
Static cooling, 12V DC
* Fan cooling of electronic unit compulsory
1 Watt = 0.86 kcal/h

Compressor speed

Electronic unit	Resistor (R1) Ω	Motor speed rpm	Contr.circ current mA
101N0210 101N0220	0	2,000	5
	277	2,500	4
	692	3,000	3
	1523	3,500	2
101N0300 with AEO	0	AEO	6
	173	2,000	5
	450	2,500	4
	865	3,000	3
	1696	3,500	2

In AEO (Adaptive Energy Optimizing) speed mode the BD compressor will always adapt its speed to the actual cooling demand.

Wire dimensions

Cross section mm²	Max length* m 12V operation	Max length* m 24V operation
2.5	2.5	5
4	4	8
6	6	12
10	10	20

*Length between battery and electronic unit

Accessories

Devices	BD50F
Standard automobile fuse DIN 7258 12V: 15A 24V: 7.5A	Not deliverable from Danfoss
Mounting accessories	
Bolt joint for one compressor	118-1917
Bolt joint in quantities	118-1918
Snap on in quantities	118-1919

Operational errors shown by LED (optional)

Number of flashes	Error type
5	**Thermal cut-out of electronic unit** (If the refrigeration system has been too heavily loaded, or if the ambient temperature is high, the electronic unit will run too hot).
4	**Minimum motor speed error** (If the refrigeration system is too heavily loaded, the motor cannot maintain minimum speed at approximately 1,850 rpm).
3	**Motor start error** (The rotor is blocked or the differential pressure in the refrigeration system is too high (>5 bar)).
2	**Fan over-current cut-out** (The fan loads the electronic unit with more than 1A ⎓).
1	**Battery protection cut-out** (The voltage is outside the cut-out setting).

Appendix A-2: Deep cycle solar battery specification

Battery Model			**Maximus 105**	
Nominal Voltage				12V
Nominal Capacity (20Hr)				105Ah
Nominal Capacity (5Hr)				85Ah
Reserve Capacity (Min)			170	
CCA (-18°C) A / IEC	490			A
Operating Temperature (°C)			[-40°C to +50°C]	
	Length			332mm
Dimensions ± 0.5mm	Width			171mm
	Height			220mm
	Total Height			230mm
Cell Layout and Type	1			
Terminals	C			
Approx. Weight	Wet Charged			24.5Kgs

Constant current discharge ratings-amperes at 25°C

F . V/Time	5 MIN	10 MIN	15 MIN	30 MIN	1 HR	3 HR	5 HR	10 HR	20 HR
1. 60V	350	240	175	105	66. 0	27. 3	19. 1	10. 6	5. 27
1. 67V	315	219	170	102	65. 9	27. 2	18. 9	10. 4	5. 25
1. 70V	299	211	164	100	65. 7	27. 2	18. 9	10. 4	5. 25
1. 75V	266	195	155	98. 0	65. 0	27. 0	18. 8	10. 2	5. 23

1. 80V	240	181	148	95. 0	64. 2	26. 9	18. 6	10. 0	5. 04
1. 85V	182	149	128	87. 4	63. 5	26. 8	18. 5	9. 83	4. 74

Constant power discharge ratings-watts at 25°C

F . V/Time	5 MIN	10 MIN	15 MIN	30 MIN	1 HR	3 HR	5 HR	10 HR	20 HR
1. 60V	577	398	310	198	130	52. 4	36. 5	21. 2	10. 5
1. 67V	547	393	307	194	126	52. 4	36. 5	20. 9	10. 5
1. 70V	511	383	302	189	122	52. 4	36. 5	20. 7	10. 5
1. 75V	476	358	284	184	121	51. 6	36. 1	20. 4	10. 5
1. 80V	427	333	267	179	119	50. 9	35. 5	20. 0	10. 1
1. 85V	342	276	233	164	118	50. 7	35. 0	19. 7	9. 48

Battery characteristics

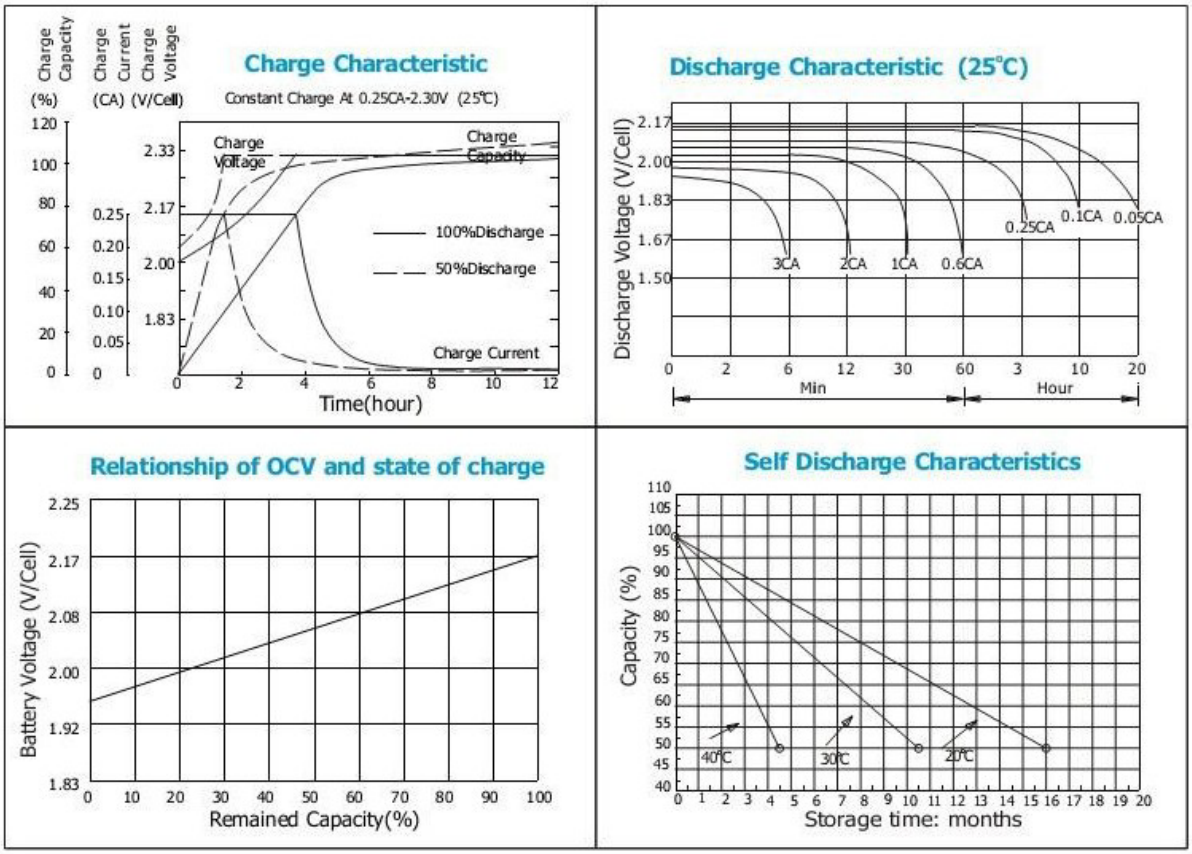

Appendix B: Technical specification of experimental instruments

Appendix B-1: Kipp & Zonen CMP06 pyranometer specification

Specifications	CMP 3	CMP 6	CMP10 & CMP 11	CMP 21	CMP 22
Classification to ISO 9060:1990	Second Class	First Class	Secondary Standard	Secondary Standard	Secondary Standard
Spectral range (50% points)	300 to 2800 nm	285 to 2800 nm	285 to 2800 nm	285 to 2800 nm	200 to 3600 nm
Sensitivity	5 to 20 µV/W/m²	5 to 20 µV/W/m²	7 to 14 µV/W/m²	7 to 14 µV/W/m²	7 to 14 µV/W/m²
Impedance	20 to 200 Ω	20 to 200 Ω	10 to 100 Ω	10 to 100 Ω	10 to 100 Ω
Expected output range (0 to 1500 W/m²)	0 to 30 mV	0 to 30 mV	0 to 20 mV	0 to 20 mV	0 to 20 mV
Maximum operational irradiance	2000 W/m²	2000 W/m²	4000 W/m²	4000 W/m²	4000 W/m²
Response time (63%) Response time (95%)	< 6 s < 18 s	< 6 s < 18 s	< 1.7 s < 5 s	< 1.7 s < 5 s	< 1.7 s < 5 s
Zero offsets (a) thermal radiation (at 200 W/m²) (b) temperature change (5 K/h)	 < 15 W/m² < 5 W/m²	 < 12 W/m² < 4 W/m²	 < 7 W/m² < 2 W/m²	 < 7 W/m² < 2 W/m²	 < 3 W/m² < 1 W/m²
Non-stability (change/year)	< 1%	< 1%	< 0.5%	< 0.5%	< 0.5%
Non-linearity (100 to 1000 W/m²)	< 1.5%	< 1%	< 0.2%	< 0.2%	< 0.2%
Directional response (up to 80° with 1000 W/m² beam)	< 20 W/m²	< 20 W/m²	< 10 W/m²	< 10 W/m²	< 5 W/m²
Spectral selectivity (350 to 1500 nm)	< 3%	< 3%	< 3%	< 3%	< 3%
Temperature response	< 5% (-10°C to +40°C)	< 4% (-10°C to +40°C)	< 1% (-10°C to +40°C)	< 1% (-20°C to +50°C)	< 0.5% (-20°C to +50°C)
Tilt response (0° to 90° at 1000 W/m²)	< 1%	< 1%	< 0.2%	< 0.2%	< 0.2%
Field of view	180°	180°	180°	180°	180°
Accuracy of bubble level	< 0.2°	< 0.1°	< 0.1°	< 0.1°	< 0.1°
Temperature sensor output				10 K Thermistor (optional Pt-100)	10 K Thermistor (optional Pt-100)
Detector type	Thermopile	Thermopile	Thermopile	Thermopile	Thermopile
Operational temperature range	-40°C to +80°C	-40°C to +80°C	-40°C to +80°C	-40°C to +80°C	-40°C to +80°C
Storage temperature range	-40°C to +80°C	-40°C to +80°C	-40°C to +80°C	-40°C to +80°C	-40°C to +80°C
Humidity range	0 to 100% non-condensing	0 to 100% non-condensing	0 to 100% non-condensing	0 to 100% non-condensing	0 to 100% non-condensing
Ingress Protection (IP) rating	67	67	67	67	67
Recommended applications	Economical solution for routine measurements in weather stations, field testing	Good quality measurements for hydrology networks, greenhouse climate control	Meteorological networks, PV panel and thermal collector testing, materials testing	Meteorological networks, reference measurements in extreme climates, polar or arid	Scientific research requiring the highest level of measurement accuracy and reliability

(Adapted from Omni, 2009)

Appendix B-2: SP-LITE silicon pyranometer specification

2. Sensor Specifications

Electrical

Nominal Impedance:	<50 Ω
Response Time:	<1 second
Sensitivity:	10 µV/(W m^{-2})
Expected signal range: (under atmospheric conditions)	0 – 15 mV
Stability:	<±2% per year
Non-linearity:	<±1% up to 1000 W m^{-2}
Temperature dependence of sensitivity:	<±0.15% /°C

Spectral

Spectral range:	400 to 1100 nm
Detector type:	BPW 34

Directional

Cosine corrected between 80° angle of incidence, error:	within ±10%
Cosine errors averaged over opposite azimuth error (at 60° angle of incidence):	within ±10%
Tilt response:	zero error

Mechanical

Housing material:	Anodized aluminum
Cable material:	Polyurethane
Weight:	110 g
Cable length:	5 m (can be extended up to 100 m)
Physical Dimensions:	See Figure 5

Environmental

Working temperature:	-30 to +70°C

Dimensions

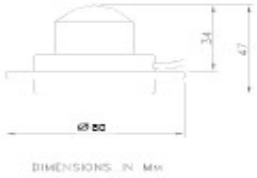

FIGURE 5. Dimensions of SP-LITE with Leveling Device

(Adapted from Campbell, 2015)

Appendix B-3: 03101 R.M Young three cup anemometer

Range:	0 to 50 m s^{-1} (112 mph), gust survival 60 m s^{-1} (134 mph)
Sensor:	12 cm diameter cup wheel assembly, 40 mm diameter hemispherical cups
Accuracy:	±0.5 m s^{-1} (1.1 mph)
Turning Factor:	75 cm (2.5 ft)
Distance Constant (63% recovery):	2.3 m (7.5 ft)
Threshold:	0.5 m s^{-1} (1.1 mph)
Transducer:	Stationary coil, 1300 ohm nominal resistance
Output:	AC sine wave signal induced by rotating magnet on cup wheel shaft 100 mV peak-to-peak at 60 rpm; 6 V peak-to-peak at 3600 rpm
Output Frequency:	1 cycle per cup wheel revolution; 0.75 m s^{-1} per Hz
Cup Wheel Diameter:	12 cm (4.7 in)
Weight:	113 g (4 oz)

(Adapted from Campbell, 2015)

Appendix C: Perez's statistical analysis of the clearness

Appendix C-1: Brightness coefficient of Perez Anisotropic Sky

ε	*f11*	*f12*	*f13*	*f21*	*f22*	*f23*
1-1.065	-0.008	0.588	-0.062	-0.06	0.072	-0.022
1.065-1.23	0.130	0.683	-0.151	-0.019	0.066	-0.029
1.23-1.5	0.330	0.487	-0.221	0.055	-0.064	-0.026
1.5-1.95	0.568	0.187	-0.295	0.109	-0.152	0.014
1.95-2.8	0.873	-0.392	-0.221	0.226	-0.462	0.001
2.8-4.5	1.132	-1.237	-0.412	0.288	-0.823	0.056
4.5-6.2	1.060	-1.6	-0.359	0.264	-1.127	0.131
6.2-∞	0.678	-0.327	-0.250	0.156	-1.377	0.251

(Adapted from Perez *et al.*, 1990)

Appendix D: Recorded data

Appendix D-1: Data recorded on 21 December 2020

TIME	AMBIENT TEMPERATURE (°C)	WIND SPEED (m/s)	SOLAR RADIATION (W/m²)
8:29 AM	19.6	0.1	167.9
9:04	20.4	0	714.7
9:34	22.2	0	752.7
10:04	23.7	1.1	803.4
10:34	25.6	0	838.3
11:04	27.7	0.5	868.2
11:34	28.6	0.1	859.6
12:04 PM	30	2.7	844.3
12:34	30.6	2.6	819.3
13:04	30.5	3	769.6
13:34	30.3	3.2	740.2
14:04	29	1.6	696.7
14:34	28.2	2.6	649.6
15:04	27.9	6.8	561.1
15:34	27.6	2	450.2
16:04	27.4	1.6	347.7
16:34	27.6	3.3	249.9
17:04	27.3	0.9	162.2
17:34	26.8	2.2	104.3
17:59	26.1	3.6	86.56

Appendix D-2: Data recorder on 22 December 2020

TIME	AMBIENT TEMPERATURE (°C)	WIND SPEED (m/s)	SOLAR RADIATION (W/m²)
8:29 AM	17.4	1.2	701.2
8:59	18.6	0	744.2
9:29	20.2	1.3	808
9:59	22.3	0.9	842.4
10:29	23.9	0	868
10:59	24.5	0.1	883.5
11:29	25.8	1.5	889.5
11:59	26.7	3	879.1
12:29 PM	27.2	0.1	856.2
12:59	27.7	1.2	828.1
13:29	28.3	5.8	792.2
13:59	27.5	2.6	722.3
14:29	27	4.4	702.8
14:59	26.8	4.1	652.5
15:29	26.5	6.1	594.5
15:59	25.5	3.3	504.6
16:29	25	5.1	406.4
16:59	24.2	2.9	309.4
17:29	25.2	2.3	223.3
17:59	24.6	4.3	149.8.1

Appendix D-3: Data recorder on 04 January 2021

TIME	AMBIENT TEMPERATURE (°C)	WIND SPEED (m/s)	SOLAR RADIATION (W/m²)
8:29 AM	22.5	0	734.7
8:59	24.3	0.8	800.2
9:29	26.2	1.1	841.5
9:59	27.8	0.4	882.2
10:29	30.8	0	907.3
10:59	31.5	0.2	911.8
11:29	33.2	1.5	924.2
11:59	34.1	2.3	99.8
12:29 PM	33.5	1.5	846.6
12:59	32.9	1.6	826.7
13:29	32.7	1.1	810
13:59	33.9	3.7	803.9
14:29	33.8	1.9	751.1
14:59	33.4	1.9	694
15:29	33	3.4	606.2
15:59	32.4	1.6	509
16:29	31.8	1.9	427.2
16:59	31	4.3	326.7
17:29	30.1	3	231.3
17:59	29.1	4.1	160.1

Appendix D-4: Data recorder on 05 January 2021

TIME	AMBIENT TEMPERATURE (°C)	WIND SPEED (m/s)	SOLAR RADIATION (W/m²)
8:29 AM	22.1	0.5	712.5
8:59	23.1	0	773.4
9:29	25.1	1.5	831.6
9:59	26.4	0.2	851.4
10:29	27.2	9.2	867.3
10:59	28.3	1.2	872
11:29	28.5	1.8	854
11:59	28.8	2.6	858.3
12:29 PM	30.2	2	859.2
12:59	30.5	3	822.8
13:29	30.7	2	790
13:59	31.2	2.9	777.5
14:29	31.4	2.7	731.8
14:59	31.1	3.6	678.9
15:29	31.3	2.3	636.4
15:59	31.3	4.3	547.9
16:29	31.1	3.3	456.4
16:59	30.4	1.1	362.8
17:29	30	2.6	271.1
17:59	29.6	3.9	196.2

Appendix D-5: Data recorder on 06 January 2021

TIME	AMBIENT TEMPERATURE (°C)	WIND SPEED (m/s)	SOLAR RADIATION (W/m²)
8:29 AM	19.5	2	713.3
8:59	21.1	1.8	728.8
9:29	22	0.4	646.7
9:59	23.1	1.5	731.3
10:29	24.6	0.1	892.1
10:59	26.4	0.9	853.7
11:29	26.5	0.6	904.4
11:59	27.1	2.3	862.1
12:29 PM	27.2	3.3	820.3
12:59	27	5.7	817.7
13:29	26.8	5.3	744
13:59	27.3	4.7	842.4
14:29	27.3	5.1	664.4
14:59	27.1	4.8	621.7
15:29	27.1	3.4	551.4
15:59	26.5	7.5	407.7
16:29	26.6	3.9	520.1
16:59	27.5	4.7	430.4
17:29	27.4	4	347
17:59	26.4	5.3	162.6

Appendix D-6: Data recorder on 07 January 2021

TIME	AMBIENT TEMPERATURE (°C)	WIND SPEED (m/s)	SOLAR RADIATION (W/m²)
8:29 AM	21.9	0.8	695.6
8:59	22.8	0.4	778.6
9:29	23.5	2.2	825.2
9:59	25	0.9	843.9
10:29	25.1	0	846.5
10:59	25.7	4.1	828.6
11:29	25.9	2.6	847.1
11:59	26.3	5	829
12:29 PM	26.8	2.7	824.4
12:59	27.3	1.6	820.8
13:29	28.1	0.8	816.6
13:59	28.6	1.5	794.6
14:29	28.5	4	718.5
14:59	28.4	3.3	679
15:29	28.3	4.1	634.1
15:59	28.5	4.7	577
16:29	28.3	4.1	498.7
16:59	27.9	4	415.5
17:29	27.2	7.5	329.6
17:59	26.5	4.1	259.4

Appendix D-7: Data recorder on 08 January 2021

TIME	AMBIENT TEMPERATURE (°C)	WIND SPEED (m/s)	SOLAR RADIATION (W/m²)
8:29 AM	22.4	0.9	712.2
8:59	24.4	0.6	774.8
9:29	24.9	0	823.1
9:59	25.7	2.2	844.2
10:29	27.1	1.6	847.5
10:59	27.6	5.1	824.6
11:29	27.4	2.2	836.4
11:59	27.6	4.1	835.2
12:29 PM	28	4	823.8
12:59	28.6	2.3	807.8
13:29	28.7	4.4	776.5
13:59	29	3	746.6
14:29	29.1	1.9	728.9
14:59	29.3	6	630.2
15:29	29	2.5	663.8
15:59	28.9	3.4	575.7
16:29	28.1	3.6	506.1
16:59	28	3.3	412.2
17:29	28.2	4.1	338
17:59	28.3	3.3	258.5

Appendix D-8: Data recorder on 09 January 2021

TIME	AMBIENT TEMPERATURE (°C)	WIND SPEED (m/s)	SOLAR RADIATION (W/m²)
8:29 AM	22.7	0.8	679.1
8:59	23.4	2	752.2
9:29	24.6	0.9	650.9
9:59	25.2	0.8	538.8
10:29	27.2	0	865
10:59	27.6	0.1	868.6
11:29	27.9	2.2	855.8
11:59	27	3.6	817.2
12:29 PM	26.5	3.6	803.2
12:59	26.7	6.2	776.3
13:29	27.8	2.7	791.3
13:59	28.2	4.6	745.8
14:29	27.9	4.8	799.1
14:59	27.5	4.3	779.2
15:29	26.9	4.6	306.5
15:59	27.5	5.7	468.3
16:29	27.4	4.3	358.7
16:59	26.8	2.9	770
17:29	25.8	5.3	124.9
17:59	24	6.8	92.5

Appendix E: Summary of the design parameters

Appendix E-1: Heat load design calculation

Table E-1: Cooling system vs heating system

Cooling system		Heating system	
Cooling load 'Q_{Load}'	3550.66588 kJ	Heating load 'Q_{Load}'	433.51 kJ
Refrigeration capacity 'Q_{Ref}'	493 W	Evaporating capacity 'Q_{Ev}'	377.4 W
Condensing capacity 'Q_{Cond}'	639 W	Heating capacity 'Q_{Cond}'	484 W
Compressor Power 'W_{In}'	148 W	Compressor Power 'W_{In}'	114 W
Mass flow rate '$\dot{m}$'	0.0039 Kg/s	Mass flow rate '$\dot{m}$'	0.003 Kg/s
Reynolds number 'Re'	331443316	Reynolds number 'Re'	142140255
Nusselt number 'Nu'	70.02	Nusselt number 'Nu'	56.75
Overall 'U_{Ref}'	0.543 W/m² K	Overall 'U_{Hp}'	0.430 W/m² K
Leakage load '$Q_{Leakage}$'	879.660 kJ	Leakage load '$Q_{Leakage}$'	224 kJ
Product load '$Q_{Product}$'	2302.31808 kJ	Product load '$Q_{Product}$'	159.6 kJ
Infiltration load '$Q_{Infiltration}$'	31.5 kJ	Infiltration load '$Q_{Infiltration}$'	10.5 kJ
Miscellaneous load 'Q_{misc}'	14.4 kJ	Miscellaneous load 'Q_{misc}'	14.4 kJ

Appendix E-2: Components design and sizing

Compressor

- Rotation speed: 2000 – 3500 rpm
- Cooling capacity: 149 – 186 W
- Power supply: 12V DC
- Displacement: 2.5 cm^3

Power demand

Power consumption: 84.8 W + 2 W @ 2500 rpm
Power demand = 86.8 x 8h x 1.3 = 902.72 Wh/day

PV panel

- Solar rad.: 5.55 kWh/day
- Total peak watt: 90W

Number of panel
= 902.72 / (90 x 5.55)
= 1.8 ~ 2 panels of 90W

Battery

- Total appliance = 86.8 x 8 = 694.4 Wh/day
- Nominal batter voltage = 12V
- Battery efficiency = 85%
- Days of autonomy = 2 days
- Type: Deep cycle battery
- Depth of Discharge: 100%

Battery Capacity (Ah) (Leonics,2013)
= Total Wh/day x Days of autonomy / (0.85 x 1 x 12V)
= (86.8 x 8 x 2) / (0.85 x 12) =136 Ah

Charge controller

- Voltage: 12V
- Maximum amperage: 10A
- Type: PWM